

UNIVERSITÀ DEGLI STUDI DI PADOVA

Department of Land, Environment, Agriculture and Forestry
Second Cycle Degree (MSc) in Forest Science

Risk Assessment of Climate Change-induced Droughts and
Heatwaves in French Vineyards

Supervisor

Prof. Paolo Tarolli

Co-supervisor

Dott. Eugenio Straffelini

Submitted by

Aude Laforest

2053897

ACADEMIC YEAR 2022-2023

Acknowledgements

I would like to thank my family for motivating me when I felt down, helping me brainstorm solutions when I would get stuck, and sharing their knowledge of French wines, geography, and viticulture. Your help was invaluable, my greatest adventure yet wouldn't have gone far without your unwavering faith in me. To my friends and classmates, thank you for taking me out to forget all about my problems. I'd like of course to thank Prof. Tarolli, my supervisor for this project, and my deepest thanks to Dr. Straffelini, my co-supervisor, for giving me a crash course on how to use Google Earth Engine and providing me with some code so that I may use the Javascript console. Finally, I'd like to thank my roommates for giving me tips on more formal writing styles, forcing me to take regular breaks to get some social interaction, and for their emotional support. Thank you everyone, I couldn't have done it without you.

Table of Contents

Acknowledgements	2
Table of Contents	2
List of tables and figures.....	3
List of acronyms and formulas	5
Abstract (Italiano).....	6
Abstract (English).....	7
1. Introduction.....	7
1.1. Literature review	7
1.2. Problem Statement	8
1.3. Research objectives.....	8
1.4. Hypothesis	9
1.5. Methodology	9
2. Materials and Methods	9
2.1. Study Area	9
2.2. Data Collection	12
2.2.1. Manipulation of the GEE datasets and the AI, HI and CI Indices.....	13
2.2.2. MeteoFrance data.....	17
2.3. Data analysis.....	17
2.3.1. Slopegraphs on R.....	18
2.3.2. Maps from p-values.....	19
3. Results	20
3.1. Context	20

3.2.	Region-by-region Assessment, with Maps and Slopegraphs	21
3.2.1.	Corsica Region	21
3.2.2.	Mediterranea.....	27
3.2.3.	Midi.....	35
3.2.4.	Bordeaux	42
3.2.5.	Loire	49
3.2.6.	Champagne.....	56
3.2.7.	Alsace.....	62
3.2.8.	Bourgogne	68
3.2.9.	Jura-Savoie.....	74
3.3.	Regression coefficients graphic representation.....	80
3.3.1.	Precipitations PT.....	80
3.3.2.	Maximum Temperatures TX.....	84
4.	Discussion.....	88
4.1.	Key Findings and their Implications.....	88
4.1.1.	High Temperature Origins and Dynamics.....	88
4.1.2.	Region-Specific Trends, Risks, and Opportunities brought on by Climate Change:.....	88
4.2.	Future research developments:	90
4.3.	Limitations:.....	93
5.	Conclusion	94
6.	Bibliography.....	95
7.	Annexes	99
7.1.	Annex 1 : Weather station names and 3-letter codes	99
7.2.	Annex 2: Topographic map of France, with mountains and rivers	101
7.3.	Annex 3: Map of wine production regions of France, with grape varieties.....	101

List of tables and figures

Figures

Figure 1	Weather stations & vineyards, raw data.....	10
Figure 2	Grid layer	11
Figure 3	Vineyards in regions and selected weather stations.....	12
Figure 4	Huglin Index formula	15
Figure 5	Corsica context	22
Figure 6	Corsica Aridity Index.....	23
Figure 7	Corsica Cool Nights Index	24
Figure 8	Corsica Huglin Index	25
Figure 9	Corsica Precipitation & Temperature Slopegraphs April to June.....	26
Figure 10	Corsica Precipitation & Temperature Slopegraphs July to September	27

Figure 11	Mediterranea context	28
Figure 12	Mediterranea Aridity Index	30
Figure 13	Mediterranea Cool Nights Index	30
Figure 14	Mediterranea Huglin Index	31
Figure 15	Mediterranea Precipitation & Temperature Slopegraphs April to June	34
Figure 16	Mediterranea Precipitation & Temperature Slopegraphs July to September	35
Figure 17	Midi context	36
Figure 18	Midi Aridity Index	38
Figure 19:	Midi Cool Nights Index	38
Figure 20	Midi Huglin Index.....	39
Figure 21	Midi Precipitation & Temperature Slopegraphs April to June	41
Figure 22	Midi Precipitation & Temperature Slopegraphs July to September	42
Figure 23	Bordeaux-Charentes context.....	43
Figure 24	Bordeaux-Charentes Aridity Index	45
Figure 25	Bordeaux-Charentes Cool Nights Index.....	45
Figure 26	Bordeaux-Charentes Huglin Index.....	46
Figure 27	Bordeaux-Charentes Precipitation & Temperature Slopegraphs April to June	48
Figure 28	Bordeaux-Charentes Precipitation & Temperature Slopegraphs July to September	49
Figure 29	Loire context.....	50
Figure 30	Loire Aridity Index	51
Figure 31	Loire Cool Nights Index.....	51
Figure 32	Loire Huglin Index.....	52
Figure 33	Loire Precipitation & Temperature Slopegraphs April to June	55
Figure 34	Loire Precipitation & Temperature Slopegraphs July to September.....	56
Figure 35	Champagne context.....	57
Figure 36	Champagne Aridity Index	58
Figure 37	Champagne Cool Nights Index	59
Figure 38	Champagne Huglin Index.....	59
Figure 39	Champagne Precipitation & Temperature Slopegraphs April to June	61
Figure 40	Champagne Precipitation & Temperature Slopegraphs July to September	62
Figure 41	Alsace context	63
Figure 42	Alsace Aridity Index	64
Figure 43	Alsace Cool Nights Index	65
Figure 44	Alsace Huglin Index.....	65
Figure 45	Alsace Precipitation & Temperature Slopegraphs April to June	67
Figure 46	Alsace Precipitation & Temperature Slopegraphs July to September	68
Figure 47	Bourgogne context	69
Figure 48	Bourgogne Aridity Index.....	70
Figure 49	Bourgogne Cool Nights Index	71
Figure 50	Bourgogne Huglin Index	71
Figure 51	Bourgogne Precipitation & Temperature Slopegraphs April to June	73
Figure 52	Bourgogne Precipitation & Temperature Slopegraphs July to September	74
Figure 53	Jura-Savoie context	75
Figure 54	Jura-Savoie Aridity Index	76
Figure 55	Jura-Savoie Cool Nights Index	77
Figure 56	Jura-Savoie Huglin Index	77
Figure 57	Jura-Savoie Precipitation & Temperature Slopegraphs April to June	79
Figure 58	Jura-Savoie Precipitation & Temperature Slopegraphs July to September	80

Figure 59 Regression coefficients for Precipitation in April	81
Figure 60 Regression coefficients for Precipitation in May.....	82
Figure 61 Regression coefficients for Precipitation in June	82
Figure 62 Regression coefficients for Precipitation in July.....	83
Figure 63 Regression coefficients for Precipitation in August	83
Figure 64 Regression coefficients for Precipitation in September.....	84
Figure 65 Regression coefficients for Maximum Temperatures in April.....	85
Figure 66 Regression coefficients for Maximum Temperatures in May	85
Figure 67 Regression coefficients for Maximum Temperatures in June.....	86
Figure 68 Regression coefficients for Maximum Temperatures in July	86
Figure 69 Regression coefficients for Maximum Temperatures in August	87
Figure 70 Regression coefficients for Maximum Temperatures in September	87
Figure 71 Topographic map of France, source: (Carte Du Relief Francais, n.d.).....	101
Figure 72 Map of grapevine varieties by regions of France, source: (abacchus, 2021).....	102

Tables

Table 1 List of Acronyms	6
Table 2 Regions.....	12
Table 3 Aridity Index classification	14
Table 4 Day lengths	15
Table 5 Hugin Index categories	15
Table 6 Cool nights Index	16
Table 7 Regression coefficients PT and TX with p-values for Corsica	26
Table 8 Regression coefficients PT and TX with p-values for Meditteranea.....	33
Table 9 Regression coefficients PT and TX with p-values for Midi.....	40
Table 10 Regression coefficients PT and TX with p-values for Bordeaux-Charentes	47
Table 11 Regression coefficients PT and TX with p-values for Loire	54
Table 12 Regression coefficients PT and TX with p-values for Champagne.....	61
Table 13 Regression coefficients PT and TX with p-values for Alsace.....	66
Table 14 Regression coefficients PT and TX with p-values for Bourgogne	72
Table 15 Regression coefficients PT and TX with p-values for Jura-Savoie.....	79
Table 16 City names and codes	100

List of acronyms and formulas

Acronym	Label
AI	Aridity Index
CC	Climate Change
CEP	Champs Electriques Pulsés (Pulsed Electromagnetic Fields)
CI	Cool Nights Index
GADM	Global Administrative District Maps
GEE	Google Earth Engine
GEVES	Variety and Seed Study and Control Group
HI	Hugin's Heliothermal Index
IFV	French Wine and Vine Institute
INAO	National Institute of Origin and Quality

INRAE	French National Research Institute for Agriculture, Food and Environment
ISVV	Science Institute of Wine and Vine
MOS	Model Output Statistics
OIV	International Organization of Vine and Wine
OLS	Ordinary Least Squares
ONERC	Observatoire National sur les Effets du Réchauffement Climatique
PCDS	Multicriteria Climatic Classification System
PDO	Protected Designation of Origin
PET	Potential Evapo-Transpiration
PT	Precipitation
TMMX	Mean Maximum Temperature

Table 1 List of Acronyms

Abstract (Italiano)

In Francia, la viticoltura è tra i principali settori socio-economici del Paese. I vigneti antichi, le pratiche tradizionali e il vino rappresentano pilastri fondamentali della cultura nazionale, ma sono ora sotto la minaccia del cambiamento climatico. Data la loro storica importanza come vitale risorsa economica e culturale, l'identificazione delle regioni a più alto rischio potrebbe aiutare a guidare le strategie di adattamento per la gestione futura dei vigneti. Questo studio mira ad indagare siccità e ondate di calore indotte dal cambiamento climatico negli ultimi anni e la loro influenza sulle regioni vitivinicole francesi. Il lavoro si concentra sulle tendenze climatiche come principale influenza sulla produzione di uva e trascurerà fattori statici locali (ad es. composizione del suolo) e fattori puntuali (ad es. disturbi). Gli obiettivi dello studio sono determinare l'estensione della superficie vitata in Francia, analizzare il cambiamento nelle tendenze climatiche durante il periodo riproduttivo della vite dagli anni 2000 al 2020 e, utilizzando indicatori bioclimatici specifici per la vite, determinare quali vigneti regionali sono più interessati da questi rischi. La metodologia prevede la creazione di un dataset di temperature e precipitazioni da stazioni meteorologiche francesi chiave attraverso gli archivi governativi, conducendo analisi statistiche e creando mappe climatiche per la visualizzazione. I risultati mostrano cambiamenti significativi nelle tendenze delle precipitazioni e delle temperature dei mesi primaverili ed estivi, risultando in una degradazione delle condizioni climatiche e nella comparsa di sfide maggiori per la viticoltura. Studi e progetti per mitigare l'effetto del cambiamento climatico e prepararsi all'adattamento a lungo termine sono in corso, e nuovi metodi di viticoltura hanno iniziato l'implementazione ufficiale nel 2022.

Abstract (English)

In France, no branch of agriculture is more important to the hearts of its citizens than viticulture, the ancestral vineyards, traditional practices, and wine filled with a rich history all a key part of the country's culture and now threatened by climate change. Given their historical importance as a vital economic and cultural asset, identification of the most high-risk regions could help guide adaptation strategies for future vineyard management. This study aims to provide a risk assessment of climate change-induced drought and heatwave trends and their influence over French vineyards. It will focus on climate trends as the main influence on grape production and disregard local static (e.g., soil composition) and punctual (e.g., pest invasions) factors. The objectives of the study are to determine the extent of the vineyard surface area in France, analyse the shift in climatic trends during the reproductive period of the grapevine from years 2000 to 2020, and using grapevine-specific bioclimatic indicators, determine which region's vineyards are most concerned by these risks. The methodology involves creating a dataset of temperature and precipitation readings from key French weather stations through the governmental archives, conducting statistical analysis, and creating climate maps for visualization. We notice significant changes to the precipitation and temperature trends of the spring and summer months, resulting in a degradation of the climate conditions and the arising of greater challenges for viticulture. Studies and projects to mitigate the effect of climate change and prepare for long-term adaptation are ongoing, and new viticulture methods have started implementation officially in 2022.

1. Introduction

1.1. Literature review

In France, reports dating back to the 1980s (Fraga et al., 2016) have highlighted a growing decoupling between enological and phenolic maturities in the grapes of French vineyards. This phenomenon has been observed primarily in Mediterranean vineyards (Salazar-Parra et al., 2018; Toda & Balda, 2015) but also in the North, for example with the Champagne region (Briche et al., 2011).

This decoupling raises concerns for the wine industry (Gutiérrez-Gamboa et al., 2021), indeed studies have shown that the enological maturity of the grape berry determines the alcohol content of the wine: as the berry ripens, its acidity is converted into sugars, later synthesized into ethanol during the fermentation process. This maturity period represents the ideal acidity-to-sugar ratio for harvest (Toda & Balda, 2015). However, the taste, tannin and phenol content of the wine is also determined by another factor: seed ripening, a process which starts as the nights cool down when they lengthen in September. But as Climate Change (CC) forces higher temperatures earlier in the year, effectively hastening grape flowering, so do berries ripen

earlier and earlier in the year, before the nights lengthen and cool down enough for the seed maturation process to finish, which leads to a shift in the ideal harvesting period (Liu et al., 2018; Verdugo-Vásquez et al., 2023). These consequences are worrisome for stakeholders: as CC is advancing harvest time and affecting grape ripening potential, wine-making regions face challenges in maintaining markets and ensuring their economic sustainability (Madelin et al., 2010). In France, where many high-end wine labels are area-specific through Protected Designation of Origin (PDO) labels, the common solution of relocating vineyards northward isn't always feasible, as it would result in losing the geographical designation that characterizes these labels (van Leeuwen et al., 2016).

To understand vineyard climates and evaluate the described parameters, researchers have developed the Multicriteria Climatic Classification System (MCCS) (Tonietto & Carbonneau, 2004). This system employs three synthetic indices: the Dryness Index (DI) to measure dryness, the Heliothermal Index of Huglin (HI) to classify land surface temperature specifically related to vine growth, and the Cool Nights Index (CI), which indicates night temperature conditions during grape maturation. These indices help in assessing the climate suitability for wine production (Ollat et al., 2021).

1.2. Problem Statement

Multiple case-studies at the vineyard level, focusing on specific areas or slopes or conducted in surrounding countries have been made using this MCCS over the years (Briche et al., 2011; Buesa et al., 2023; Doutreloup et al., 2022; Knauss, 2023.; Madelin et al., 2010; Roucher et al., 2022), but a comprehensive climate change-driven risk assessment encompassing the entire country's vineyards and comparing their different climatic conditions has not been conducted in the past 15 years (last assessment by: (Agenis-Nevers, 2006)). Gaining an understanding of these dynamics is vital to mitigate the impact of climate change on viticulture, safeguard French wine quality and uniqueness, and provide valuable insights for developing sustainable vineyard management strategies and potential adaptation measures. To do so, our study aims to determine national trends, identify the most severely affected regions, and take note of the way the situation is evolving in each of them.

1.3. Research objectives

General Objective

Determine the direct impact of climate change on the French grape production from 2000 to 2020.

Specific Objectives

1. Graphically model and analyse shifts in temperature and precipitation trends during the grapevine's flowering cycle in relevant regions of France from 2000 to 2020, using the MCCA's indices.
2. Identify the regions and vineyards most affected by climate-change.
3. Propose solutions for future management based on previous studies.

1.4. Hypothesis

As climate change continues, it is possible that the existing locations of French vineyards may become increasingly unsuitable for grape production intended for winemaking. We also anticipate the progression of this phenomenon to not be uniform across regions nor follow a linear trend over time. We also suspect the heatwave events that took place in 2003 and 2022 might offer insights into what the climatic conditions might be like in a few years.

1.5. Methodology

The methodology includes creating a dataset of temperature and precipitation readings from key French weather stations (2000-2020) using free access monthly reports for 100 stations. We'll perform a statistical analysis and generate climate maps using Google Earth Engine (GEE) data on QGIS for visualizing the shifting climate trends.

2. Materials and Methods

2.1. Study Area

To start this project, we must first define the study area. We consider the entire vineyard surface of metropolitan France, including the island of Corsica, but acknowledging only the vineyard surface area will not be enough to get an accurate reading of the climatic conditions, so we must also consider a surrounding buffer area affected by similar climate conditions to give us more context. Though the vineyard surface of France represents 1,4% of the metropolitan territory and takes 3% of the agricultural surface (*Infographie - La viticulture française*, 2022) it is also spread over most of the country. As such, we think a complete view of France might be necessary to accurately spot and assess both changes to the climate and potential trends.

To this end, we found a dataset on the official government census website for forestry and geographical information, the Institut National de l'Information Géographique et Forestière (IGN) that accurately represents and geographically places the totality of Protected Designation of Origin (PDO, or AOP in French) vineyards in France (*Cartes des grandes régions productrices de vins AOP en France - data.gouv.fr*, n.d.). We then transformed this dataset into a polygon layer in QGIS, version 3.16.13. At the same time, we also sought and found a dataset of the administrative borders of France and its regions in the GADM database (*GADM*, 4.0.),

to better delimitate our study area. We inserted it in our QGIS project along with the vineyard layers, as polygon vector layers over a base OpenStreetMap layer from the basic QGIS package. We then found on the official French weather archive (*Données Publiques de Météo-France - Bulletins Climatiques de France Métropolitaine et Outre-Mer*, n.d.) a compilation of the weather measures of 100 stations all over France, which seemed complete enough and that we obtained along with the GPS coordinates associated with these 100 stations. We compiled in an Excel dataset the station's names, a 3-letter name code we created for easier reference (Table 16 City names and codes), and their GPS coordinates to input on our map in QGIS as a delimited text layer named "Weather stations" and added labels bearing the station names (Figure 1 Weather stations & vineyards).

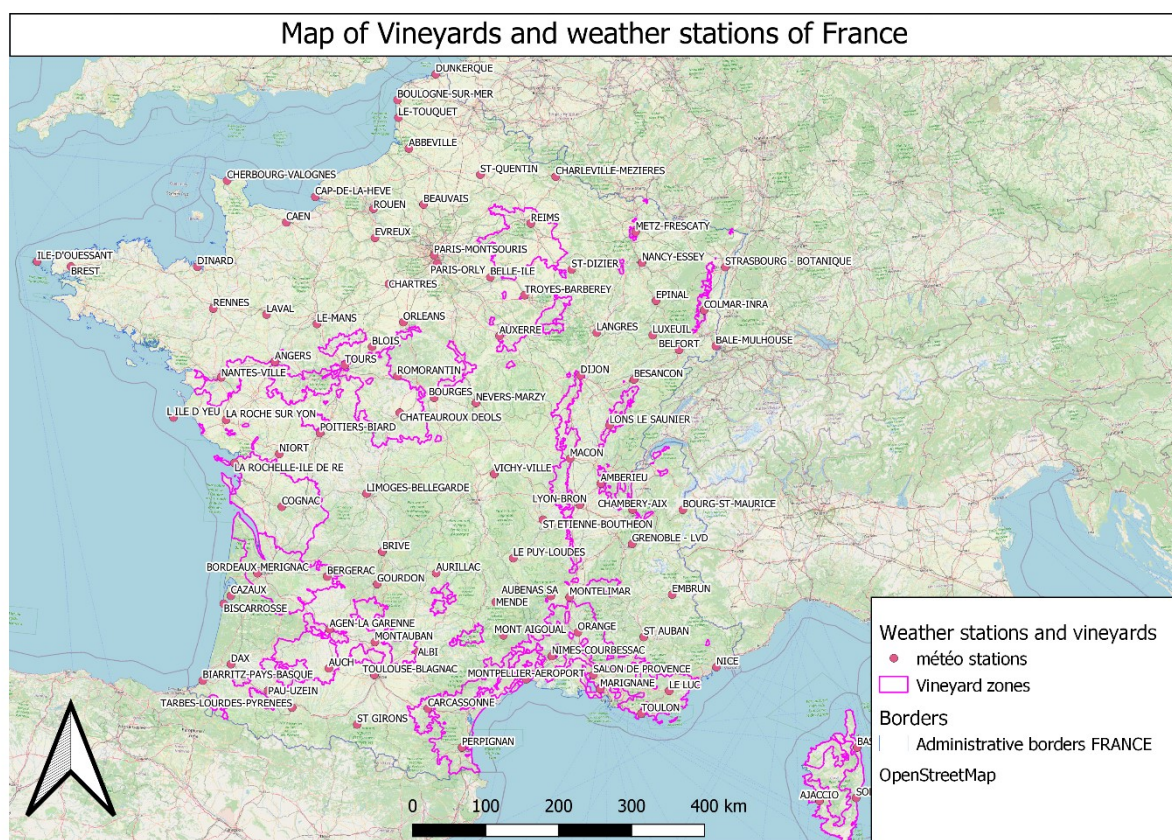


Figure 1 Weather stations & vineyards, raw data

We then intended to put the vineyards and close-by weather stations in relation with each-other on our QGIS map. Data from weather stations can be used for Model Output Statistics (MOS) with sufficient accuracy with a resolution of 10km in complex terrain (Müller, 2011). We aimed to select on our project all weather stations that were within a 10km radius of the vineyard area. For this, we started with using the "Create grid" tool to make a grid containing the whole of the vineyard area. we set the grid to the map canvas, use a hexagonal shape to better approximate a circle, and set the horizontal and vertical spacings to a 20 km diameter. Our resulting layer is a multi-polygon vector layer called "Grid20km". From this grid, we used the "Select by

location” tool to automatically select the hexagons containing part of the vineyard layers. We obtained a vector layer we called “aopgrid.” (Figure 2 Grid layer).

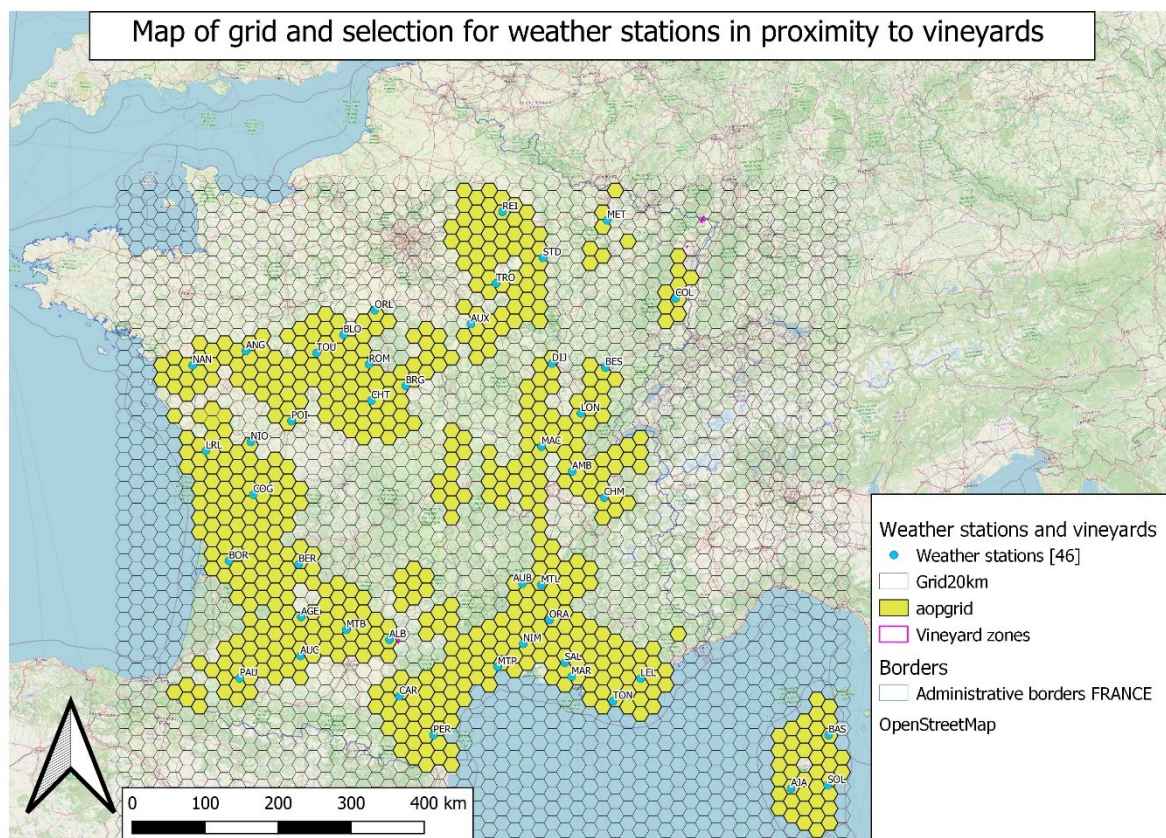


Figure 2 Grid layer

Then, we extracted from the weather stations layer the points present within the “aopgrid” layer’s confines and copied them onto another layer by using the “extract selected features” tool, on which we used the “extract by location” tool to create a point selection containing only the weather stations within 20km’s proximity of the vineyards. We thus obtained 46 relevant stations out of 100, counted via attribute table, so less than half of the original count. We renamed the output points layer the new “Weather stations” with shortened 3-letter names (see Table 16 City names and codes).

Afterwards, we checked two well-rated wine guides (abacchus, 2021; *Vin-Vigne : Le Guide Des Vins et Des Vignes de France*, n.d.) for a map of the delimitations of the great vineyards of France (see Figure 72 Map of grapevine varieties by regions of France) and manually parcelled the study area in 9 regions on a polygon vector layer (see Table 2 Regions) we named: Alsace, Bordeaux-Charentes, Bourgogne, Champagne, Corsica, Jura-Savoie, Loire, Midi and Mediterranean (see Figure 3 Vineyards in regions and selected weather stations).

Region	Stations
Alsace-Lorraine	COL, MET
Bordeaux-Charentes	BOR, COG, LRL, NIO
Bourgogne	AUX, DIJ, MAC
Champagne	REI, STD, TRO
Corsica	AJA, BAS, SOL
Jura-Savoie	AMB, BES, CHM, LON
Loire-Centre	ANG, BLO, BRG, CHT, NAN, ORL, POI, ROM, TOU
Mediterranea	AUB, CAR, LEL, MAR, MTL, MTP, NIM, ORA, PER, SAL, TON
Midi	AGE, ALB, AUC, BER, MTB, PAU

Table 2 Regions

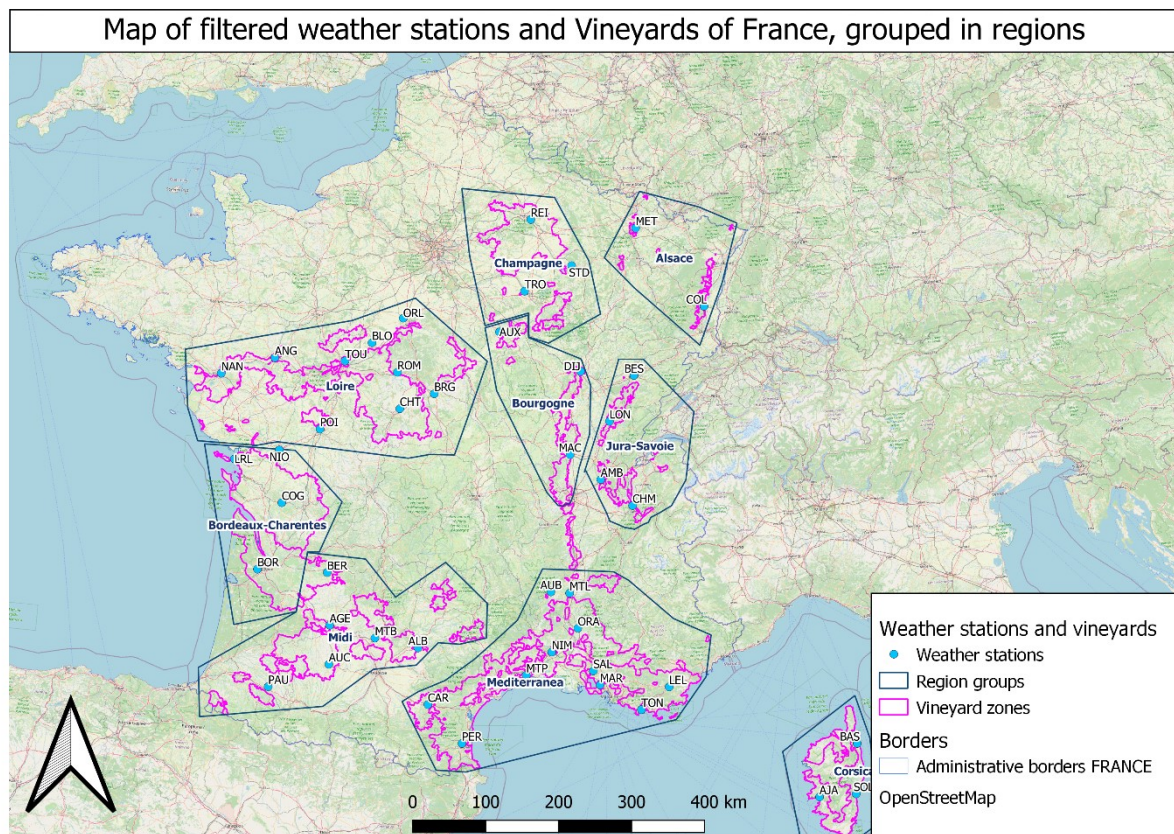


Figure 3 Vineyards in regions and selected weather stations

2.2. Data Collection

In this section, we explain our data-collecting process, and how we went about manipulating this data. We examined three main datasets: two datasets from NASA's MODIS satellite and the University of California Merced, officially named MODIS/061/MOD11A2 and

IDAHO_EPSCOR/TERRACLIMATE respectively, manipulated through Google Earth Engine (GEE) and one from the national weather archives of MeteoFrance (*Données Publiques de Météo-France - Bulletins Climatiques de France Métropolitaine et Outre-Mer*, n.d.) to help us analyse trends and perform statistical analysis. The Multicriteria Climatic Classification System (MCCS) mentioned earlier introduced us to the concept of the Cool nights Index (CI), Dryness Index (DI) and Huglin Index (HI), as pivotal metrics adapted to the assessment of climate conditions regarding the growth of grapevine for wine production. However, we ran into a problem regarding the DI, where we were confronted to a lack of available data concerning some of the factors needed for its computing. So as a substitute, we used the Aridity Index (AI) to measure shifts in the precipitation-evapotranspiration of the area, and for better accuracy, we used the data from MeteoFrance to create slopegraphs to help us visualize the shifts in climate and associated trends.

2.2.1. Manipulation of the GEE datasets and the AI, HI and CI Indices

We intended to compute and use three bioclimatic indices over our study area, the Aridity Index (AI), Huglin's Index (HI) and Cool Nights Index (CI), which paired together, are specifically designed to assess the climate's suitability for grapevine growth with the goal of wine production in each area.

Through Google Earth Engine (GEE), we acquired two essential datasets: the MODIS LST Land Surface Temperature (LST) dataset from NASA held precious data regarding daily and nightly LST, and the TerraClimate dataset from the University of California Merced, later updated and completed by the University of Idaho, contained useful data on accumulated precipitation (PT), projected evapotranspiration (PET), and mean maximum temperatures (TMMX).

Before computing the data rasters on GEE, we manually delineated a polygon containing the entire study area, both Metropolitan France and Corsica, that we used as a base for all our downloads on GEE.

2.2.1.1. The Aridity Index (AI)

The Aridity Index (AI) of an area is determined by dividing the mean of its yearly accumulated precipitation (PT) by the mean of the yearly accumulated potential evapotranspiration (PET) (Zomer et al., 2022).

$$AI = \frac{\text{meanPT}}{\text{meanPET}}$$

The official classification for the Aridity Index, as defined by the World Atlas of Desertification (WAD | *World Atlas of Desertification*, n.d.), are:

Aridity Index	Climate Type and categories
AI < 0.03	Hyper-Arid (+3)
0.03 < Arid < 0.2	Arid (+2)
0.2 < AI < 0.5	Semi-Arid (+1)
0.5 < AI < 0.65	Dry Sub-Humid (-1)
AI > 0.65	Humid (-2)

Table 3 Aridity Index classification

We modified Dr. Straffellini’s Javascript code to function with the TerraClimate (IDAHO_EPSCOR/TERRACLIMATE) dataset on GEE. We computed the monthly accumulated precipitation (PT) and potential evapotranspiration (PET) for the 12 months of the entire period of 2000 to 2020, with the addition of the entire year of 2022. We obtained this way 264 data files for PT and another 264 files for PET, that we downloaded on our computer under the GeoTIFF format.

Then, we uploaded the files as raster layers onto QGIS and calculated, first the sums of PT and of PET through the months for every year, then we divided the summed PT by the corresponding summed PET rasters to obtain 22 layers of the AI.

Afterwards, we clipped these rasters to the borders of France using the “Clip raster to mask layer” tool and “Administrative Borders FRANCE” mask layer to eventually obtain 22 raster layers named “AI_YYYY” of the finished AI. To eliminate interannual variability, we calculated 3 more layers using the “raster calculator” tool on QGIS, for the years 2000 to 2006, 2007 to 2013 and 2014 to 2020. We called these layers “AI 2000-06”, “AI 2007-13” and “AI 2014-20,”, for a total of 25 layers in this index.

2.2.1.2. The Huglin Index (HI)

To get a better understanding of the evolution of heat accumulation during the grapevine growth period over the years, we computed the Huglin Index (HI). This index was created in 1978 by Huglin, specifically to assess the suitability of an area to cultivate grapes based on its average temperatures in the vegetative period of the grapevine life cycle, and day length based on the area’s latitude. It’s calculated from the months of April to September, with T mean temperatures of the month, Tx maximum temperature of the month, and d day length coefficient, such as:

$$HI = \sum_{01.04}^{30.09} \frac{[(T - 10) + (T_x - 10)]}{2} d$$

Figure 4 Huglin Index formula

In the Northern Hemisphere, the daylength variable d varies from 1.02 to 1.06 between 40° and 50° of latitude.

Latitude	Daylength coefficient d
≤ 40°00'	1.00
40°01'–42°00'	1.02
42°01'–44°00'	1.03
44°01'–46°00'	1.04
46°01'–48°00'	1.05
48°01'–50°00'	1.06

Table 4 Day lengths

The Index is composed of 6 categories describing the influence of the temperature on potential precocity of grape ripening:

Values	Categories
HI ≤ 15	Very Cool (-3)
15 < HI < 18	Cool (-2)
18 < HI < 21	Temperate (-1)
21 < HI < 24	Temperate-warm (+1)
24 < HI < 30	Warm (+2)
HI > 30	Very warm (+3)

Table 5 Huglin Index categories

On our side, we computed day LST data through the MODIS dataset on GEE from the months of April to September, from the years 2000 to 2020, with the addition of 2022, and a further step for temperature unit conversion from Kelvin to degrees Celsius, to obtain 132 GeoTIFF files. We repeated this process on the Terraclimate dataset with TMMX data, to obtain 132 GeoTIFF files as well. We named the resulting 264 files respectively “LSTDay MM_YYYY” and “TX MM_YYYY” and downloaded them.

The main issue with the Huglin Index’s formula was that we couldn’t calculate it on QGIS, as our raster data couldn’t be computed with the area-dependant d factor on QGIS’s Python

console. To solve this issue, we computed Huglin’s Index on the R console, version 4.3.1. We downloaded the “raster” and “sf” packages for spatial data manipulation and accessed the files through the R console (*Raster Package - RDocumentation*, n.d.; *Sp Package - RDocumentation*, n.d.).

We then defined the latitude-dependent coefficients (d) to account for day length variations, based on latitude ranges as instructed from the MCCA, allowing us to adjust the index calculation according to its coordinates.

Afterwards, we calculated the HI in earnest: using the LSTDay and TX values, along with the calculated coefficients, we applied a predefined formula to compute the Huglin Index for each pixel in the raster grid of the study area and generated the output as raster files in the GeoTIFF format, that we saved on our computer using the “writeRaster” function from the raster package.

Finally, the output files were transferred as 132 raster layers to QGIS, where we summed the months of every year then clipped them to the borders of France using the “Clip raster to mask layer” tool and “Administrative Borders FRANCE” mask layer to eventually obtain 22 raster layers named “HI_YYYY” of the finished HI. To eliminate interannual variability, we calculated 3 more layers using the “raster calculator” tool on QGIS, for the years 2000 to 2006, 2007 to 2013 and 2014 to 2020. We called these layers “HI 2000-06”, “HI 2007-13” and “HI 2014-20,” for a total of 25 layers in this index.

2.2.1.3. The Cool Nights Index (CI)

The Cool Nights Index is a parameter made from the nighttime Land Surface Temperature (LST) in the month of September for the North Hemisphere, grouped into 4 classes as per the MCCA:

Values	Classes
CI < 12°C	Very Cool nights (+2)
12°C < CI < 14°C	Cool nights (+1)
14°C < CI < 16°C	Warm Nights (-1)
CI > 18°C	Very Warm Nights (-2)

Table 6 Cool nights Index

It is meant to rank the temperatures in how they affect grape seed ripening in September. To construct it, we started by compiling LSTNight (LST during the night) data with 1km resolution, for the month of September across the years 2000 to 2020, with the addition of 2022. We obtained a series of 22 GeoTIFF files, extracted from the MODIS/061/MOD11A2 dataset

(MODIS), that we then had to convert from Kelvins to degrees Celsius to match the values of the Indexes categories.

After computing our files, we uploaded them as raster layers into QGIS, and corrected the edges with the tool “Clip raster to mask layer” and the “Administrative borders FRANCE” layer as a mask, so they would match the borders of France. The resulting layers were named “CI_YYYY”, one for every year from 2000 to 2020, and another for 2022. We also calculated the means of our resulting rasters over 7 years, thrice, to obtain 3 layers with the mean values for: 2000 to 2006, 2007 to 2013, and 2014 to 2020, and this way remove the yearly variability to better showcase the index’s evolution. We obtained 25 layers in total, that we named: “CI 2000-06”, “CI 2007-13” and “CI 2014-20” on top of the original 22.

2.2.1.4. 2022 Heatwave and drought maps

After having configured our base data, we searched in the France’s weather archives for recent occurrences of heatwaves similar to those seen in 2022. We found that in 2003, a canicule swept over the entirety of France, with severe consequences. We thus selected the year in our indexes for separate study and comparison with 2022, to know if the 2022 heatwaves were worse or on the same level as the 2003 heatwaves.

Our exploration then led us back to the MeteoFrance archives, where we parsed through the archives' monthly summaries and weather newsletters for more data.

2.2.2. Meteofrance data

Through the MeteoFrance archive, we obtained a dataset of monthly values for our 100 weather stations, for the months of April to September, from 2000 to 2020. These include mean minimum temperatures, absolute minimum temperature with date, mean maximum temperatures, absolute maximum temperature with date, insulation, and accumulated precipitation (TN, TNN with TNN-D, TX, TXX with TXX-D and PT), available respectively in degrees Celsius and millimeters. With this data, we created a file on Microsoft Excel with the relevant variables of TX and PT and the station names as the three-letter code we had previously established. We then filtered the data so that only the 46 weather stations we had pointed out as relevant were kept, and input the resulting dataset in R through the “readxl” package for statistical analysis (*Readxl Package - RDocumentation*, n.d.).

2.3. Data analysis

To analyse our numerical data from MeteoFrance, we used the R console, version 4.3.1. We first organized our data in slopegraphs to show the progression of maximum temperature (TX)

and precipitation (PT) values for each of our 9 studied regions, through the months of April to September, then computed the linear regression of these values and input the regression lines in the slopegraphs.

The regression lines and coefficients were calculated through the Linear Models function, “lm()” in R, that uses Ordinary Least Squares (OLS) regression to fit the model. Afterwards, we programmed R to calculate the regression coefficients of these lines with the “tidy()” function from the “broom” package (*Broom Package - RDocumentation*, version 1.0.4). We used this method to extract the coefficients, standard error, t-value, and through it the p-value from the lm() output, and loaded the resulting values in an Excel file to input in QGIS as a points layer showing the intensity of the resulting trends.

Finally, we set an error margin at 95% and extracted all significant regression coefficient values with p-value < 0.05, then created a polygon layer in QGIS to visualize the resulting trends.

2.3.1. Slopegraphs on R

Using the R console, we first realised slopegraphs from the MeteoFrance dataset to better visualize TX or PT variations for each month over the two decades of our study period. In this section, we go through the methodology employed to create these slopegraphs. The goal here was to provide a clear representation of the evolution of TX and PT trends over time, while also focusing on the specific groups of cities associated with our 9 grapevine-growing regions.

The MeteoFrance dataset we used as a template for these graphs contained five key variables: "Année" (years), "Mois" (months), "TX" (maximum temperature values), "PT" (precipitation accumulation values) and "Stations" (three letter city codes). The dataset covered the months of April to September for the years 2000 to 2020 and included PT and TX readings for the 46 cities within 20 km of our vineyard zones.

We chose slopegraphs to visualize the data as this graphical method is designed for displaying changes in a variable between two or more points in time. We used the R programming language for this data analysis and visualization.

We used the “ggplot2” graphics package (*Ggplot2 Package - RDocumentation*, version 3.4.3) to create the slopegraphs. The evolution of PT or TX values was put on the y-axis, while years were set on the x-axis.

Given the considerable number of cities in the dataset, we thought to improve the clarity of the slopegraphs' visualization by separating the slopegraphs in groups of close-by stations. For this, we used the 9 vineyard regions we had already defined (see Table 2 Regions). Each city in the studied region's slopegraph was then assigned a unique colour for easy identification.

As a trial run, we focused on the three stations located in Corsica, namely "AJA," "SOL," and "BAS," representing respectively the cities of Ajaccio, Solenzara, and Bastia. To this end, we used the "dplyr" package (*Dplyr Package - RDocumentation*, 1.0.10) to filter the dataset based on the selected city codes. As the values obtained in our test run were very wildly fluctuating, we also decided to add the regression line of each city's curve for better visualisation. We then tested the analysis programming, and after debugging we computed the slopegraphs for the rest of the regions. The resulting slopegraphs provided a better visual representation of the variable's evolution in a specific region, and so allowed for a quicker assessment of PT and TX changes on the region while still providing insights into variations unique to each city.

After analysis of our newly made slopegraphs, we decided to calculate the regression coefficients of the regression lines on said graphs. To this end, we used our R console again to calculate both the regression coefficient and the p-value of every regression line and do this for the entire dataset. The goal was to assess the slope of the trend and determine if it was significant. We used here a margin of error of 95%. As such, we only considered the trend given by the regression line of a station's PT or TX as significant if the p-value of its regression coefficient was $P < 0.05$.

Through Excel, we sorted the regression coefficient values we obtained into their respective months and stations, added their GPS coordinates, and converted the original RStudio output file to one CSV format file for every month, for PT and for TX, for a total of 12 files. We then imported them as points vector layers with x, y, and M values such as: x = latitude, y = longitude, and M = regression coefficients. We changed the symbology of the layers to a blue-to-red gradient to give a better visual representation of the regression slope's magnitude and used a blue gradient to represent negative slopes (decreasing trend) and a red one for positive ones (increasing trend).

2.3.2. Maps from p-values

For the last part of our analysis, we decided to do a graphical representation on our project's QGIS map of the location of the significant regression coefficients, for PT as well as TX, and for the 6 months of our study. Out of the 276 values of the PT dataset, we found 26 significant values, spread over 4 months of the study period, April, June, July, and September. To represent

them, we created 4 vector layers in QGIS and manually created a polygon around all the concerned cities to highlight the trends formed.

For also 276 values in the TX dataset, we found 46 significant ones, spread over 3 months: April, July, and September. We created 3 layers in QGIS to represent and highlight their trends. We obtained a total of 7 QGIS layers displaying the weather stations whose PT and TX values over the 2000-2020 period, had regression coefficients with a significant ($P < 0.05$) p-value.

3. Results

3.1. Context

The main viticulture practice in France involves cultivating the grapes not in terraced hills as in Italy, but in either flat plains, or slopes of varying steepness. The greatest cultures of vineyards are also found almost entirely near a source of water, be it the banks of a river for the majority, or sometimes in around a lake or in proximity to the sea. As a result of this constraint, the grapevine-growing regions tend to be confined near their rivers away from of the more typical natural barriers like mountain ranges, forested areas, and urban areas. Because of this and of climatic restrictions in the northernmost parts of France, the shape, size and location of the vineyard-filled areas can vary wildly. It can also lead to some geographical outliers, like the vineyards on the hills of Paris, whose growth conditions are too impacted by the city itself to be of much use when discussing the influence of climate change on the national scale.

It is also worth noting that the vineyards themselves can influence the temperature at the local scale when covering a large area, and that the same can be said about city centers or lakes near which some vineyards may be located.

The grapevine is a hardy species, with an extensive root system and a great tolerance for both heat and water stresses, that can nevertheless survive frosty winters and bounce back the following year. It has been cultivated since the Antiquity and has since evolved into an array of varieties with different levels of resistance and adaptation to diverse conditions, which is why the species can be found between 28° and 50° latitude in places as far south as Algeria, and as far up as England. However, because there are over 200 grapevine varieties present in France, this study will not consider all their respective qualities and preferred climate despite the relevance of this factor but will briefly list the most cultivated varieties in each region.

First, we elaborated on each region's geographical characteristics with help from an official topography map (see Figure 71 Topographic map of France) (*Carte Du Relief Francais*, n.d.), and their peculiarities if relevant, but the study of local factors such as soil composition, altitude, or

exposure types, even if important, are outside the scope of this project. Second, we assessed their climatic conditions and evolution through the years 2000 to 2020 with the aid of the AI, HI, and CI. We also took note of the effects of the heatwave phenomenon that swept over most of France in 2003 and 2022 with the same indicators. Finally, given the somewhat generalized nature of the AI and the relatively stable maps generated through it, we conducted a numerical analysis using MeteoFrance weather data.

To learn if there were any trends in precipitation and maximum temperatures from April to September, we conducted a two-fold analysis: a series of slopegraphs done on RStudio to represent the evolution of the PT or TX variables for each month of the study period and in each region, coupled with their corresponding regression lines. We calculated the regression coefficients, and their significance level (p-values), to establish a list of selected cities where the trend direction was significant ($p < 0.05$) for a given month. To better visualize the results, we regrouped in QGIS the selected regions and drew hypothesis as to the reasons and provenance of the spread.

3.2. Region-by-region Assessment, with Maps and Slopegraphs

3.2.1. Corsica Region

3.2.1.1. Geoclimatical Context

Corsica is a mountainous island to the southeast of the French metropolis, at the periphery of Italy. Because of the mountains and rougher terrain inland, all the vineyards there are confined to the vicinity of the coastline. The island being situated in the warm waters of the Mediterranean Sea, the grape varieties cultivated there are accustomed to a Mediterranean climate with the trademark mild winters, rainy springs, and hot and dry summers. The proximity of the vineyards to the sea offers a degree of protection against extreme temperatures.

There are many grape varieties cultivated in Corsica. The most common ones are:

- For red wines: grenache, mourvèdre, cinsault, niellucio, sciacarello, black carajolo.
- For white wines: vermentino, sémillon, white ugni, and white carajolo.

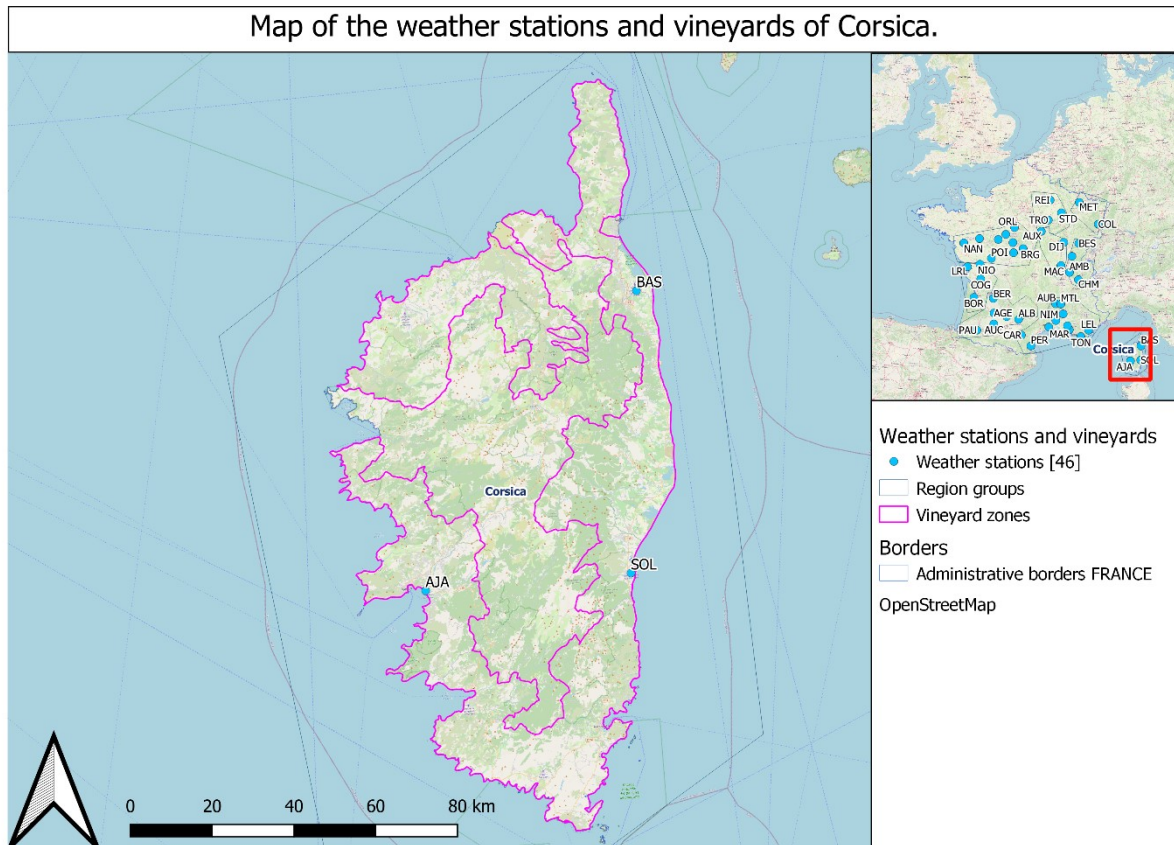


Figure 5 Corsica context

3.2.1.2. Index Shift Analysis:

Through the maps we have created to illustrate the evolution of HI, AI and CI, we observe the following results:

The AI shows the island is mainly in the arid (+2) category, with the coast of the southern point in the hyper-arid (+3) category. In the 21 years of the study, this hyper-aridity spreads a bit north but remains mostly close to the coasts. However in 2003 and 2022, about three quarters of Corsica's coasts turned to the red category (+3), including in 2022 the entire east side where it encroached further inland and part of the north, against a more even spread of red all around the periphery of the island for the 2003 event. The rest of the island remained firmly in the +2 category.

The HI shows most of the coasts of Corsica were already in the warm (+2) category in 2000. The following years saw further warming and very warm (+3) hotspots started forming near Solenzara (SOL on the maps), but not much change was otherwise observed there. On the other hand, the warm (+2) zone spread considerably inland on the north and west coasts of Corsica in 2003, with large very warm (+3) hotspots also appearing on the north of the island. This event was mirrored in 2022, though a bit less severely.

Analysing results of the CI, we see the coasts of Corsica were in the warm (-1) category already in 2000. This process has spread further since and was a permanent feature the foothills of the mountain sides of Corsica by 2020. The year 2003 saw a wide spread of warm (-1) category temperatures over the coasts and far inland and overtaking the cool (+1) zones while 2022 saw little deterioration on the mountain sides but the start of a shift to the very warm (-2) category around the very edge of the coasts in the north, west and south sides of the island. This phenomenon is probably due to the water of the Mediterranean Sea releasing the heat absorbed during the day and keeping the coastside warm at night.

Overall from 2000 to 2020, the climate near the vineyards appears relatively stable though slowly becoming warmer and drier, with dramatic climatic alterations only manifesting during the extreme heatwave events of 2003 and 2022. The grapevine cultivated in the region was already selected for its adaptation to especially warm and dry conditions as evidenced by the 2000 data. The Corsica region is significantly influenced by climate change, as evidenced by the growing warmer conditions, particularly observable in the southern part of Corsica. The effects on the area’s grapevine growth will probably cause a heightened risk of extreme hydric stress in the coming years, as the cultures there already are in the upper range of AI and HI for grape cultivation (Tonietto & Carbonneau, 2004).

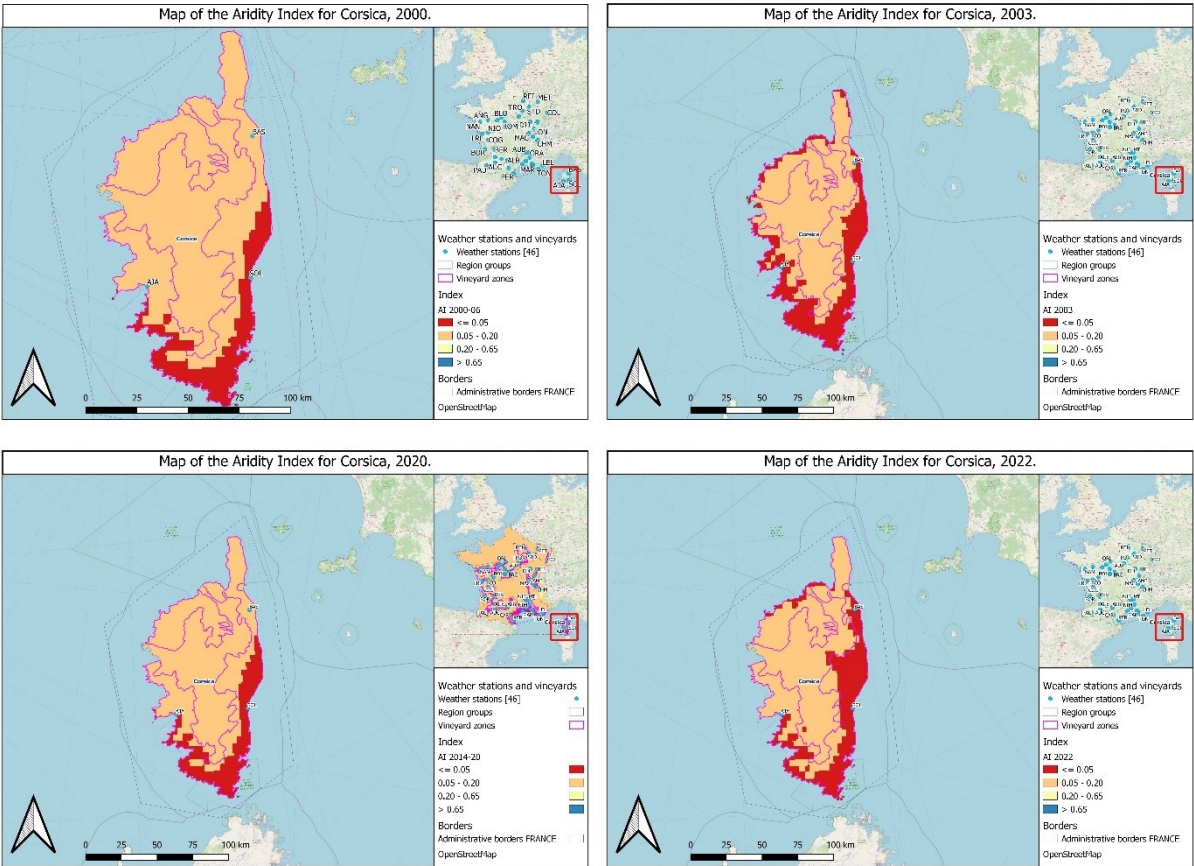


Figure 6 Corsica Aridity Index

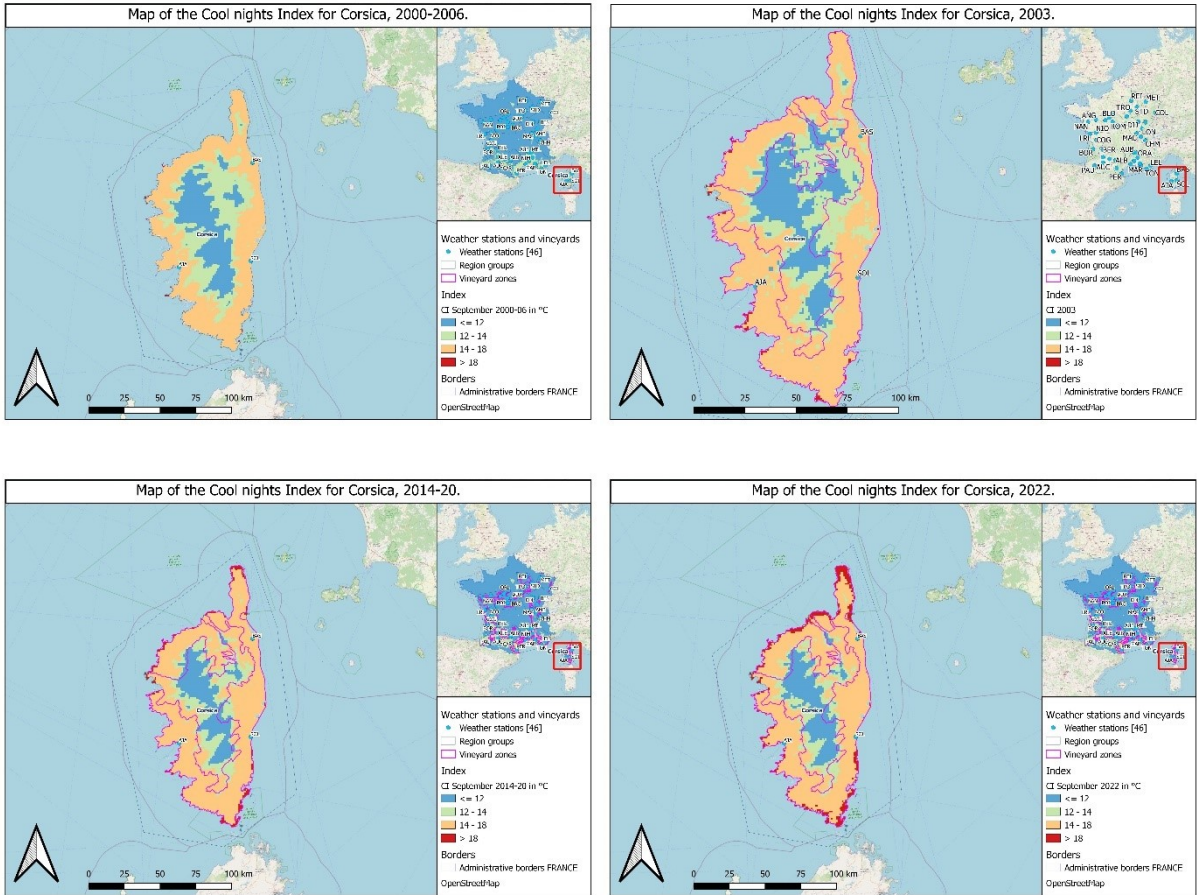
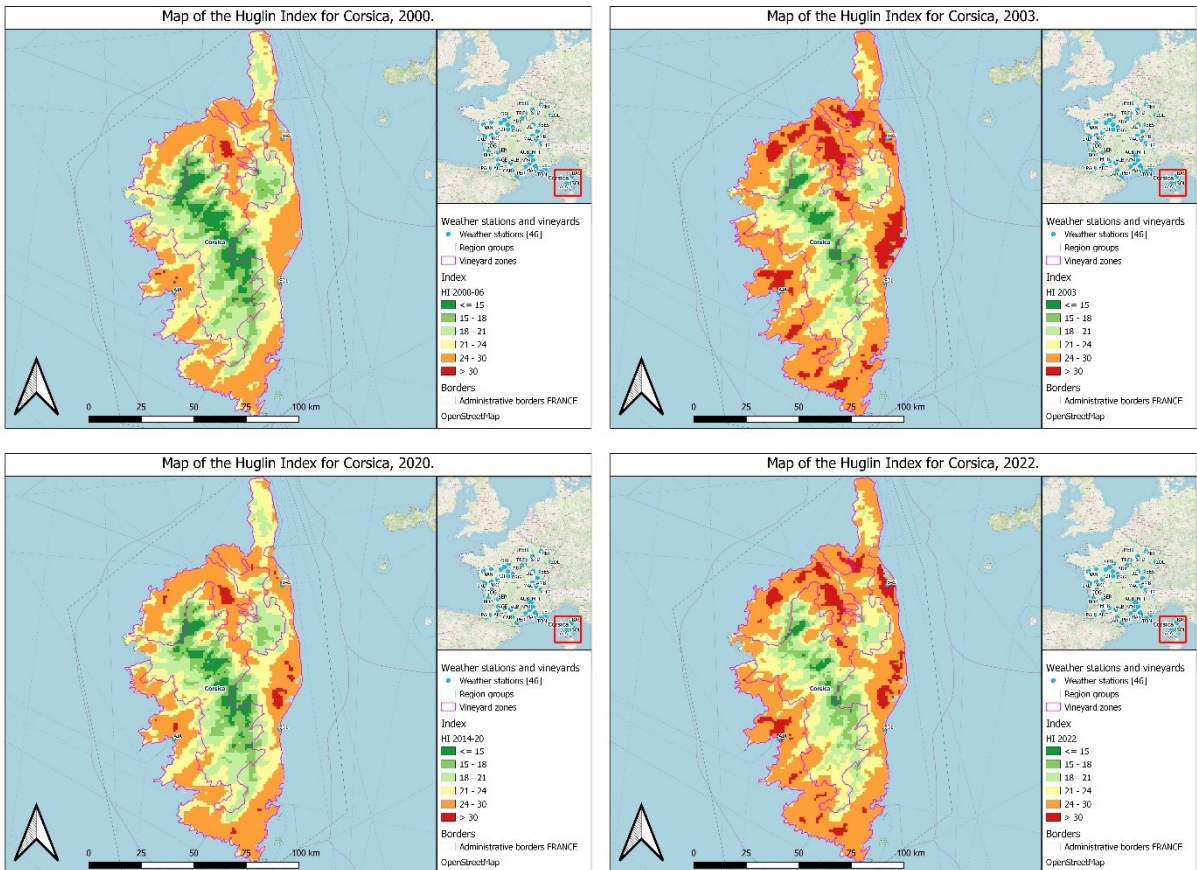


Figure 7 Corsica Cool Nights Index



3.2.1.3. Slopegraphs

Within Corsica, our limited dataset with only three spatial data points may not seem relevant enough, but if we keep in mind that our aim is a national scale assessment and the island's limited vineyards size, it aligns with our overall spatial resolution. We added the regression lines for every city to our precipitation and temperature graphs to better discern the region's PT or TX trends over the years.

The similarity of PT trends among different cities in May, July, and September shows that they are consistent whether they increase, decrease, or stay constant. Deviations from the main pattern are observed in June and August charts. The trends over the months of April, June and August are less similar, some increase while others decrease or stay constant, but these variations remain modest, the greatest fluctuation being an increase in PT that didn't exceed 30 mm of difference over the 21-year span, at Ajaccio (AJA) in June. The sharp spikes in precipitation are outliers, for example, the episode in Solenzara in September 2006 is the result of a freak storm event where 465 mm of rain fell in two days (*Pluies Diluviennes Sur Le Languedoc et La Corse - Pluies Extrêmes En France Métropolitaine*, n.d.).

In accordance with these visual observations, none of the p-values calculated from the regression coefficients of the stations in Corsica are significant, as they are all over the 0.05 threshold. We can thus conclude that the changes in total precipitation in Corsica hasn't been significant from the years 2000 to 2020.

Regarding maximum temperature (TX) slopegraphs, we see the values are somewhat aligned between cities over the years, especially in May. Their regression lines however show that the trend for TX is clearly increasing, and the city trends are either parallel to each other or converge. The only slightly decreasing trend, in May, is of less than 0.5°C, against an increase of 1.5°C in April and September for all three cities, and almost 2°C for Ajaccio (AJA) in July. The p-values calculated for these trends are significant in the months of April and September for the three cities of Ajaccio, Bastia and Solenzara (AJA, BAS, and SOL on the maps), as well as for Ajaccio in July. We can thus conclude that there has been a significant increase in maximum temperatures in Corsica from 2000 to 2020 for the months of April, September, and July for the western side of Corsica, highlighted in blue on the p-value table (see Table 7 Regression coefficients PT and TX with p-values for Corsica).

Month	Stations	Regression Coeffs PT	p.value PT	Regression Coeffs TX	p.value TX
April	AJA	-0.257	0.823	0.0800	0.00549
April	BAS	-0.309	0.797	0.0669	0.0197

April	SOL	-1.92	0.345	0.0692	0.00714
May	AJA	1.03	0.669	-0.0316	0.508
May	BAS	0.953	0.588	-0.0378	0.410
May	SOL	0.674	0.743	-0.0403	0.384
June	AJA	1.46	0.106	0.0129	0.768
June	BAS	-0.720	0.555	0.000909	0.983
June	SOL	-0.552	0.275	-0.00364	0.924
July	AJA	0.559	0.360	0.0969	0.0265
July	BAS	0.763	0.473	0.0656	0.130
July	SOL	0.284	0.570	0.0327	0.376
August	AJA	-0.700	0.342	0.0756	0.137
August	BAS	0.692	0.352	0.0506	0.276
August	SOL	-1.27	0.127	0.0177	0.654
September	AJA	0.132	0.904	0.0855	0.0232
September	BAS	-0.688	0.710	0.0879	0.00303
September	SOL	-1.67	0.696	0.0644	0.0396

Table 7 Regression coefficients PT and TX with p-values for Corsica

Trends for Corsica

Precipitations and temperatures from April to June

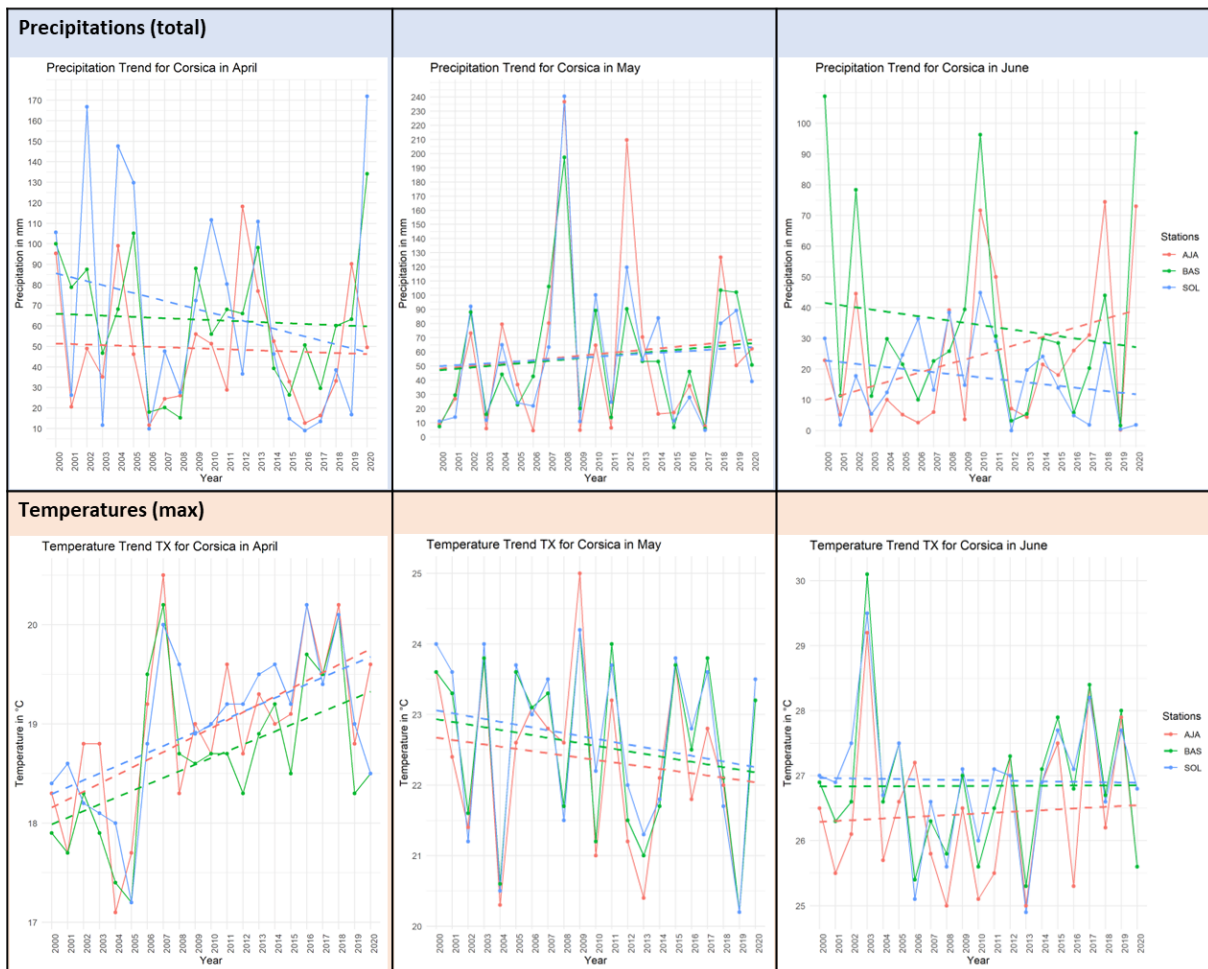


Figure 9 Corsica Precipitation & Temperature Slopegraphs April to June

Trends for Corsica

Precipitations and temperatures from July to September

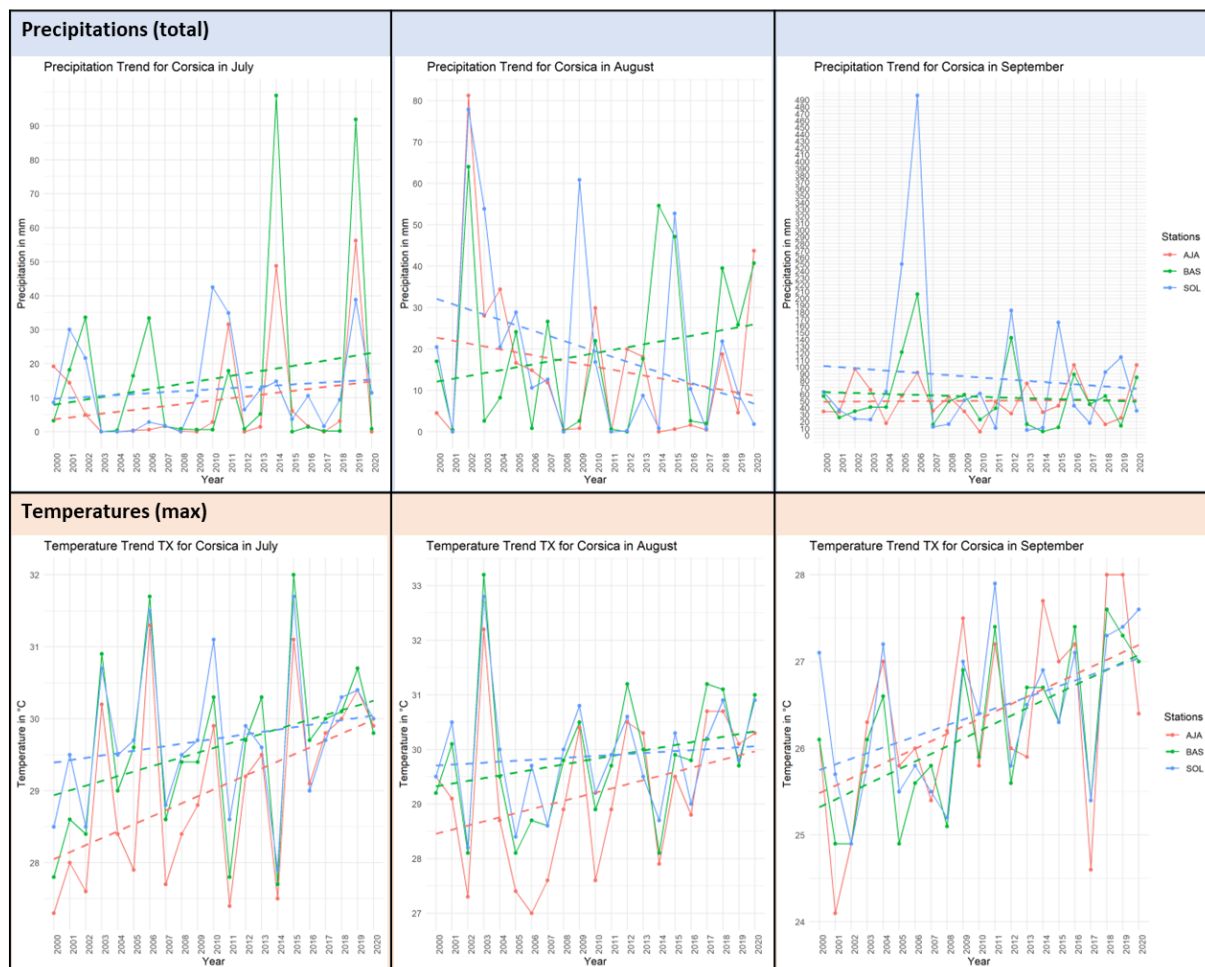


Figure 10 Corsica Precipitation & Temperature Slopegraphs July to September

3.2.2. Méditerranée

3.2.2.1. Géoclimatique Contexte

Situé dans le sud-est de la France, l'aire que nous avons étiquetée Méditerranée est une grande zone composée de la Provence, du Languedoc-Roussillon et d'une partie des Bouches-du-Rhône. Nous les avons regroupés ensemble car leur géographie et leurs conditions climatiques sont très proches, les variétés de raisin sont similaires, les vins produits ont des caractéristiques proches, et ils sont souvent appelés une grande région viticole sur les cartes. L'aire est une plaine bordant la Méditerranée à l'est, délimitée par les Alpes à l'est, et le Massif Central au nord. Les vignes couvrent toute la côte de la ville de Cannes à la frontière espagnole, s'étendant également vers le nord le long du fleuve Rhône et dans la vallée au sud de Lyon.

Les vignes de Méditerranée cultivent historiquement des variétés de raisin qui prospèrent dans le climat méditerranéen chaud, plusieurs d'entre elles sont également cultivées dans la région de Corse. Les plus connues sont :

- For reds: syrah, grenache (red and white), carignan and mourvèdre.
- For whites: muscat, clairette, bourboulenc, maccabeu, white piquepoul, cinsault, sangiovese, sémillon, and white ugni.

Climate-wise, the area beneficiates from a similar buffering influence of the Mediterranean Sea as Corsica, which plays a role in temperature regulation along the coastline, although only up to a certain degree. The region is rich in hills, mountains, and forests, so most viticulture fields are sloped with varying steepness. We add to this geography warm winds from the south (scirocco, marin) and cold ones from the north and west (tramontane, mistral) that often impact the region’s weather, coupled with a Mediterranean climate that brings hot and arid summers with mild winters.

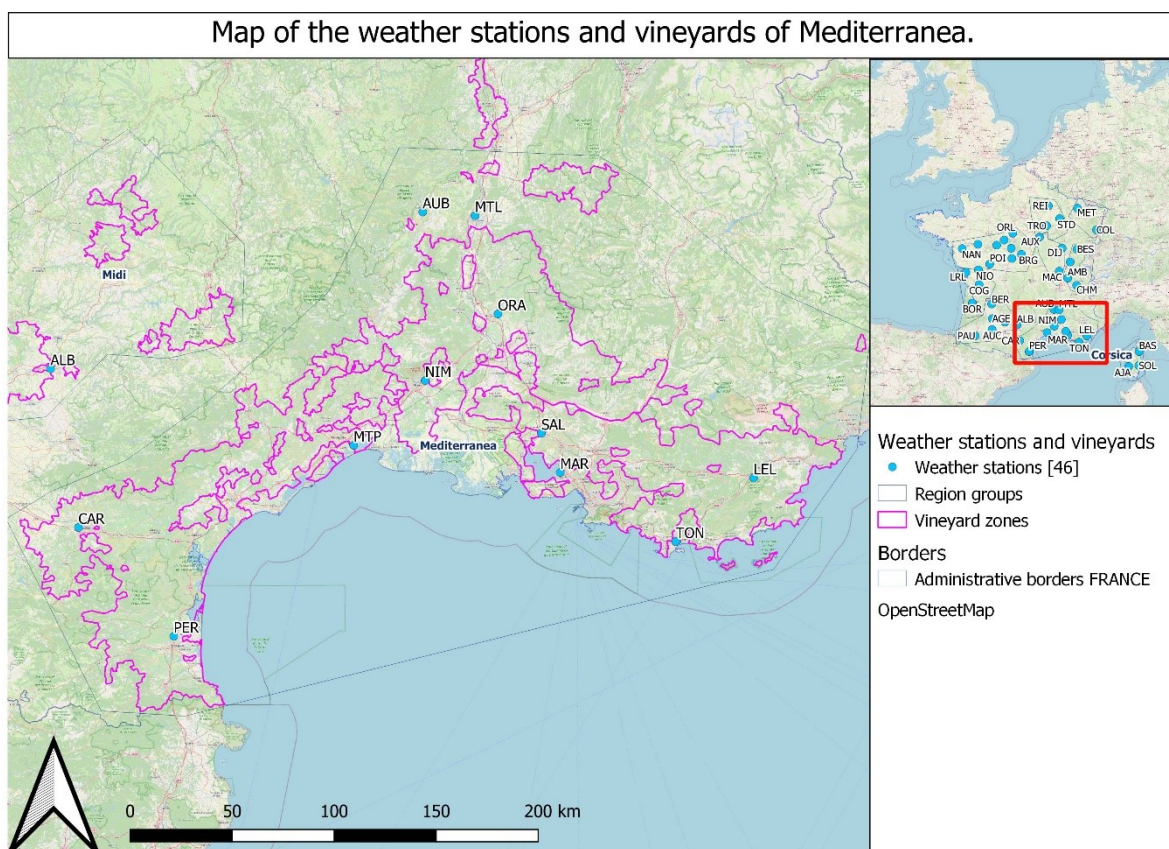


Figure 11 *Mediterranea context*

3.2.2.2. Index Shift Analysis

The AI shows that the coast was already in hyper-arid (+3) conditions in 2000, with the rest of the region in the arid (+2) category. There have been few changes over the past two decades, just an even but slight spreading of hyper-aridity inland from the Golfe du Lion between the Languedoc and Roussillon. However, the heatwaves of 2022 caused a spread of hyper-aridity (+3) over the entire length of the coastline from Spain to Italy, though it didn’t spread inland more than it already had in the other years.

The HI maps contain several changes from 2000 to 2020. The entire zone was already almost entirely in the warm (+2) category in 2000 with some hotspots in the very warm (+3) category near the coast and went colder as we got closer to the mountains. But by 2020, though the warm zones hadn't much changed, the +3 hotspots had gotten much bigger and spanned the entire Languedoc. In 2022, it worsened as the warm zone spread inland into every valley, while the +3 category spread replaced many areas where the orange had previously been, all along the coastline and far inland into both the Rhone and Causses valleys. Must be precised that the +3 category represents values above 3000, but we can't know the exact temperature of the highest points, except that they are above our measure upper limit.

The CI has a somewhat different trend. There has been a gradual warming of night-time temperatures over the years, as the dominant cool (+1) category was overtaken through the years by a rise in the warm (-1) category that spread inland through the Rhone and Causses valleys, indicating a rise in September night temperature averages from 14°C to 16°C. However, the heatwaves of 2022 didn't impact the area's night-time temperatures the same way they did the daytime temperatures. Instead of encroaching further inland, they caused a smoothing of the warm (-1) category areas, indicating uniform temperatures up to 16°C and inducing the disappearance of cold spots in the Languedoc.

As a sidenote, we looked at some hotspots of very warm (-2) category near the coast. These are a result of the warmth from the sea being transferred on the land. The hotspot showing near Marignane (MAR) is the location of a large lake, which remains likewise at a stable warm temperature.

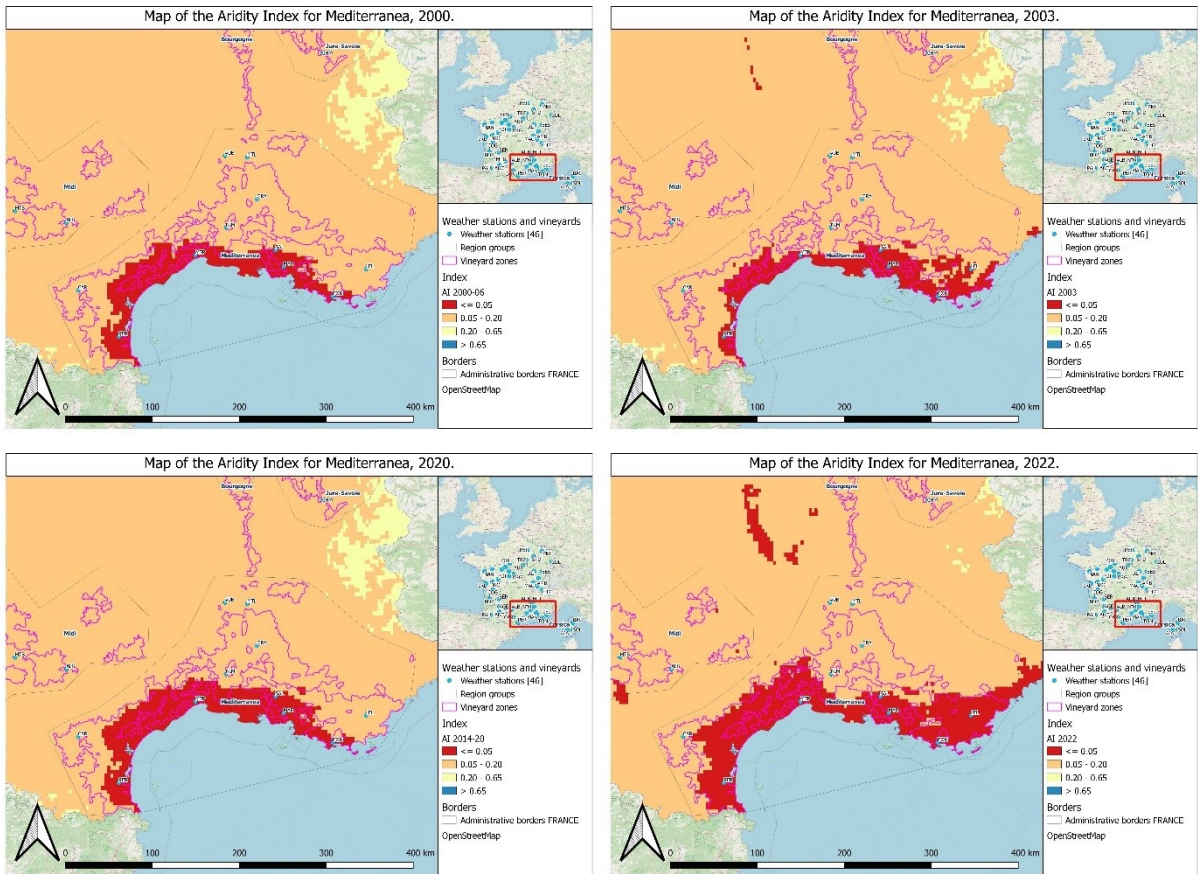


Figure 12 *Mediterranea Aridity Index*

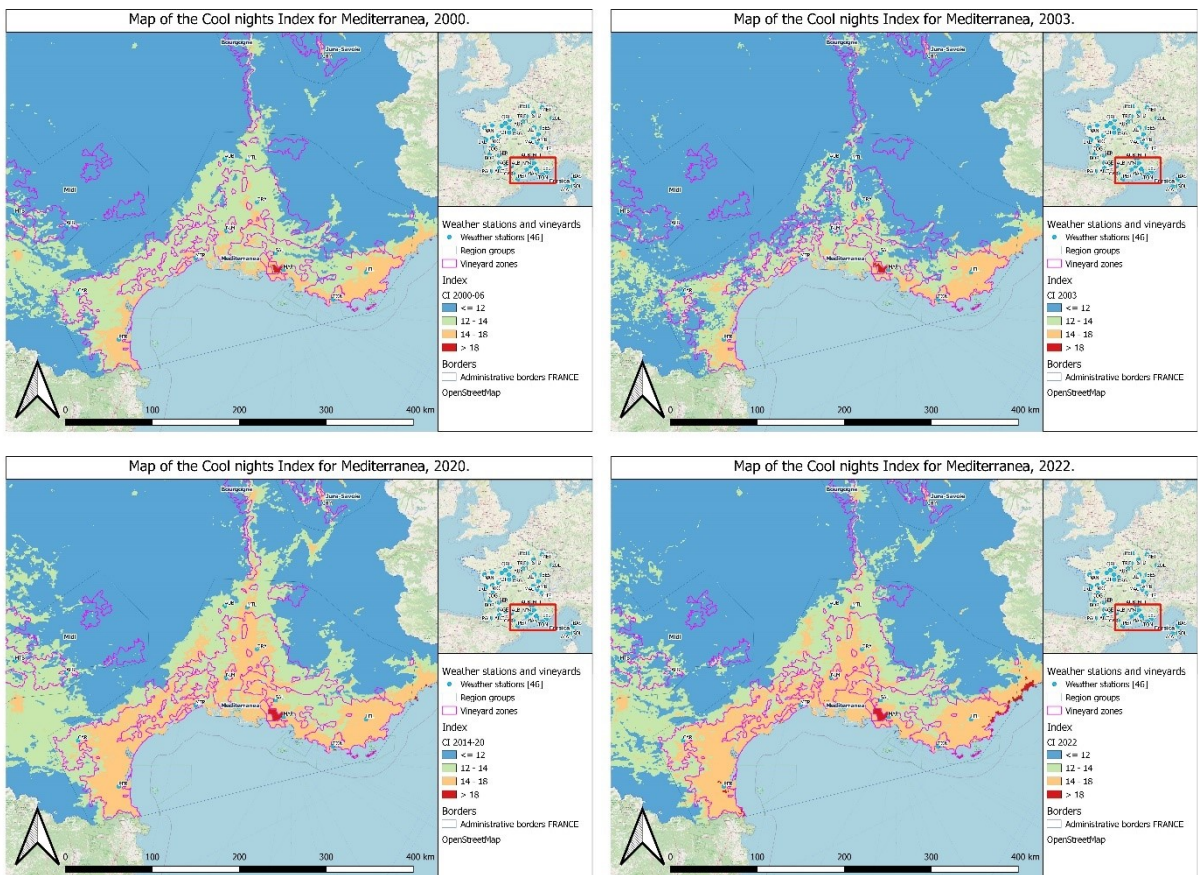


Figure 13 *Mediterranea Cool Nights Index*

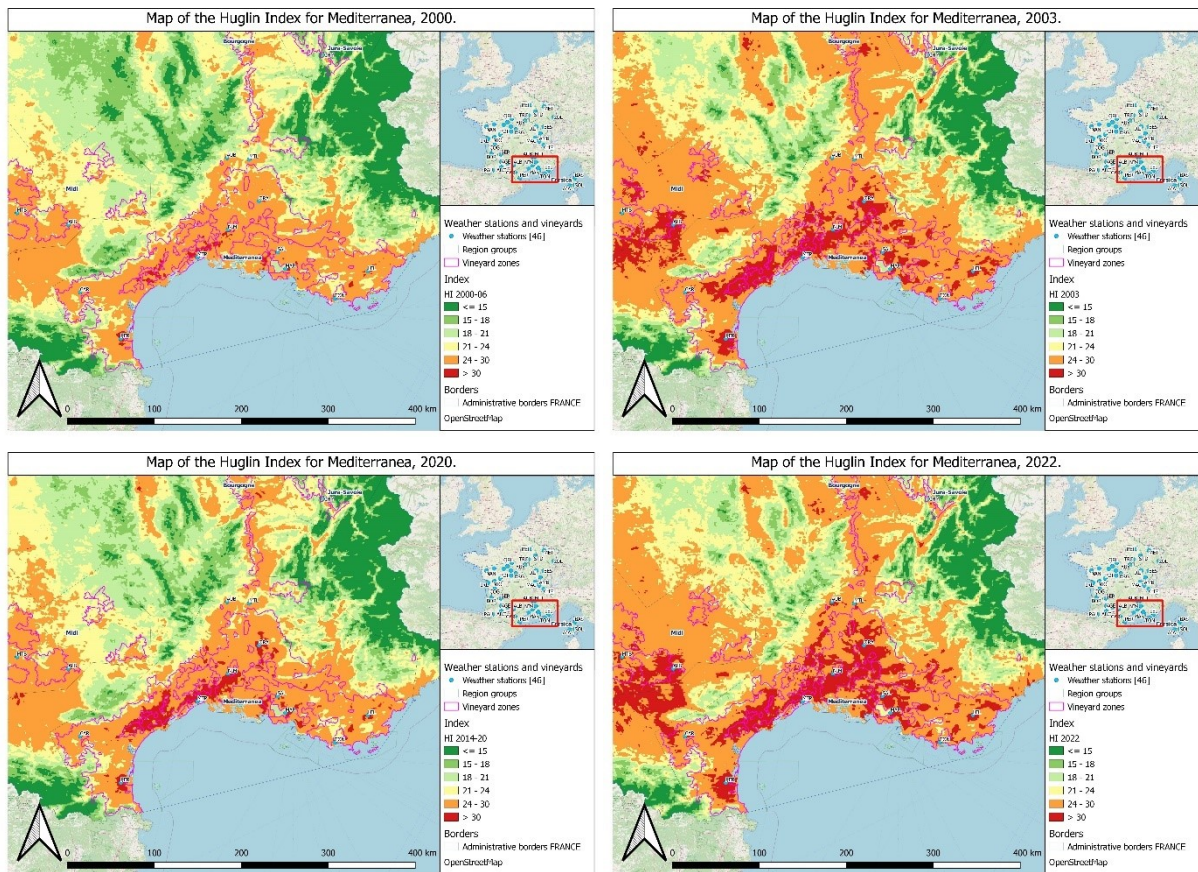


Figure 14 *Mediterranea Huglin Index*

3.2.2.3. Slopegraphs

The slopegraphs we made for the *Mediterranea* region include 11 spatial data points, that span the entire area's coast and extend north along the Rhone. This allows us to be more precise and better detect any local shifts in precipitation or temperature maximums.

The precipitation graphs of the *Mediterranea* area show scattered values over the 6 months of our study, and they tend to have either high or low values over the years without passing by a middle-ground. However, they still form and follow a recognisable pattern, as an indicator of drier and wetter years.

In some of the charts, we observe outliers with very high precipitation values for a single city: these are the results of Mediterranean episodes, an event common in the region where clouds formed above the sea are pushed to the mountains by a warm wind to accumulate there until hit by a cold northern wind, where they will condensate and cause an extreme amount of precipitation to fall in a very short time, on a very localised area. We consider a rainfall as a Mediterranean event when it falls over 200mm of rainfall in a single day, but they are not representative of the normal weather of the region.

Regarding the regression lines, we observe that they nearly overlap and appear mostly constant, with only slight group increases or decreases. Greater variations are found for the cities of Aubenas, Montpellier and Carcassonne (AUB, MTP and CAR on the graphs) in May and July: those are probably because of their location, as they're far more inland than the rest of the cities. When looking at the p-values of the regression coefficients of these graphs, we see only one significant value, a decrease in PT in Orange (ORA) for September. The graph shows a significant decrease in total monthly precipitation of 130 mm in 21 years.

The analysis of TX values results in patterns that overlap but notably increase, especially in the later months of the study period of observation. Regarding the trends illustrated by regression lines, we notice the different cities lines follow each other but are spread apart from around 3°C from lowest to highest. The lines themselves have an increasing trend for April, July, August and September, and stagnate the other two months. We also note that the LEL station seems to be an outlier, as its regression line is very separate from the rest of the cluster, although following in the same direction. Looking at the significant p-values of the regression coefficients, here highlighted in blue, we spot 6 stations in July (AUB, NIM, MAR, TON, MTP and PER) with significant increases going from 2.5°C for TON to 3°C for AUB, which seems to indicate a significant warming trend in the Languedoc region and along the coast. In September, we have a similar result, with all the stations of the area except for LEL bearing significant p-values, and the trends increasing of around 2.5°C in 21 years. We can conclude from this analysis that the warming trend in September is significant over all the region except in eastern Provence.

Month	Stations	Regression Coeffs PT	p.value PT	Regression Coeffs TX	p.value TX
April	AUB	0.165	0.910	0.0977	0.157
April	CAR	-0.592	0.629	0.0832	0.141
April	LEL	0.106	0.939	0.0687	0.121
April	MAR	-0.208	0.843	0.0416	0.340
April	MTL	-0.421	0.790	0.0916	0.143
April	MTP	-0.108	0.937	0.0443	0.310
April	NIM	0.395	0.762	0.0718	0.208
April	ORA	-0.263	0.830	0.0582	0.310
April	PER	0.652	0.810	0.0631	0.143
April	SAL	-0.473	0.683	0.0488	0.288
April	TON	-0.276	0.793	0.0913	0.0558
May	AUB	1.05	0.611	-0.0294	0.637
May	CAR	1.61	0.155	-0.0166	0.755
May	LEL	0.838	0.662	-0.0375	0.472
May	MAR	-1.18	0.304	-0.0170	0.756
May	MTL	0.144	0.938	-0.0475	0.458
May	MTP	-0.687	0.557	0.0138	0.723
May	NIM	-1.14	0.476	0.00377	0.943

May	ORA	-0.816	0.593	-0.0423	0.480
May	PER	-1.39	0.243	0.0134	0.768
May	SAL	-0.956	0.379	-0.0183	0.746
May	TON	0.194	0.886	0.0277	0.508
June	AUB	1.06	0.397	-0.0101	0.874
June	CAR	-0.719	0.319	-0.0235	0.719
June	LEL	0.846	0.739	-0.0312	0.549
June	MAR	0.519	0.618	-0.000779	0.987
June	MTL	0.728	0.459	-0.0105	0.873
June	MTP	0.45	0.580	-0.00325	0.934
June	NIM	-0.0506	0.964	0.0165	0.771
June	ORA	0.444	0.600	-0.00247	0.968
June	PER	0.281	0.668	0.0173	0.706
June	SAL	1.72	0.128	-0.00922	0.858
June	TON	0.467	0.621	0.0199	0.692
July	AUB	0.373	0.812	0.147	0.0473
July	CAR	0.524	0.562	0.0856	0.221
July	LEL	-0.0510	0.938	0.103	0.0694
July	MAR	0.00597	0.994	0.110	0.0403
July	MTL	-1.05	0.486	0.126	0.0821
July	MTP	-0.403	0.607	0.120	0.0146
July	NIM	-1.38	0.283	0.150	0.0295
July	ORA	-1.76	0.151	0.126	0.0826
July	PER	0.551	0.286	0.114	0.0449
July	SAL	-0.106	0.875	0.105	0.0594
July	TON	-0.141	0.681	0.128	0.0111
August	AUB	-1.39	0.391	0.0870	0.267
August	CAR	-0.483	0.585	0.0701	0.332
August	LEL	0.0503	0.951	0.0577	0.280
August	MAR	0.663	0.519	0.0605	0.233
August	MTL	-0.842	0.654	0.0706	0.380
August	MTP	1.00	0.595	0.0547	0.210
August	NIM	-1.90	0.274	0.0862	0.176
August	ORA	0.381	0.759	0.0494	0.494
August	PER	-0.394	0.666	0.0640	0.233
August	SAL	0.268	0.796	0.0438	0.435
August	TON	0.522	0.397	0.0862	0.558
September	AUB	-2.98	0.346	0.163	0.00796
September	CAR	0.756	0.473	0.115	0.0179
September	LEL	-1.42	0.475	0.0813	0.0607
September	MAR	-3.56	0.0995	0.111	0.0207
September	MTL	-2.23	0.405	0.144	0.0244
September	MTP	-5.59	0.102	0.110	0.0101
September	NIM	-4.84	0.0964	0.168	0.0215
September	ORA	-6.71	0.0371	0.146	0.0134
September	PER	1.57	0.0869	0.107	0.0191
September	SAL	-2.58	0.0799	0.121	0.0173
September	TON	-1.97	0.344	0.101	0.0225

Table 8 Regression coefficients PT and TX with p-values for *Mediterranea*

Trends for Mediterranean

Precipitations and temperatures from April to June

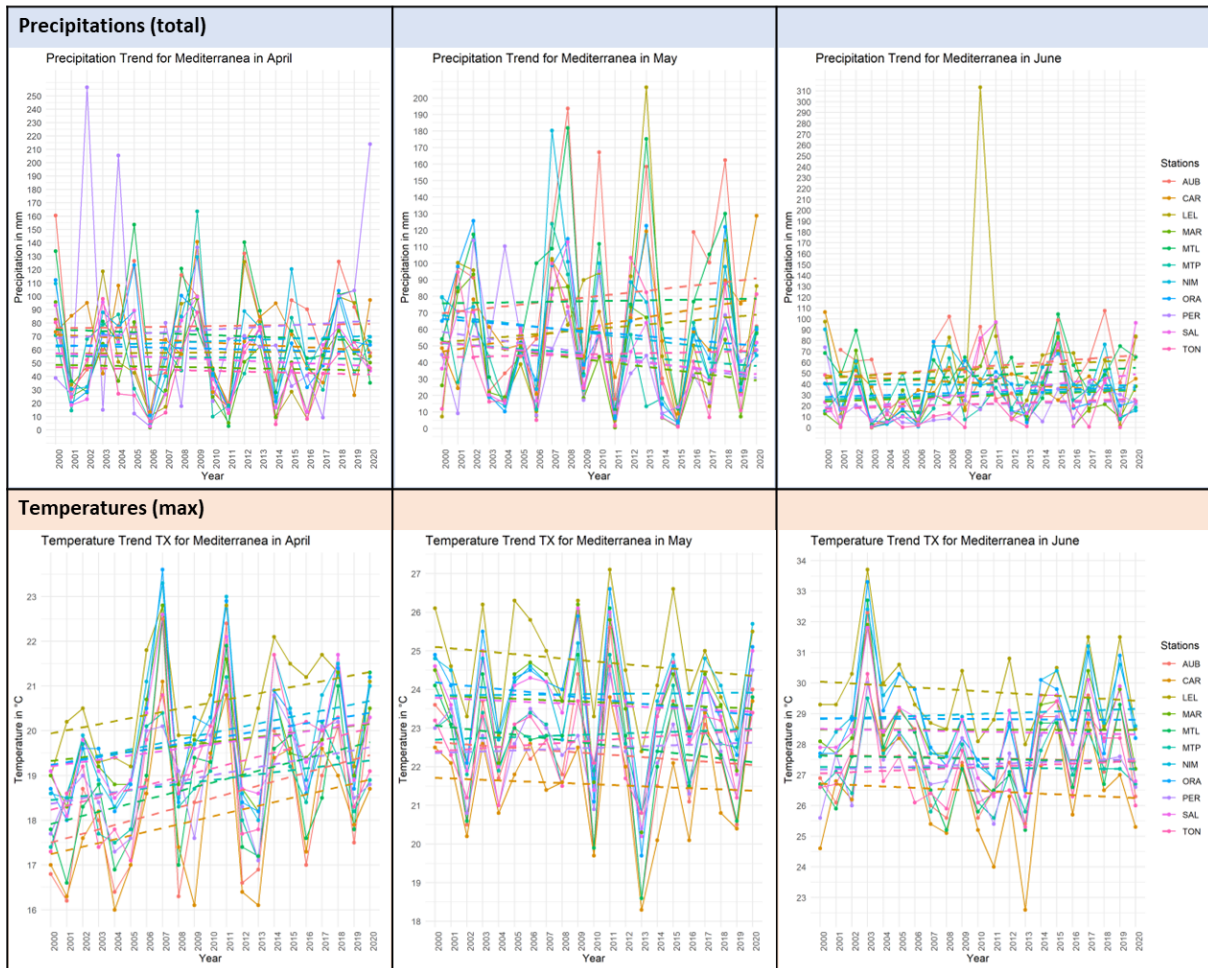


Figure 15 Mediterranean Precipitation & Temperature Slopegraphs April to June

Trends for Mediterraneana

Precipitations and temperatures from July to September

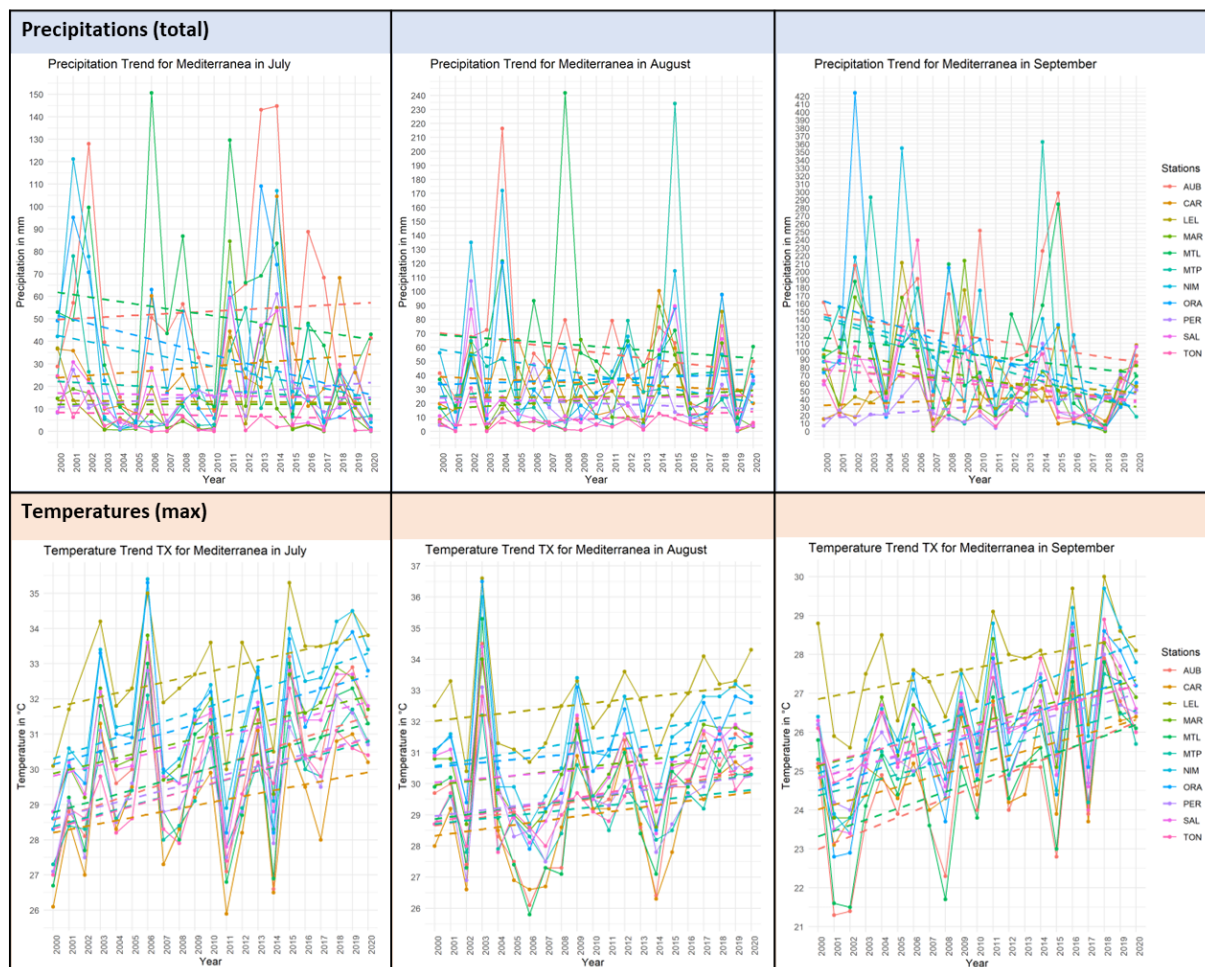


Figure 16 Mediterraneana Precipitation & Temperature Slopegraphs July to September

3.2.3. Midi

3.2.3.1. Geoclimatical Context

The area labelled Midi straddles two regions called Midi-Pyrénées and Aquitaine, and delineates the Sud-Ouest (or South-West) vineyard area. Located to the west of the Mediterranean area we've previously seen, it's bordered by the Massif Central to the northeast, and leads to another great vineyard region to the northwest. The climate is oceanic and remains as such far inland, for most of the area is composed of flat plains and gently sloped hills that enable the rapid advance and spread of air masses from the Atlantic, either from depressions or anticyclones, and so makes this part of the country very exposed to weather extremes. The area near Pau (PAU) is prone to flooding, as it has a low elevation. The gap of the Causses linking the Mediterranean area to the Midi also facilitates the circulation of warm winds from the

Mediterranean Sea. These traits contribute to facilitating extreme temperature events near the center of the basin.

The vineyards are in the southern part of the Aquitaine basin fronting the Atlantic. Because of the size of the available area and fair climate, viticulture in the area is alternated with other agricultural land-uses such as the culture of wheat, maize, and sunflower, as well as cattle rearing. Midi's vineyards house a great diversity of grape varieties, mostly:

- For red wines: cabernet sauvignon, cabernet franc, malbec, tannat, black jurançon.
- For white wines: big manseng, small manseng, mauzac, sauvignon, and arruffiac.

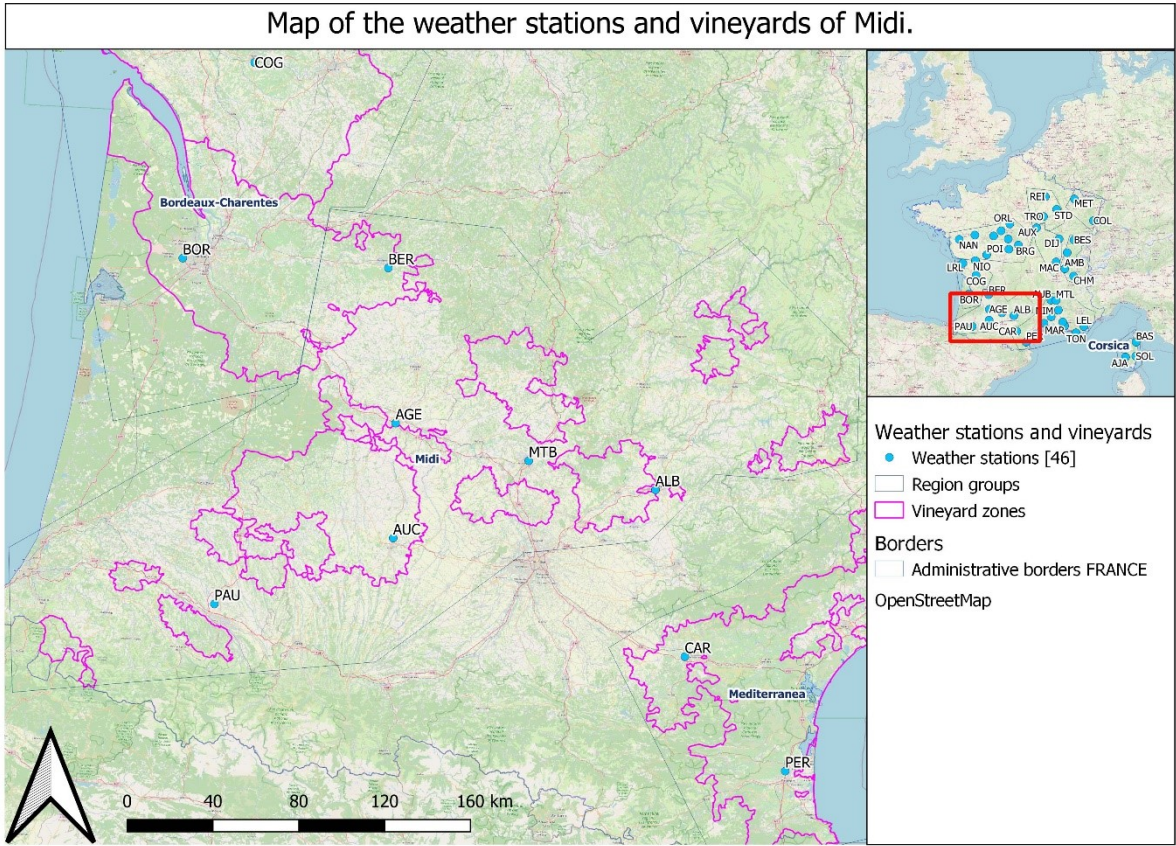


Figure 17 Midi context

3.2.3.2. Index Shift Analysis

With our maps, we see the entire area is firmly in the arid (+2) category of the AI, and we only note a lack of any significant changes over the last two decades. Even the heatwaves in 2003 and 2022 didn't cause any significant changes, though we observe a few hotspots that transitioned from arid to hyper-arid (+3) conditions in some places. These correspond to the city centers of Toulouse, Millau and Espalion and so can be considered outliers.

Regarding the HI, we found that in 2000, the area was predominantly in the warm-temperate (+1) category and edging into the temperate (-1) category towards the mountains. It has since advanced into the next up category because of the spreading warmth in the plains. By 2020, more than half of the vineyard area was in the warm (+2) category though the areas that had been in the temperate (-1) categories in 2000 remained mostly untouched. In 2003 like in 2022 however, the entire area went orange from the impact of the heatwaves, while a large zone between Agen, Auch and Albi (AGE, AUC and ALB) had gone in the red, very warm (+3) category. The behaviour of the temperature map alerts us that the changing conditions can spread all over the area with an extreme ease.

The same way, we saw in the CI maps the influence of CC on the nights of September over the years: over the span of 20 years, there has been a substantial warming of the average September nighttime temperatures across most of the area. The CI shifted from a predominantly +2 (very cool) state with only the middle of the plain and a minor part of the vineyard surface in the cool (+1) category to a widespread +1 (cool) temperature that included almost all the vineyard surface area. This transition reflecting a change from $\leq 12^{\circ}\text{C}$ to temperatures up to 14°C on the regional scale. This worrying pattern however was not impacted negatively by the 2003 heatwave, for which the area stayed almost entirely in the very cool (+2) category, but the 2022 heatwave brought about a parcelling of the area in the cool (+1) category with the very cool (+2) one. The spread of the affected area on the other hand remained just as large as it was in 2020.

In summary, since the turn of the century the shifts in aridity and temperature patterns in this area have had consequent repercussions on daily and nightly temperature norms, which has a high probability to influence the methods and strategies employed in viticulture within the area in the long term.

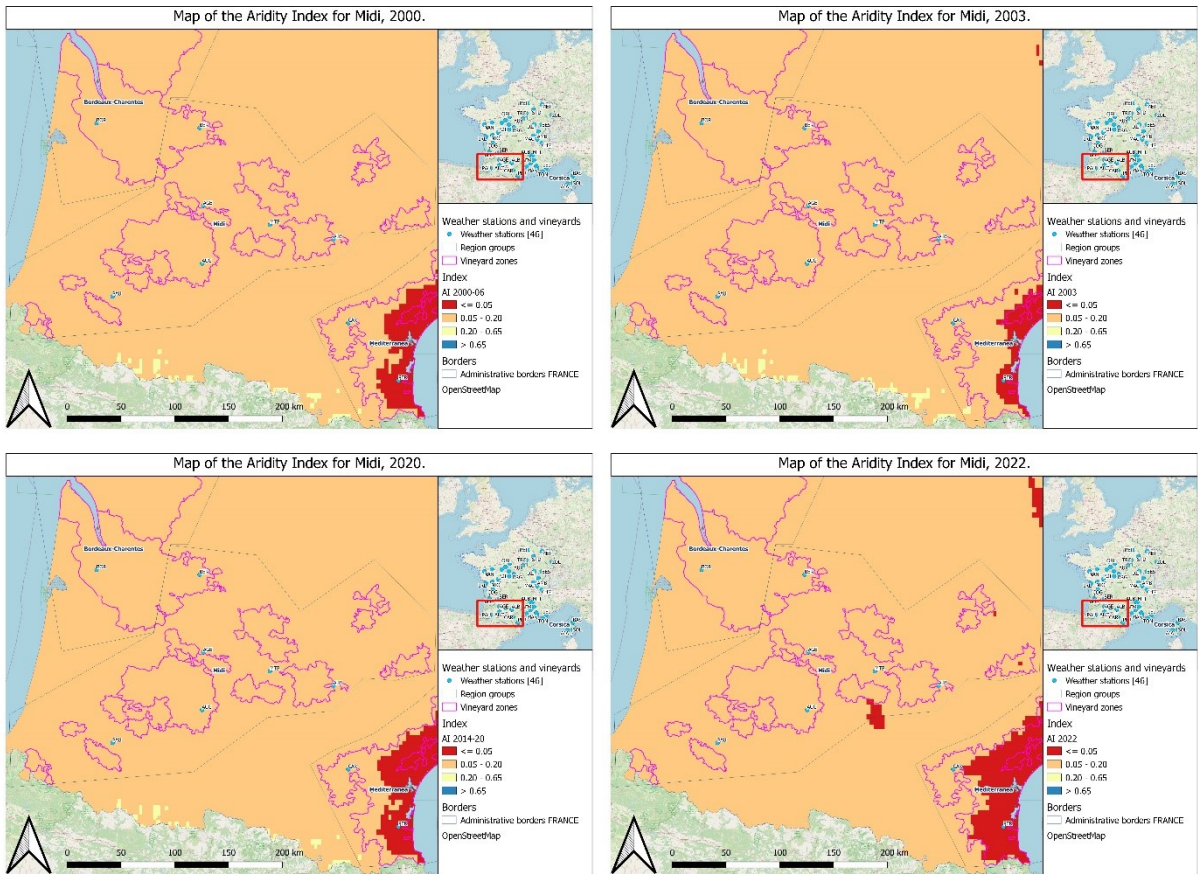


Figure 18 Midi Aridity Index

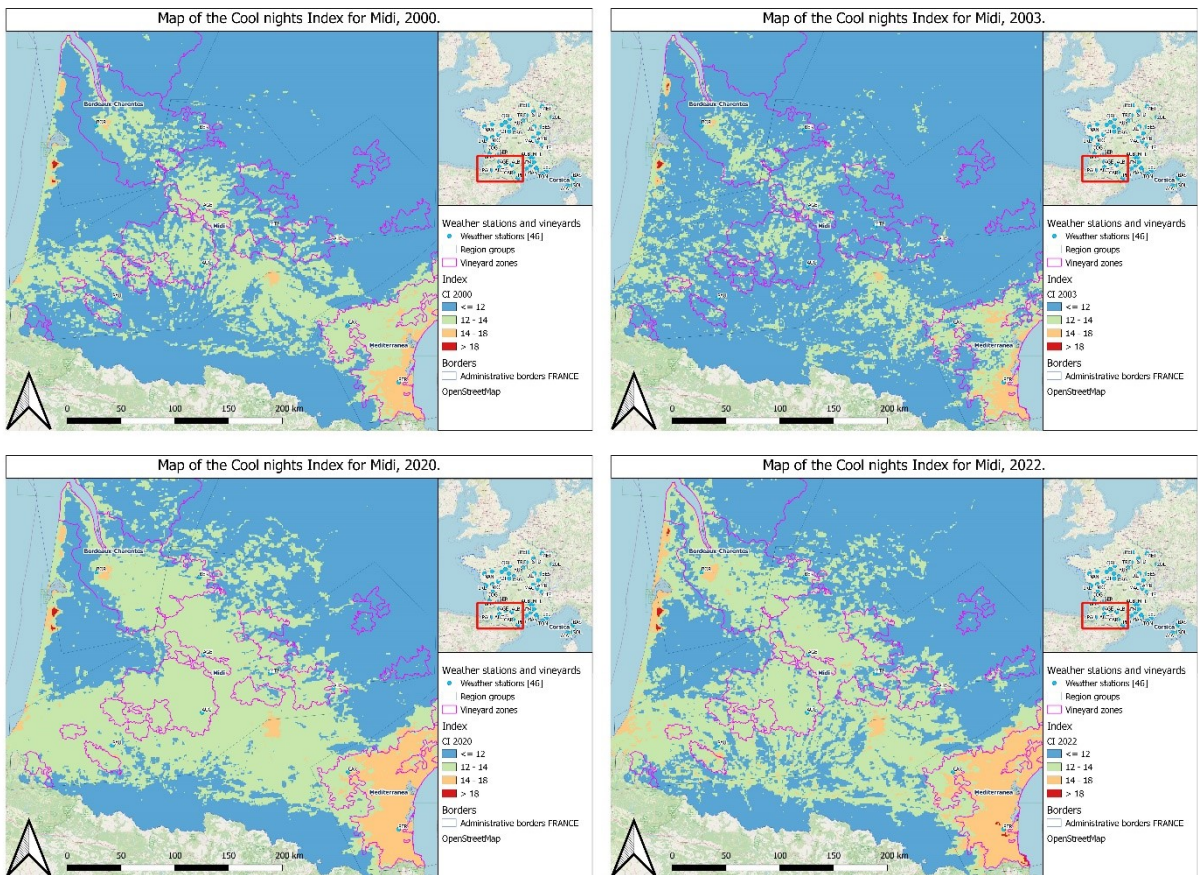


Figure 19: Midi Cool Nights Index

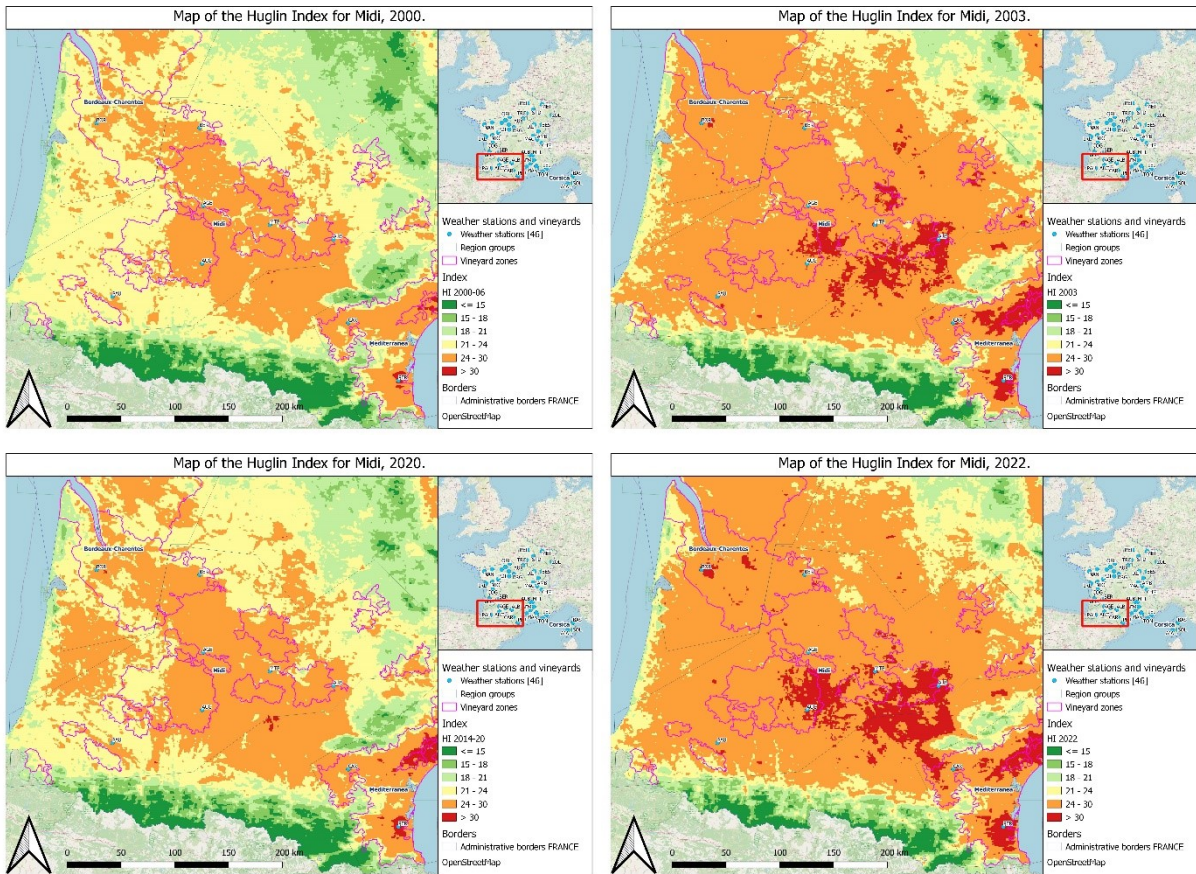


Figure 20 Midi Huglin Index

3.2.3.3. Slopegraphs

In the Midi, we have readings from 6 weather stations. They are spread rather evenly from each other and cover most of the area, apart from the easternmost zone, which is mainly at the foot of the Massif Central mountain range.

Regarding PT values, we noted they reach extremes in some years, especially for April and May where they have collectively gone over 150 mm in some years. The regression lines we have calculated from these values reveal a steady and constant trend for most cities in all months. They also indicate some cities like Pau and Bergerac (PAU and BER) are removed from the cluster formed by the other cities and deviate somewhat from the direction they follow.

The p-values extracted from the regression coefficients of these graphs, here highlighted in blue, indicate that in June, the 3 cities of Agen, Bergerac and Montauban (AGE, BER, and MTB) saw a significant increase in PT. It shows that the north of the area has been seen a significant increase in precipitation from 2000 to 2020, which has provoked several floods over large surfaces, due in no small part to the flatness of the terrain.

In contrast, the TX values of our slopegraphs almost overlap on both high and low values. The only outlier to this pattern is Pau (PAU), which follows it an average of 1°C under the rest of

the cities. The regression lines generated from these graphs show an increase in maximum temperatures of 1.5°C in July and August, and 2°C in April and September. These trends are also followed by the outlier.

The calculated p-values however show only one of these values is significant: the city of Bergerac (BER) in July, where the trend increases of 3°C in our 21 years timeframe. This deviation from the norm on only one city means it's probably part of a bigger phenomenon up north.

Month	Stations	Regression Coeffs PT	p.value PT	Regression Coeffs TX	p.value TX
April	AGE	-0.446	0.753	0.0916	0.172
April	ALB	0.0725	0.965	0.0996	0.146
April	AUC	-0.215	0.818	0.107	0.0949
April	BER	-1.28	0.398	0.126	0.0974
April	MTB	0.911	0.555	0.126	0.0682
April	PAU	-0.554	0.729	0.106	0.0864
May	AGE	-0.221	0.845	-0.00442	0.942
May	ALB	0.984	0.397	-0.0132	0.836
May	AUC	0.891	0.464	-0.00273	0.965
May	BER	-0.0253	0.984	0.0260	0.675
May	MTB	2.20	0.120	0.0125	0.842
May	PAU	1.87	0.309	-0.00208	0.976
June	AGE	2.05	0.0355	-0.0457	0.495
June	ALB	-0.739	0.456	-0.0547	0.466
June	AUC	-0.846	0.361	-0.0236	0.734
June	BER	2.10	0.0165	-0.0435	0.480
June	MTB	2.35	0.0382	-0.0781	0.260
June	PAU	2.46	0.0845	-0.0465	0.435
July	AGE	-0.657	0.447	0.102	0.133
July	ALB	0.397	0.713	0.0940	0.219
July	AUC	-0.952	0.386	0.101	0.144
July	BER	-2.01	0.187	0.143	0.0337
July	MTB	0.840	0.499	0.0662	0.326
July	PAU	0.167	0.880	0.0700	0.230
August	AGE	0.149	0.879	0.0514	0.437
August	ALB	-0.469	0.585	0.0729	0.367
August	AUC	-0.344	0.740	0.0639	0.391
August	BER	-1.06	0.321	0.0812	0.281
August	MTB	-0.273	0.811	0.0513	0.492
August	PAU	0.354	0.737	0.0491	0.461
September	AGE	-0.659	0.514	0.0862	0.151
September	ALB	-0.592	0.534	0.0843	0.155
September	AUC	-0.258	0.766	0.0825	0.159
September	BER	0.764	0.416	0.115	0.0585
September	MTB	0.364	0.733	0.109	0.0769
September	PAU	0.0621	0.961	0.0717	0.203

Table 9 Regression coefficients PT and TX with p-values for Midi

Trends for Midi

Precipitations and temperatures from April to June

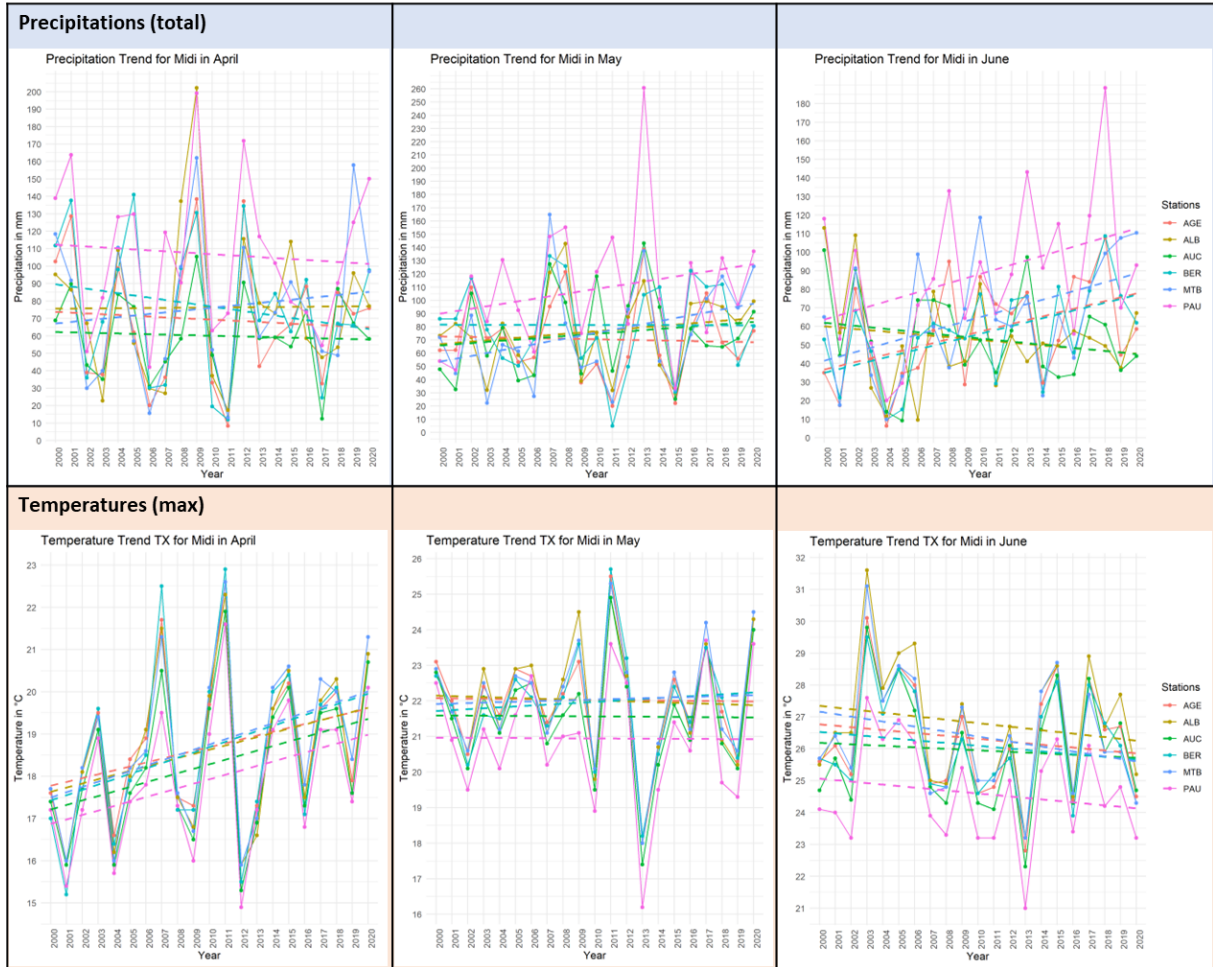


Figure 21 Midi Precipitation & Temperature Slopegraphs April to June

Trends for Midi

Precipitations and temperatures from July to September

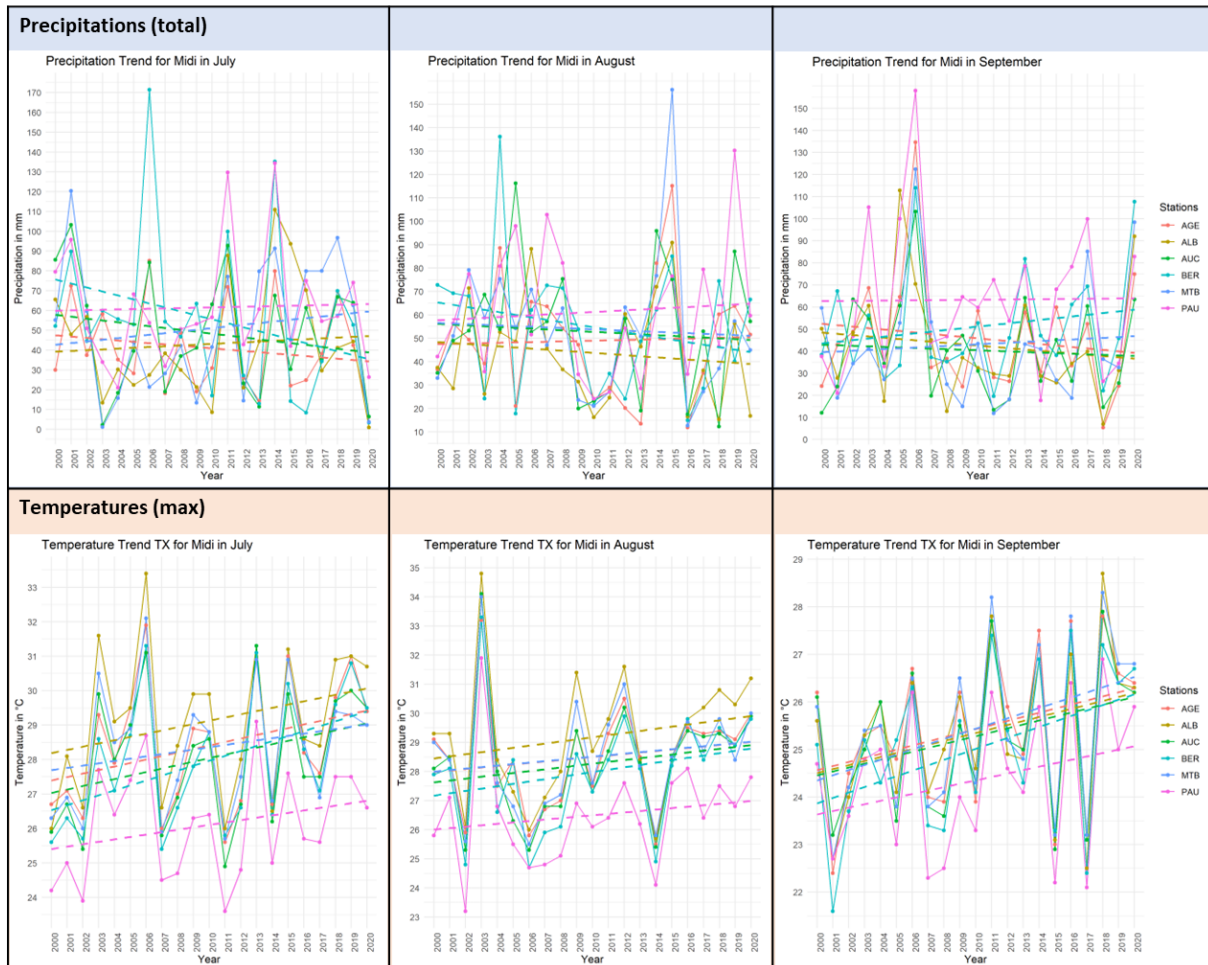


Figure 22 Midi Precipitation & Temperature Slopegraphs July to September

3.2.4. Bordeaux

3.2.4.1. Geoclimatical Context

We named our area Bordeaux-Charentes here, after the two departments it encompasses, the Bordelais and Charentais. It's set on the north side of the Aquitaine basin, facing the Atlantic on the west front, the Massif Central to the east, the Poitevin wetlands to the north and the Loire to the Northeast. Its vineyard is very densely packed in the Bordelais, where the two rivers Garonne and Dordogne cross the region to finish their course in the estuary at Bordeaux. The area's climate is oceanic, with much the same conditions as the Midi. Its closeness to Britain and higher latitude impacts the northern side of the area, as that part of France is famously very rainy. The proximity to the Atlantic Ocean also exposes the vineyards to cold ocean winds and coastal fogs that contribute to climate regulation. This set of climatic conditions plays a role in cultivating several famous grape varieties, that include:

- For reds: merlot, cabernet sauvignon and cabernet franc.
- For whites: sauvignon, sémillon, and muscadelle.

These grape varieties serve to make some of the most famous wines in the world, like Saint-Emilion’s Château Cheval Blanc, Château Ausone, Château Angélus and Château Pavie as well as the 16 Crus Classés (Classified Growths), from which we find the Domaine de Chevalier, Châteaux Pape Clément, Château Haut-Bailly, Château Smith-Haut-Lafitte or the Château La Mission Haut-Brion.

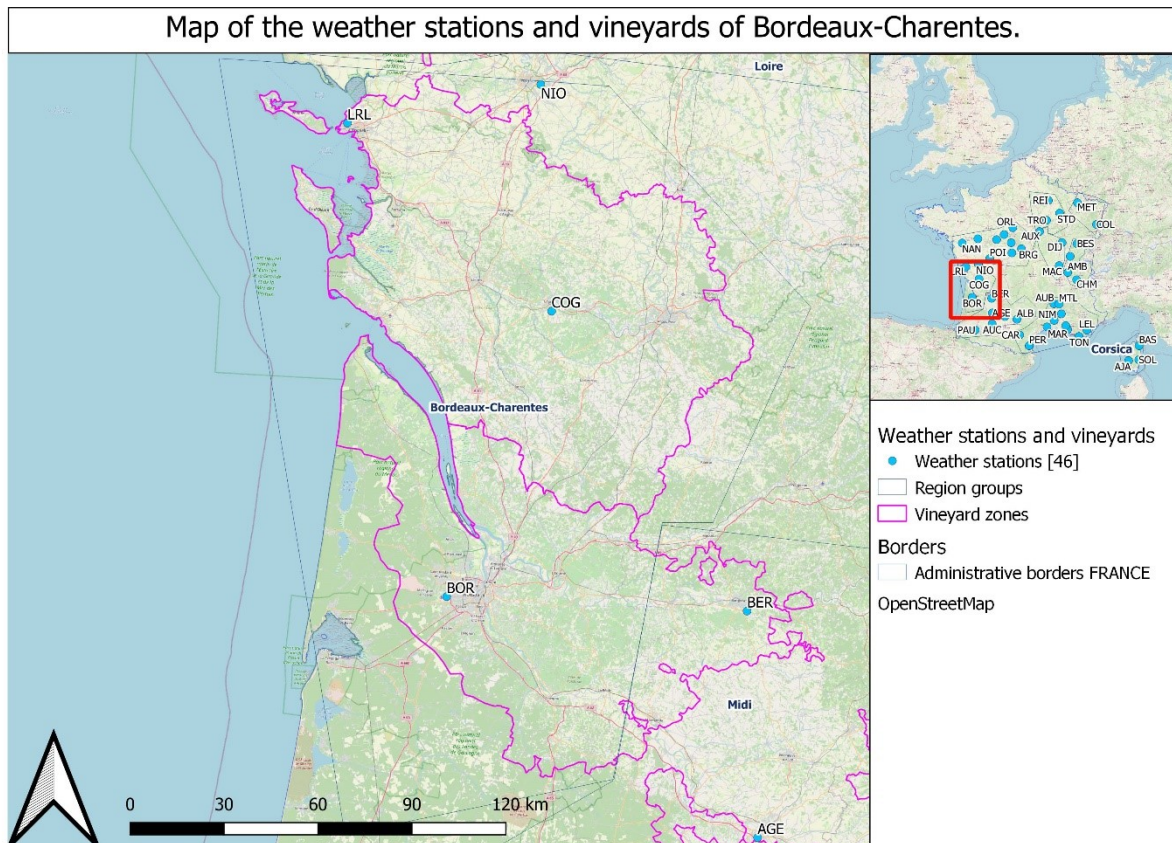


Figure 23 Bordeaux-Charentes context

3.2.4.2. Index Shift Analysis

When assessing the AI for the region, we note there hasn’t been any change during the last 20 years, 2003 and 2022 included, as the area firmly remains in the arid (+1) category. This tells us that the precipitation-evapotranspiration balance of the area is stable, and most likely remains so because of external factors, and given the area’s location, it’s very likely the Atlantic Ocean’s influence allows the region to maintain itself stable on that front.

The HI reveals a similar trend to the one we observed in the Midi region. Namely, the vineyard area that was parcelled equally into warm-temperate (+1) and warm (+2) zones in 2000 has seen the warm (+2) category spread over the last 20 years. This change was accelerated in 2022

because of the heatwaves, which led to the area warming up until the entire region slipped into the +2 category and even some spots reached the very warm (+3) category. We must however note that of the two big spots in the south of the area, only the one to the east is relevant, the other being the city of Bordeaux (BOR) itself. The 2003 heatwaves also caused a temporary shift of the whole region into the orange, with a bit less areas slipping into the red.

While looking at the CI, we realised that the locally cultivated grape varieties were used to much cooler nights than the regions we've previously seen, and that much of the area was in the very cool (+2) category in 2000, with only the sides of the rivers and the coast being a category up into the cool (+1). The blue category of the CI gathers all the temperatures under 12°C, and to have a large area covered in it means the temperatures there could go all the way from just under 12 to the negatives. It isn't very likely this far south but should be kept in mind for the regions more to the north.

By 2020, the half of the Bordelais region that houses the vineyards had shifted to the cool (+1) category everywhere except for the very edges, and these warmer nighttime temperatures were even starting to affect the northern part of the area in the Charentais. The 2003 heatwaves had very little impact on the region's night temperatures. In comparison, the 2022 heatwave's aftereffects saw a great warming of the south of the area while the north side remained under 12°C, back into the very cool (+2) category with the only spots still in +1 category being made by cities.

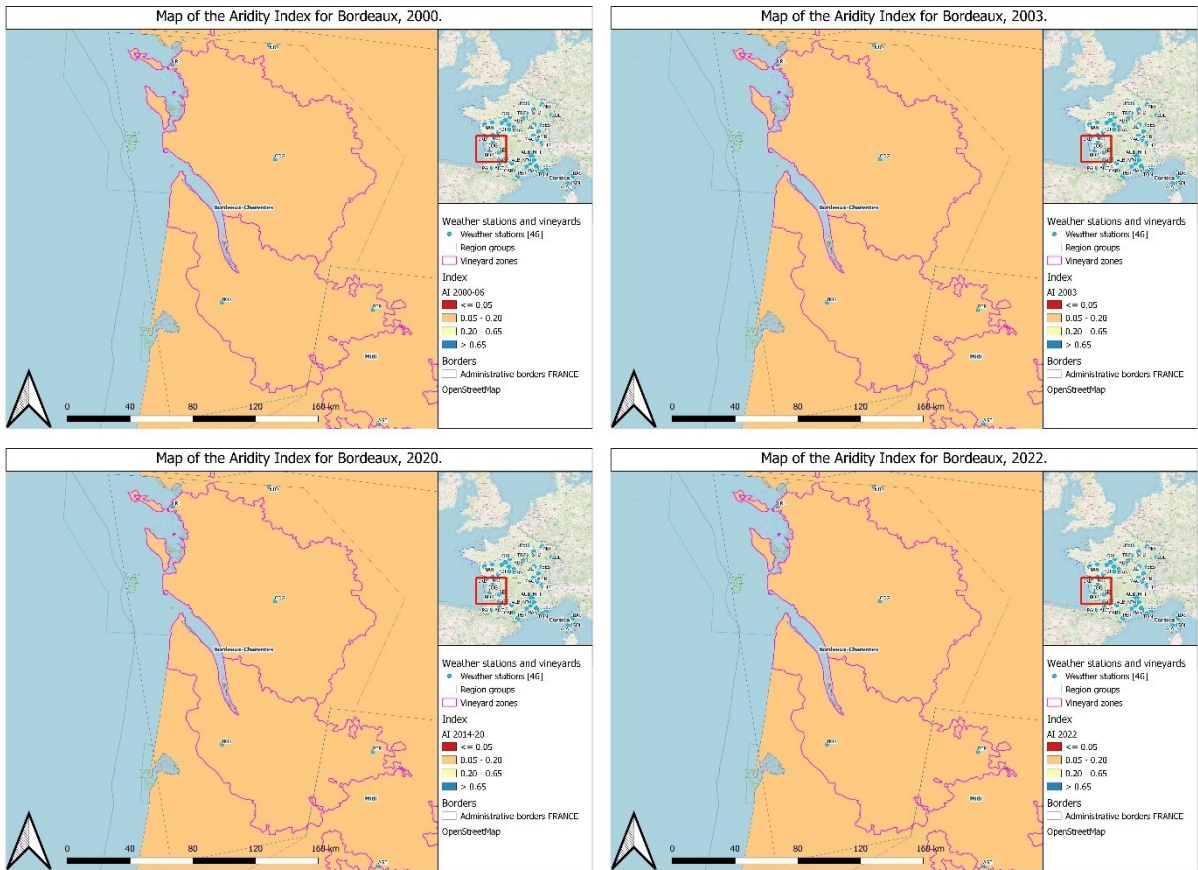


Figure 24 Bordeaux-Charentes Aridity Index

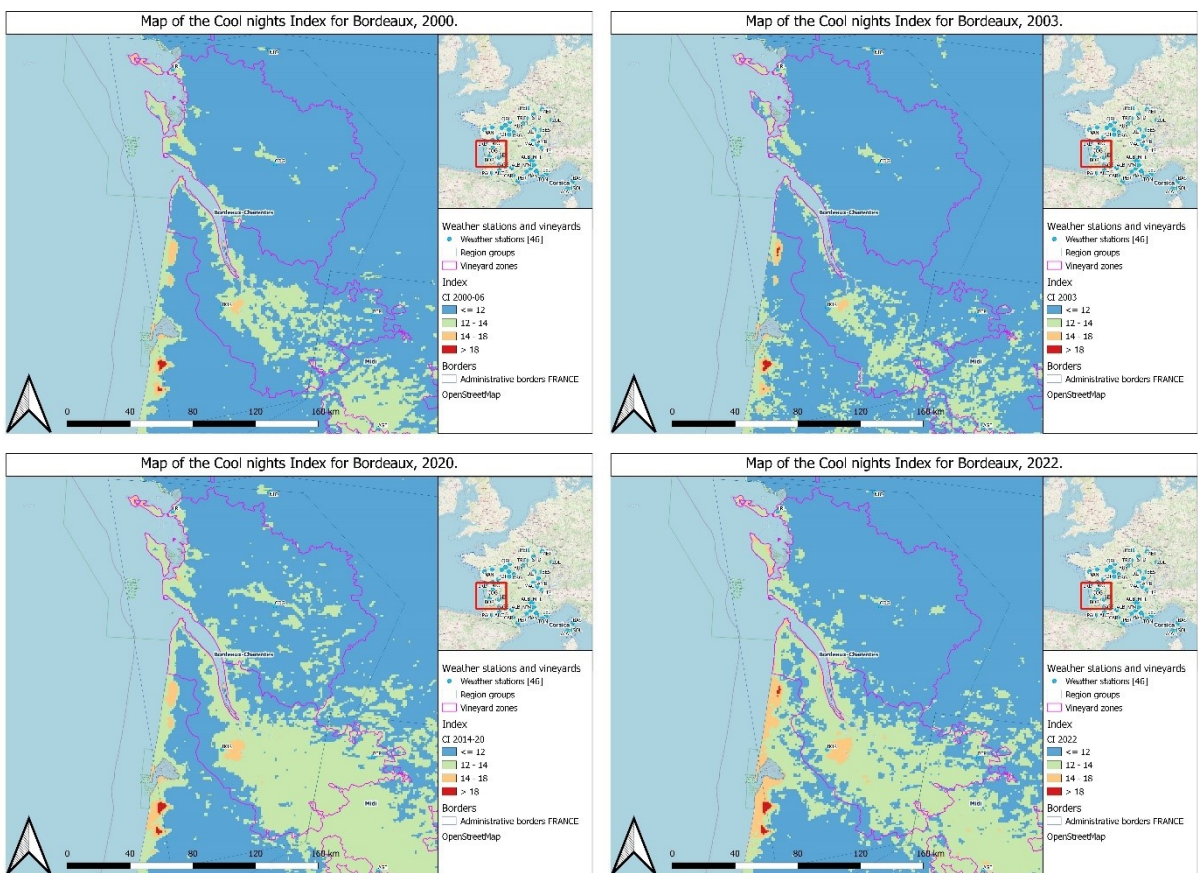


Figure 25 Bordeaux-Charentes Cool Nights Index

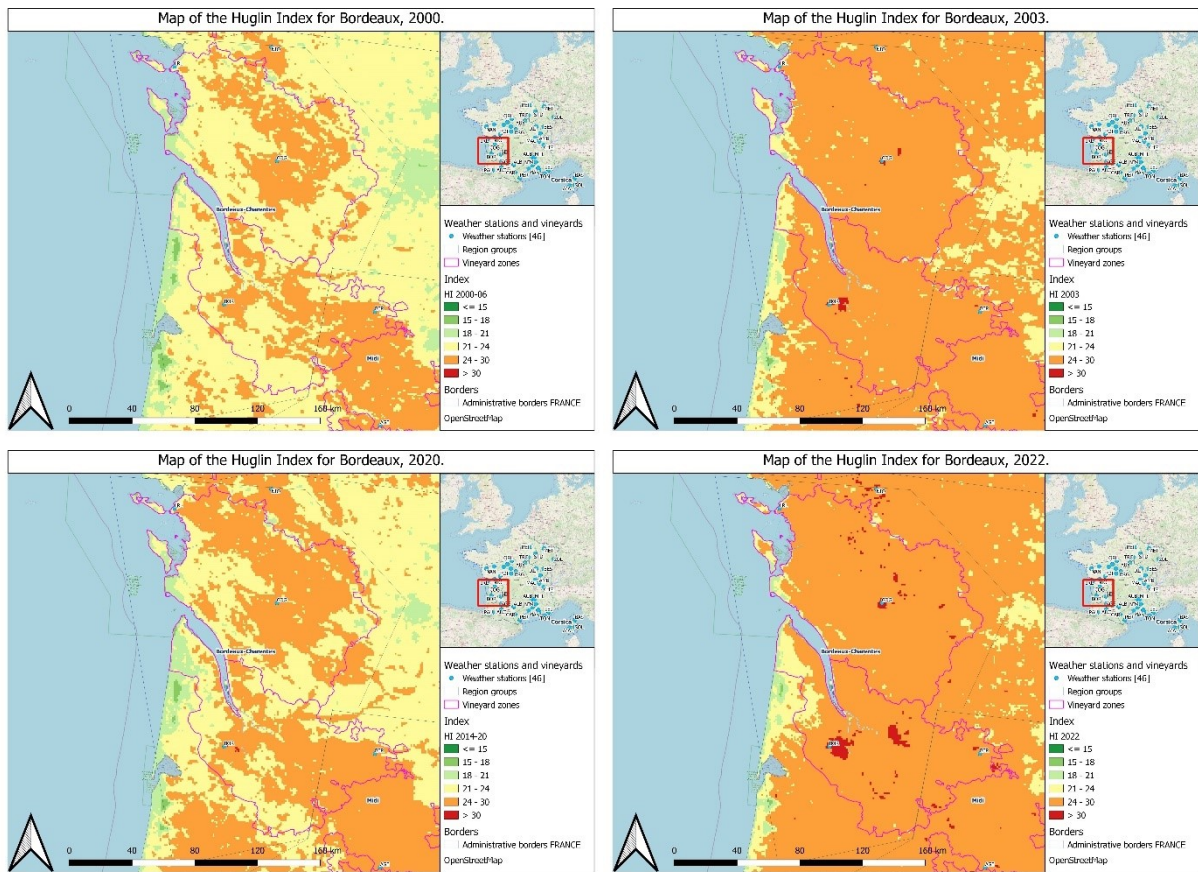


Figure 26 Bordeaux-Charentes Huglin Index

3.2.4.3. Slopegraphs

The precipitation values of our slopegraphs look particularly jagged, with values going up to 150 mm some years and a marked drought in May of 2011. However, these values establish a stable trend, staying flat over April, May, August, and September and closely followed by all stations except La Rochelle (LRL). This station seems to be a geographic outlier, being both far north and right next to the ocean. We observe a sharp increase of precipitations over the years in June followed by a sharp decrease in July, and when looking at the p-values under 0.05 of the regression coefficients, highlighted in blue in the table, we see that in June, the 3 stations of Bordeaux, La Rochelle and Cognac (BOR, LRL and COG) show a significant increase in precipitation rates over the years, a phenomenon that thus englobes all the coast of the Bordelais-Charentais, while the significant fall of precipitation rates in July regarding La Rochelle and Niort (LRL and NIO) means that trend is mostly located north and the upper part of the Charentais is only catching a small part of it.

The temperature values are very similar, with LRL again being an outlier following the same pattern two degrees lower than the rest. The regression lines have the same tendency, all closely clustered with LRL as an outlier one to two degrees colder. The trends made by the regression lines are either increasing throughout the months or remaining stable. We can probably credit the slight drop in temperatures in June to the rise of precipitations in the same month. Looking

at the significant p-values of the regression coefficients, we see that in July, the stations of BOR, COG and NIO have had a significant increase of 2°C in the last 20 years.

Month	Stations	Regression Coeffs PT	p.value PT	Regression Coeffs TX	p.value TX
April	BOR	-0.140	0.934	0.0990	0.171
April	COG	-1.04	0.415	0.119	0.121
April	LRL	-0.411	0.706	0.0956	0.180
April	NIO	-0.105	0.934	0.114	0.150
May	BOR	0.182	0.903	0.00247	0.968
May	COG	0.934	0.406	0.0134	0.825
May	LRL	0.583	0.444	0.0397	0.414
May	NIO	0.798	0.485	0.0255	0.48
June	BOR	3.12	0.00815	-0.0570	0.360
June	COG	2.99	0.00480	-0.0596	0.310
June	LRL	1.28	0.0295	0.00312	0.953
June	NIO	1.74	0.0667	-0.0590	0.337
July	BOR	-1.33	0.113	0.139	0.0461
July	COG	-1.43	0.147	0.135	0.0499
July	LRL	-2.63	0.0145	0.131	0.0511
July	NIO	-2.78	0.0191	0.139	0.0441
August	BOR	-0.415	0.699	0.0597	0.380
August	COG	-1.03	0.406	0.0549	0.449
August	LRL	-0.837	0.485	0.0571	0.337
August	NIO	-0.550	0.742	0.0569	0.475
September	BOR	0.304	0.746	0.0944	0.103
September	COG	1.04	0.272	0.0788	0.166
September	LRL	-0.0347	0.978	0.0601	0.266
September	NIO	1.24	0.263	0.0731	0.218

Table 10 Regression coefficients PT and TX with p-values for Bordeaux-Charentes

Trends for Bordeaux-Charentais

Precipitations and temperatures from April to June

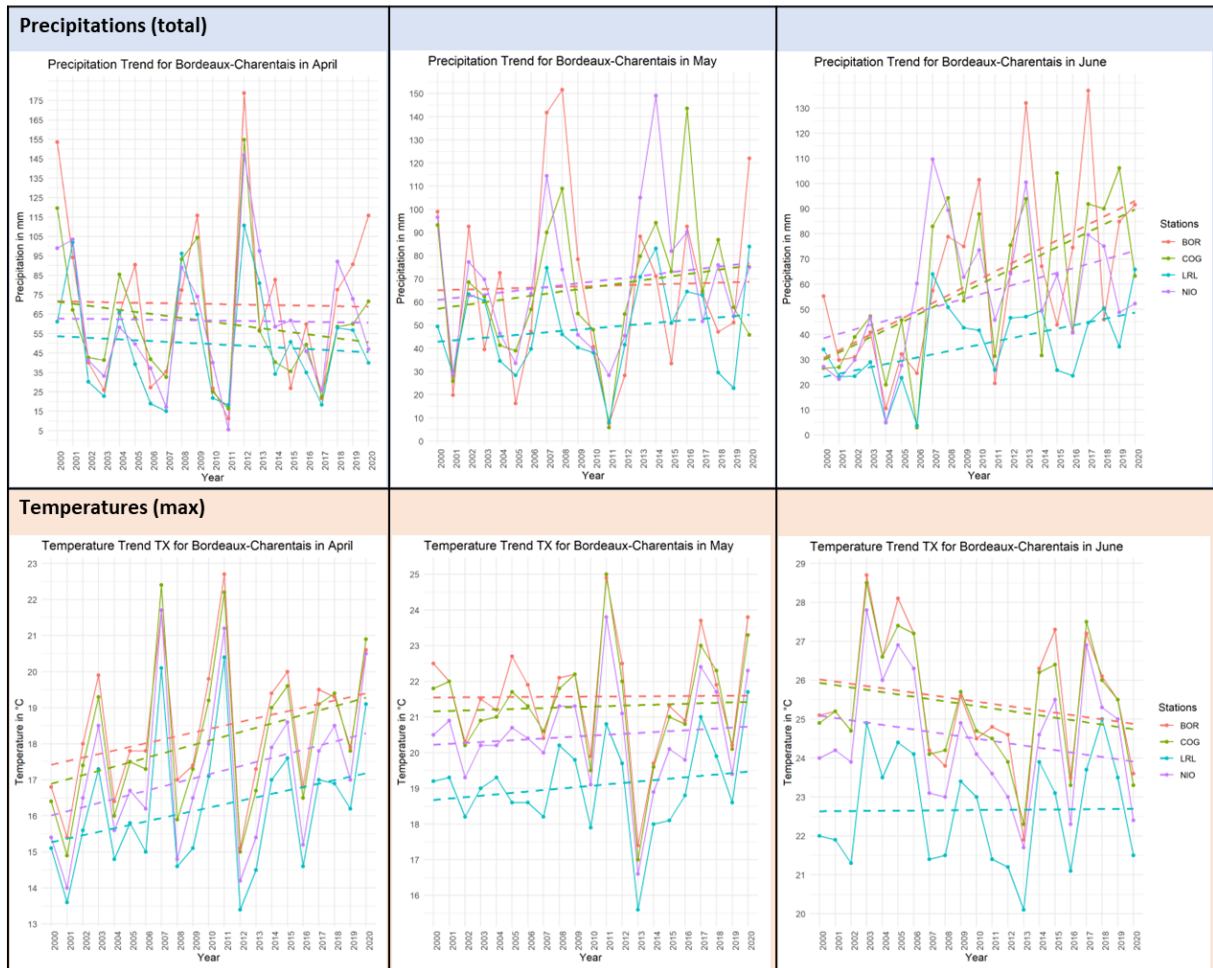


Figure 27 Bordeaux-Charentes Precipitation & Temperature Slopegraphs April to June

Trends for Bordeaux-Charentais

Precipitations and temperatures from July to September

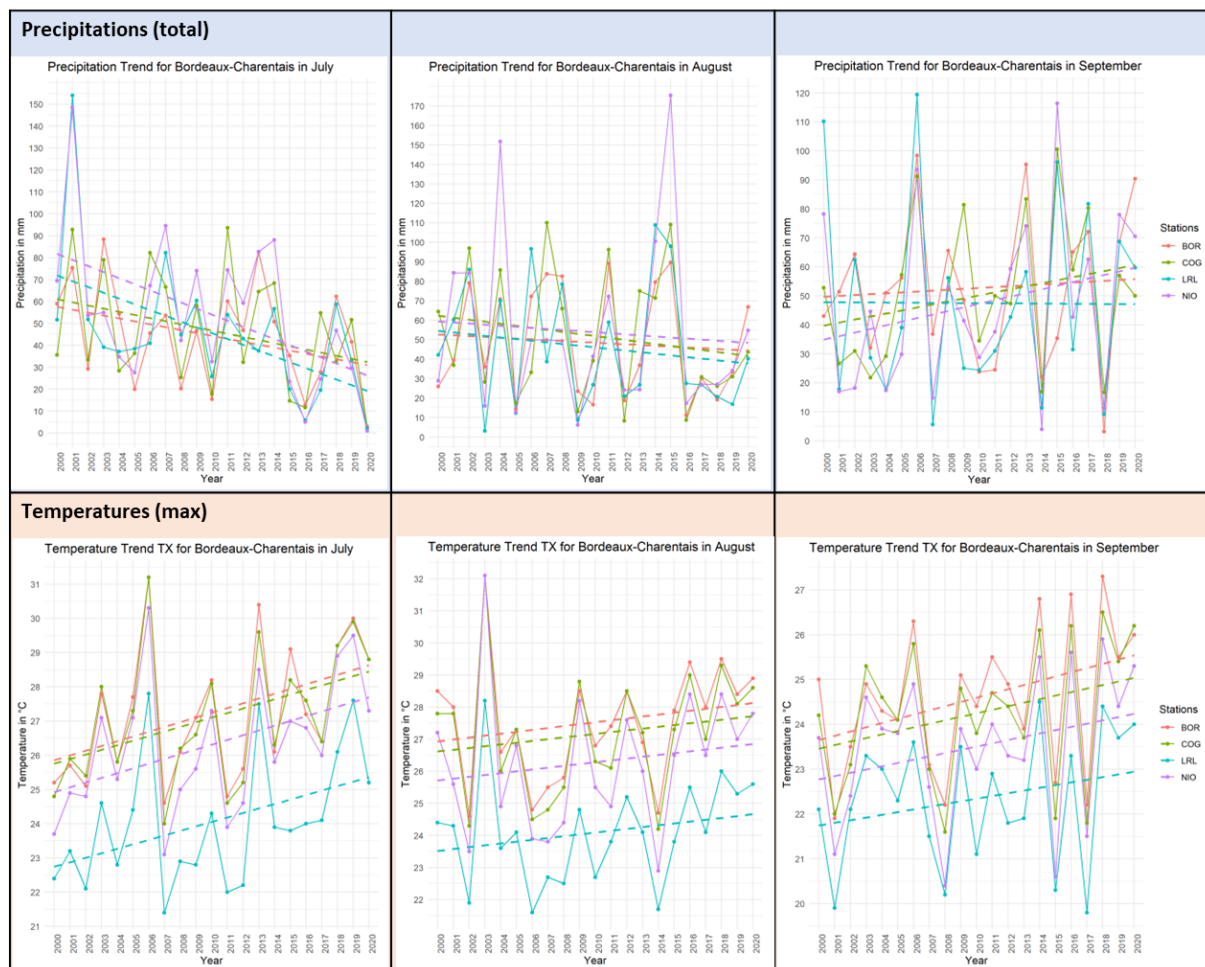


Figure 28 Bordeaux-Charentes Precipitation & Temperature Slopegraphs July to September

3.2.5. Loire

3.2.5.1. Geoclimatical Context

This vineyard area, usually called Val de Loire or the Loire Valley is placed over the Loire and Centre regions of France under Britain and north of the Charentais. The area starts at the Atlantic and heads inland under the Armorican arm for more than 400 km until reaching south of Paris. The vineyards follow the course of the Loire River and its tributaries (mainly the Loir, Indre and Cher) and circle around the forests of Sologne while spreading over the large flats of the Parisian Basin.

The Loire valley's climate ranges from oceanic to continental, which allows the cultivation of a wide range of grape varieties:

- For red wines: cabernet franc, gamay, and grolleau.
- For whites: melon de Bourgogne, chenin, and sauvignon.

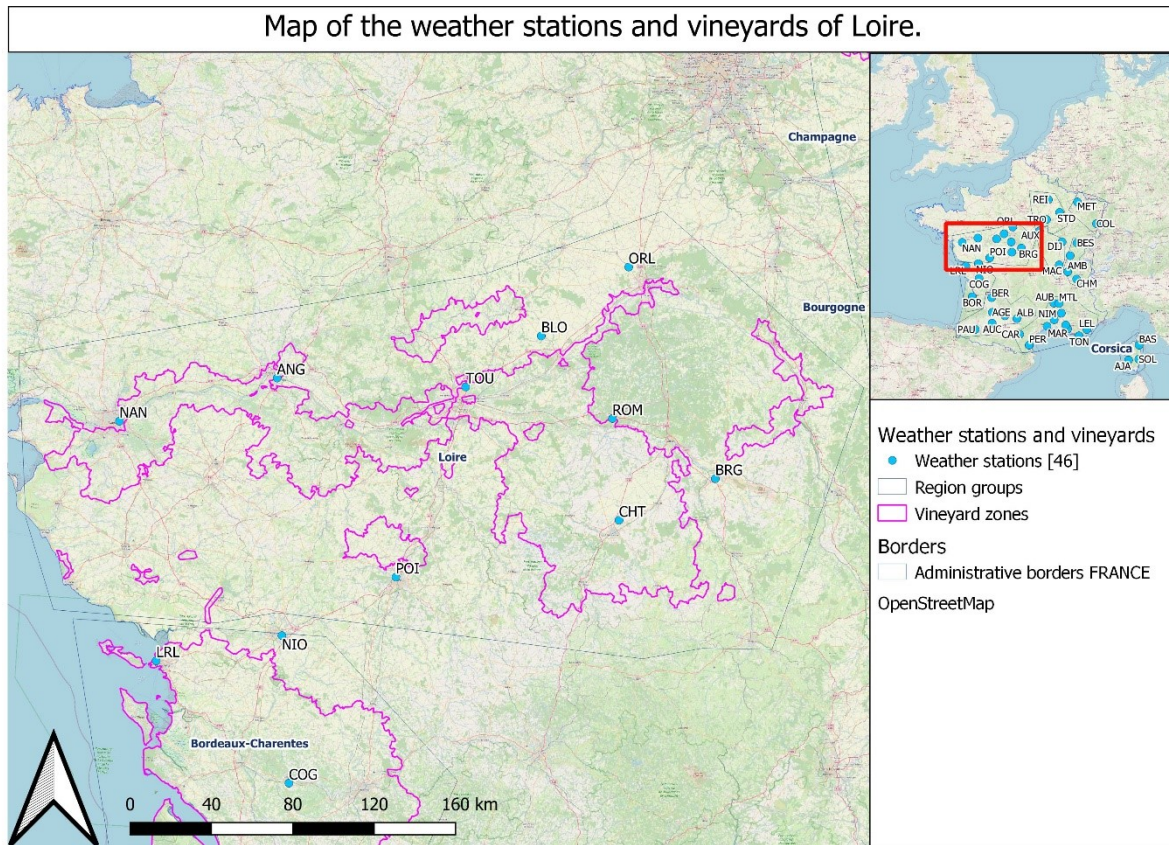


Figure 29 Loire context

3.2.5.2. Index Shift Analysis

The AI, as expected this far north and west, remains constant through the years. Neither the heat events of 2003 nor 2022 managed to cause any significant shifts in this region's precipitation-evapotranspiration balance.

Regarding the HI, we note in 2000 the region was predominantly temperate (-1) or warm-temperate (+1) with some spots of warm (+2) namely north of Poitiers (POI) and around Châteauroux (CHT). But between 2000 and 2020, a severe shift happened: half of the vineyard area transitioned into +2 (warm) territory as the temperate (-1) areas shrunk. This process was worsened when the 2022 heatwave happened: the entire region went into the +2 category, leaving only the forests of Orléans and Sologne free though well into the warm-temperate (+1) category. It was worse there than it had been in 2003, for that year the heatwaves had mostly spared the north of the Loire river from Nantes to Tours (NAN and TOU on the map).

With the CI, we see the nighttime temperatures of the region haven't changed in any serious way, remaining firmly in the very cool (+2) category the whole time from 2000 to 2022. The only changes to the map, some spots gone in the (+1) category, are placed over cities and the Loire River.

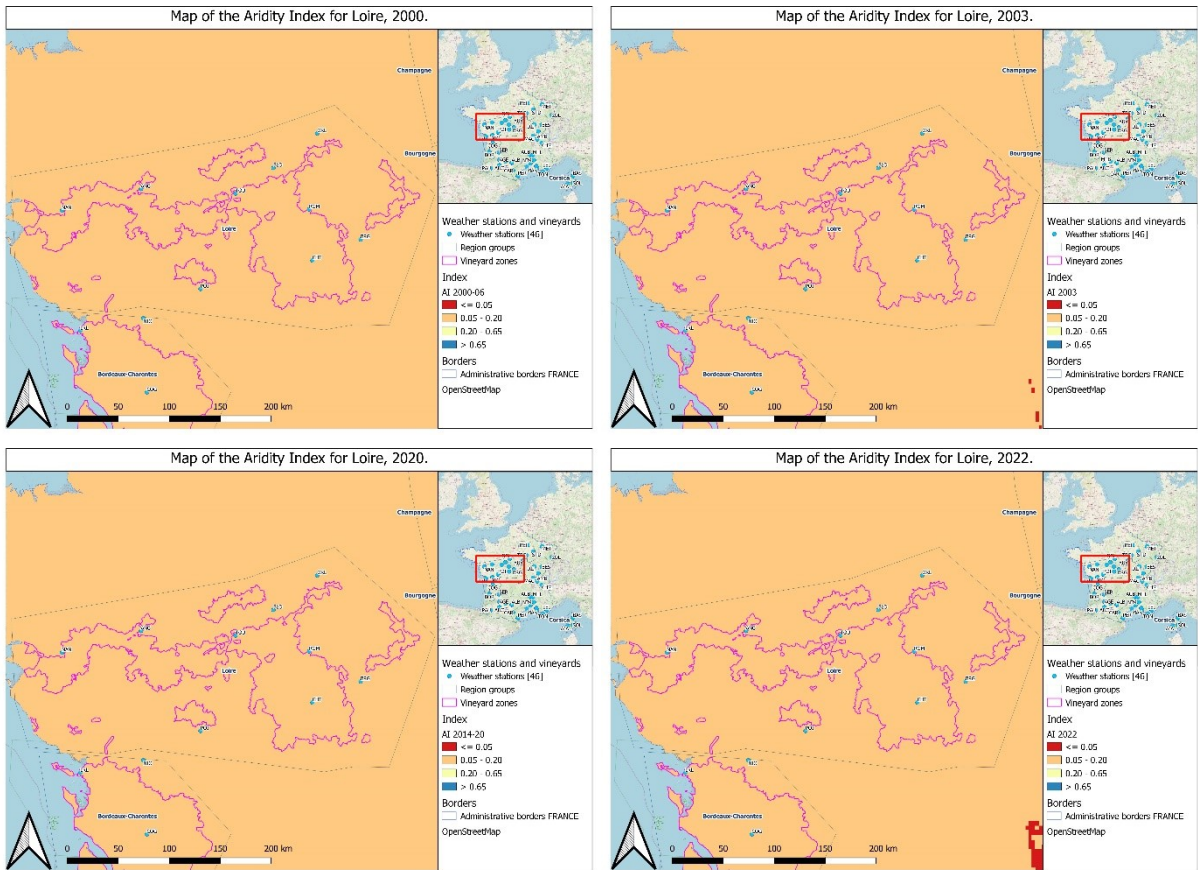


Figure 30 Loire Aridity Index

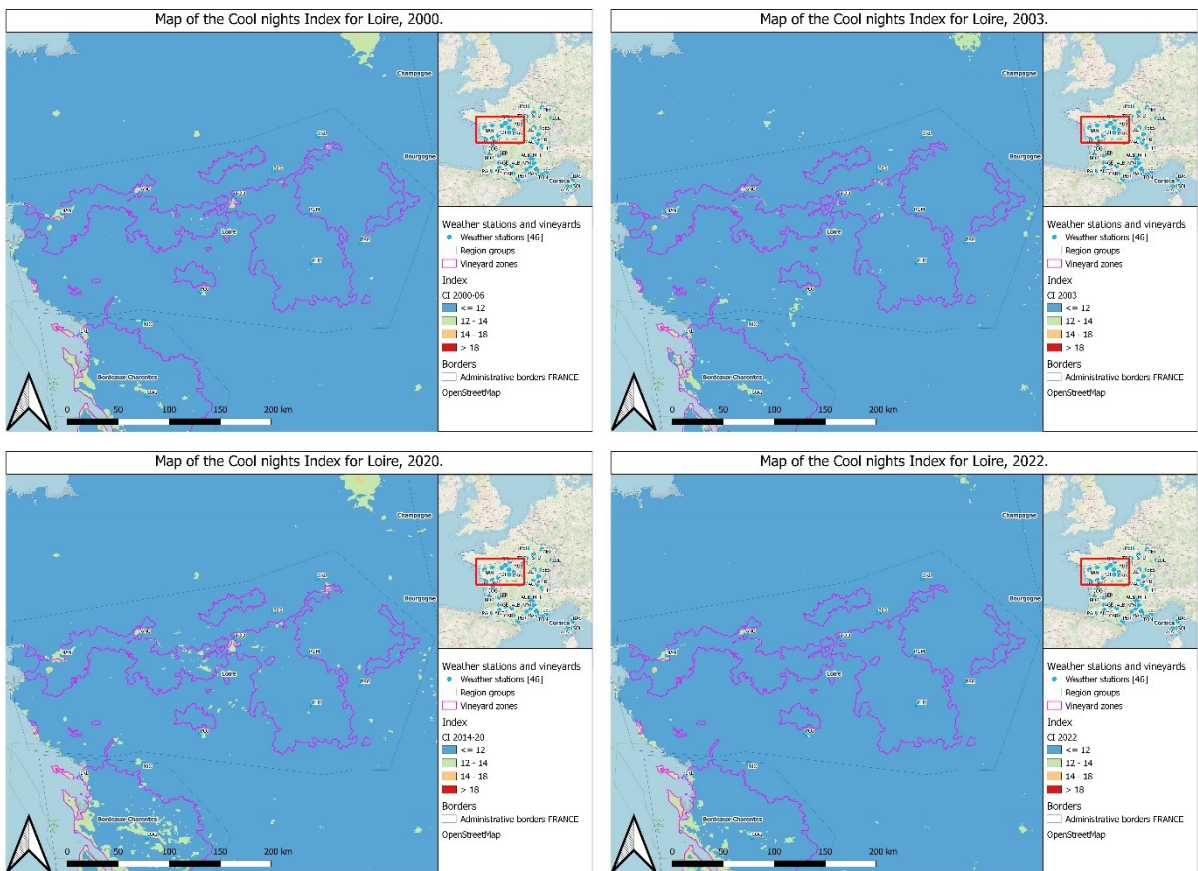


Figure 31 Loire Cool Nights Index

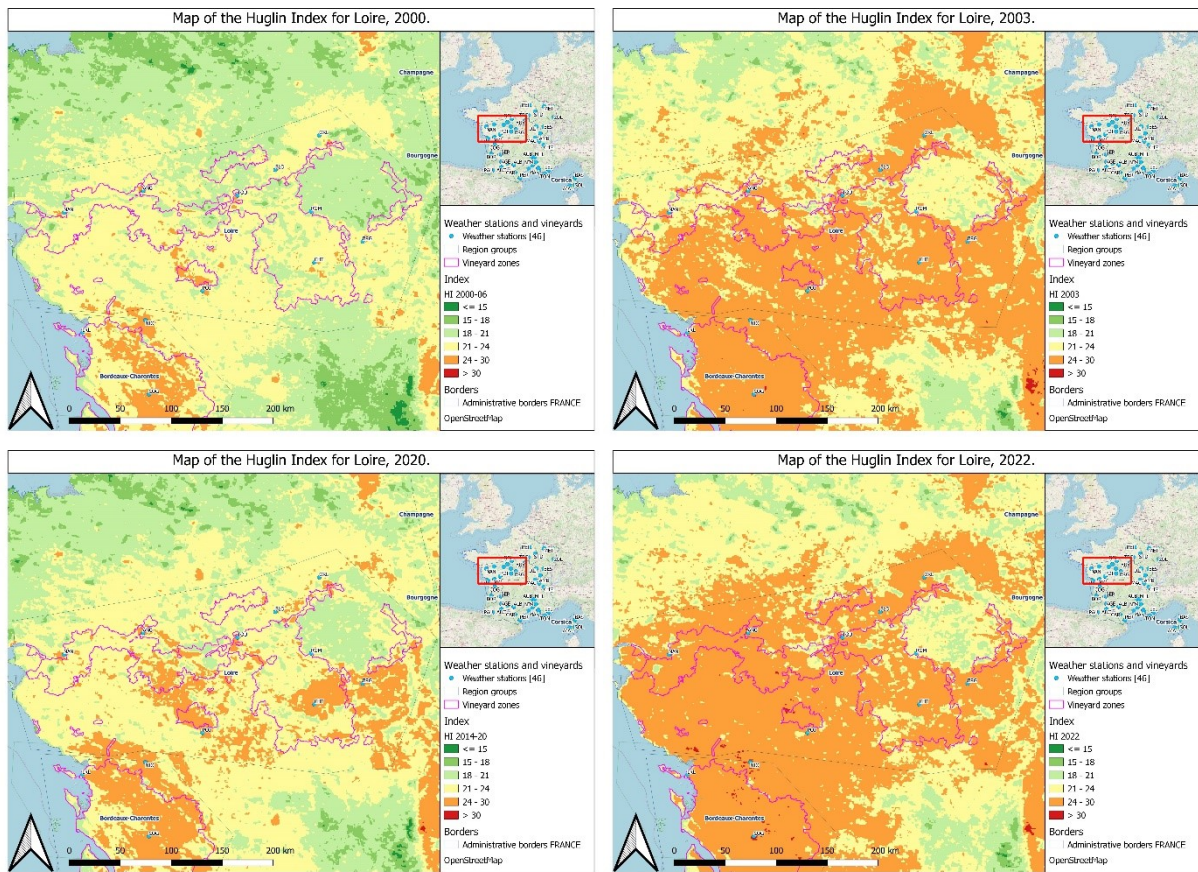


Figure 32 Loire Huglin Index

3.2.5.3. Slopegraphs

The slopegraphs we made for the Loire region include 9 spatial data points, a bit grouped in the Centre region but nonetheless spanning the entire area's length along the Loire River. This allows us to be precise and easily detect any local shifts in PT or TX.

Regarding precipitation values, they show a series of wild fluctuations going easily from 10 to 100 mm. They are similar over the months from one city to another, suggesting a considerable year-to-year variability. Despite the high level of fluctuation, the regression lines calculated from these values have only slight variations between cities no matter the direction of the trend. The p-values calculated from the regression coefficients of these lines show us there are significant ($p\text{-value} < 0.05$) increases to the precipitation trends of Angers, Nantes and Tours (ANG, NAN and TOU) in June, as well as significant decreases to the precipitation trends of Angers, Blois, Bourges, Nantes, Orléans, Poitiers and Tours (ANG, BLO, BRG, NAN, ORL, POI and TOU) in July.

The June increase in precipitation rates over the years coincides with the trend observed also in the Bordeaux-Charentes and Midi areas and indicates a rise in the influence of the Atlantic over the west coast of France, spreading further inland to the north and south. The July trend, on the

other hand, spreads over the whole length of the region and to the east, probably continuing further up north.

Analysing our TX graphs, we notice the values are extremely similar and clustered through high and low temperature extremes both, meaning the precipitation events must spread quickly and evenly over the whole region. The trends uncovered by the regression lines tell a similar story, temperatures being grouped into one bundle with less than 1°C of difference from the highest to the lowest value. These trends are stable during May and June but show an increase of precipitations over the years in April, July, August and September.

Through looking at the p-values, highlighted in blue in the table, we notice that all the stations of the regions except Angers (ANG), so Blois, Bourges, Châteauroux, Nantes, Orléans, Poitiers, Romorantin and Tours (BLO, BRG, CHT, NAN, ORL, POI, ROM, and TOU) show a significant increase in TX over the years in July. This pattern shared with most of Bordeaux-Charentes, and a piece of the Midi is certainly part of a bigger trend that continues over other regions. In September one city also has a significant increase in TX over the years: Châteauroux (CHT), situated in the south of the region, forms a lone hotspot.

Month	Stations	Regression Coeffs PT	p.value PT	Regression Coeffs TX	p.value TX
April	ANG	-0.571	0.568	0.116	0.128
April	BLO	-0.263	0.783	0.136	0.0873
April	BRG	-1.28	0.290	0.123	0.152
April	CHT	-1.79	0.179	0.121	0.134
April	NAN	-0.597	0.574	0.120	0.0938
April	ORL	-0.446	0.629	0.113	0.153
April	POI	-0.863	0.459	0.119	0.130
April	ROM	-0.729	0.521	0.135	0.112
April	TOU	-0.983	0.404	0.125	0.0975
May	ANG	-0.312	0.767	0.0390	0.468
May	BLO	1.60	0.295	0.0305	0.603
May	BRG	1.37	0.346	-0.00273	0.966
May	CHT	0.512	0.670	-0.00195	0.974
May	NAN	-0.513	0.637	0.0758	0.139
May	ORL	1.37	0.340	0.00987	0.862
May	POI	1.52	0.120	0.00805	0.884
May	ROM	1.05	0.370	0.0178	0.766
May	TOU	0.115	0.903	0.0290	0.605
June	ANG	2.57	0.00311	-0.0539	0.378
June	BLO	1.10	0.355	-0.00662	0.913
June	BRG	1.41	0.215	0.0230	0.749
June	CHT	0.979	0.299	-0.0358	0.565
June	NAN	2.69	0.0241	-0.0164	0.766
June	ORL	1.17	0.267	-0.0123	0.826
June	POI	1.61	0.130	-0.0495	0.440

June	ROM	1.18	0.231	-0.0242	0.698
June	TOU	2.55	0.0108	-0.0175	0.767
July	ANG	-3.16	0.0110	0.133	0.730
July	BLO	-2.73	0.0195	0.177	0.0239
July	BRG	-3.13	0.0403	0.191	0.0153
July	CHT	-2.52	0.0841	0.161	0.0253
July	NAN	-2.02	0.0284	0.145	0.0408
July	ORL	-3.52	0.0302	0.144	0.0480
July	POI	-2.35	0.00747	0.145	0.0399
July	ROM	-2.09	0.0821	0.151	0.0413
July	TOU	-2.45	0.0150	0.151	0.0297
August	ANG	0.645	0.567	0.0596	0.397
August	BLO	-0.885	0.409	0.0935	0.208
August	BRG	0.476	0.749	0.115	0.176
August	CHT	-1.62	0.279	0.109	0.214
August	NAN	0.324	0.779	0.0556	0.434
August	ORL	-2.09	0.157	0.0736	0.365
August	POI	-0.480	0.727	0.0726	0.378
August	ROM	-1.75	0.208	0.0847	0.319
August	TOU	-1.27	0.217	0.0666	0.369
September	ANG	-0.259	0.817	0.0487	0.396
September	BLO	-0.232	0.773	0.106	0.0990
September	BRG	0.454	0.581	0.113	0.101
September	CHT	-0.342	0.670	0.129	0.0332
September	NAN	-0.0475	0.965	0.0453	0.405
September	ORL	0.895	0.288	0.0935	0.136
September	POI	0.818	0.251	0.0892	0.136
September	ROM	-0.265	0.717	0.112	0.0757

Table 11 Regression coefficients PT and TX with p-values for Loire

Trends for Loire

Precipitations and temperatures from April to June

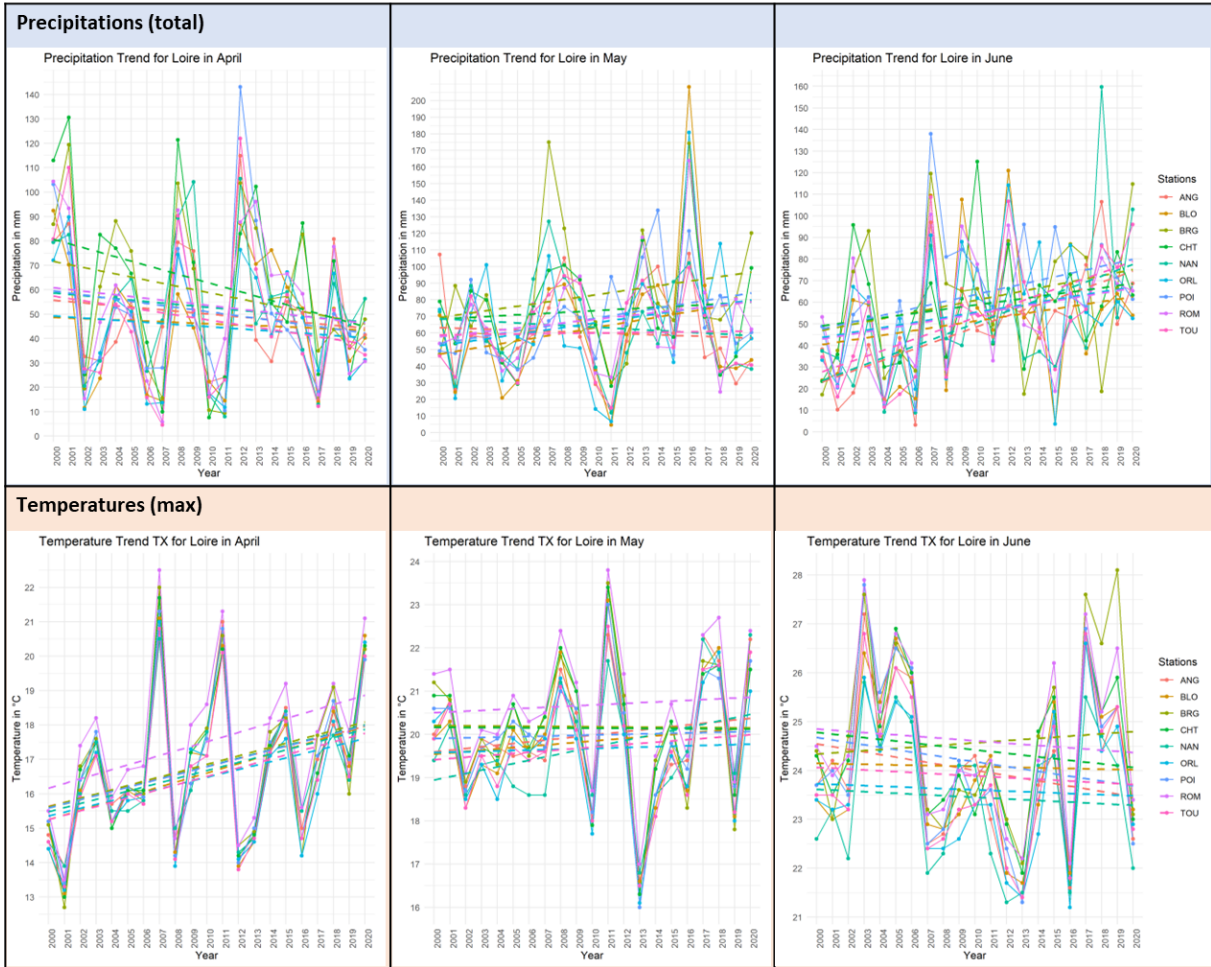


Figure 33 Loire Precipitation & Temperature Slopegraphs April to June

Trends for Loire

Precipitations and temperatures from July to September

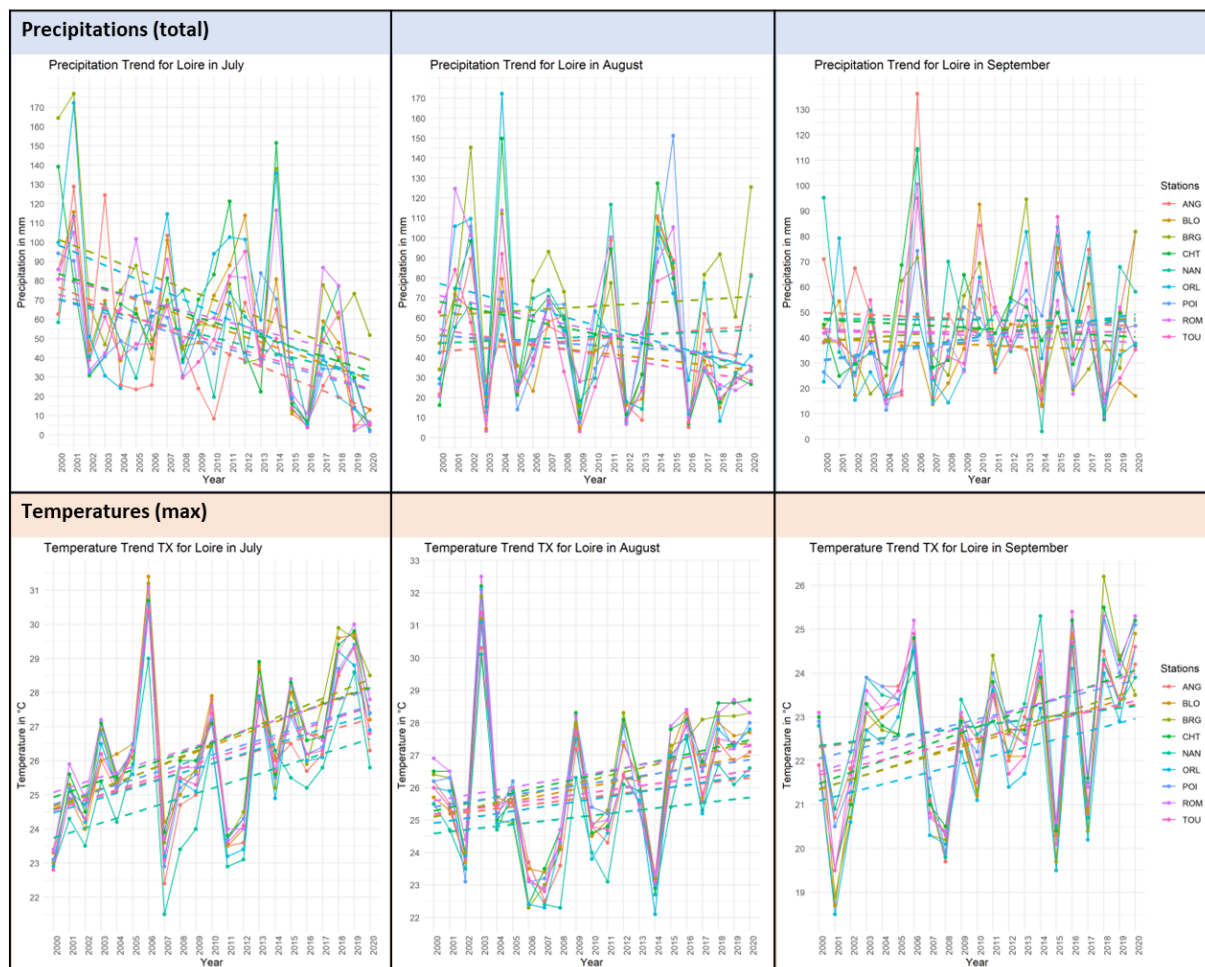


Figure 34 Loire Precipitation & Temperature Slopegraphs July to September

3.2.6. Champagne

3.2.6.1. Geoclimatical Context

The Champagne region, known worldwide for its iconic sparkling white wine, possesses the northernmost vineyards of France, to the northeast of Paris. The area is bordered by the Langres plateau on the southwest, the Ardennes mountains in the northeast, and nears the 50th parallel on the north side, beyond which the grapevine isn't considered to grow well enough to consider winemaking. Despite its international fame and the worldwide demand, Champagne features a relatively small vineyard surface, peppered around forests, lakes, fields, and diverse other land uses.

Champagne's fame lies in its specialty sparkling white, which alone constitutes over 90% of the production, and is made from a single white grape variety. Two other varieties can be found as well in the region, to be blended into a less-known rosé:

- For Champagne: Chardonnay grape variety.
- For the rosé: black Pinot and Pinot Meunier varieties.

The area is in the north side of the Parisian Basin, and so enjoys both a cool climate and some regulating influence from the English Channel.

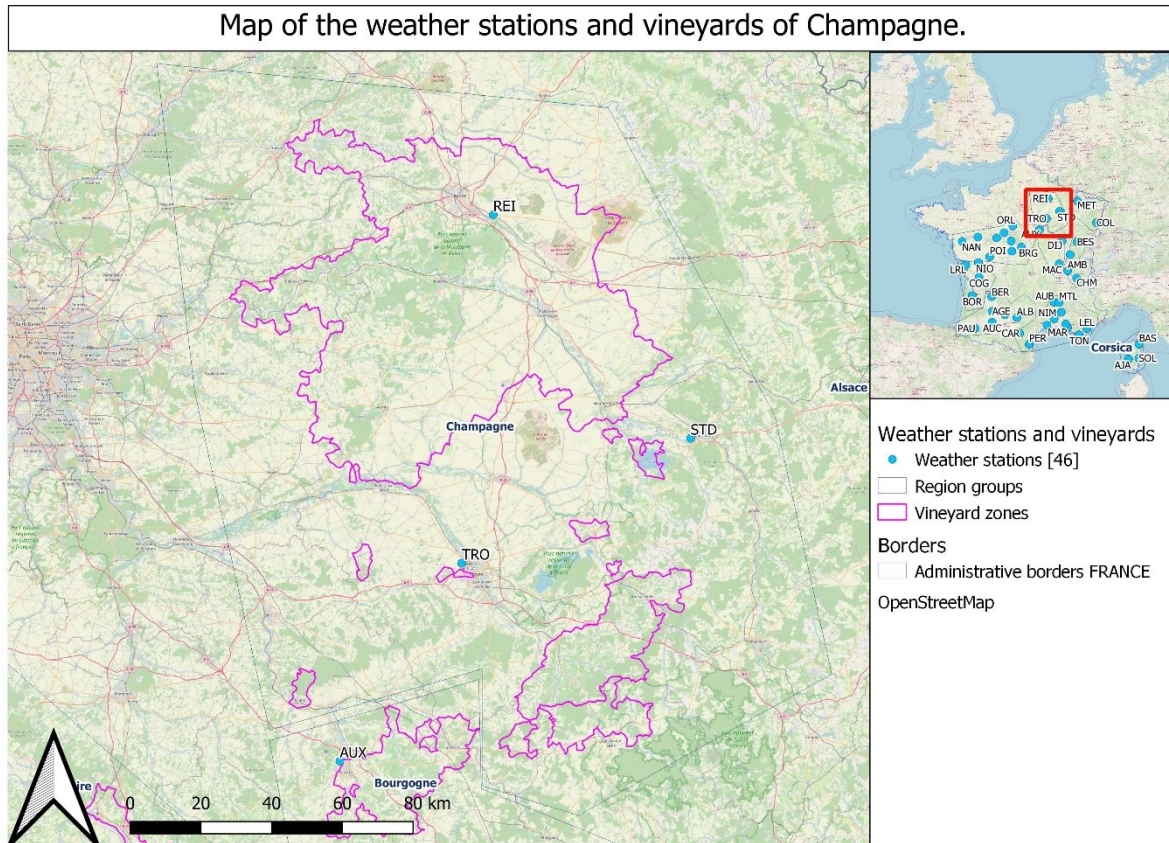


Figure 35 Champagne context

3.2.6.2. Index Shift Analysis

The AI, as expected this far north, remains constant throughout the years. Neither the heatwave events of 2003 nor 2022 managed to induce a significant shift in this region's precipitation-evapotranspiration balance.

Analysing the HI, we observe that the region originally experienced cool temperatures around the warm-temperate (+1), temperate (-1), and even cool (-2) categories in 2000, with the only points of warm (+2) temperatures being over the major cities of Troyes (TRO) and Reims (REI). However, a noticeable warming of the region has since seen the categories shift until in 2020 they reached in majority the warm-temperate (+1) with some temperate (-1) temperatures on the edges of the basin. The cities were still the only parts of the map in the warm (+2) category, though that changed with the 2022 heatwave events. As they did for the 2003 event, the warm

temperatures came from the southwest to reach all the way north to Reims and caused half of the vineyard area to shift into the orange warm (+2) category.

In terms of the CI, the night temperatures of Champagne have remained consistently cool through the last 22 years without a sign of change from the very cool (+2) category of the CI. The only spots on the area's map in warmer categories correspond to the lakes of the Der-Chantecoq, the Auzon Temple and of Orient, and should be considered outliers and disregarded.

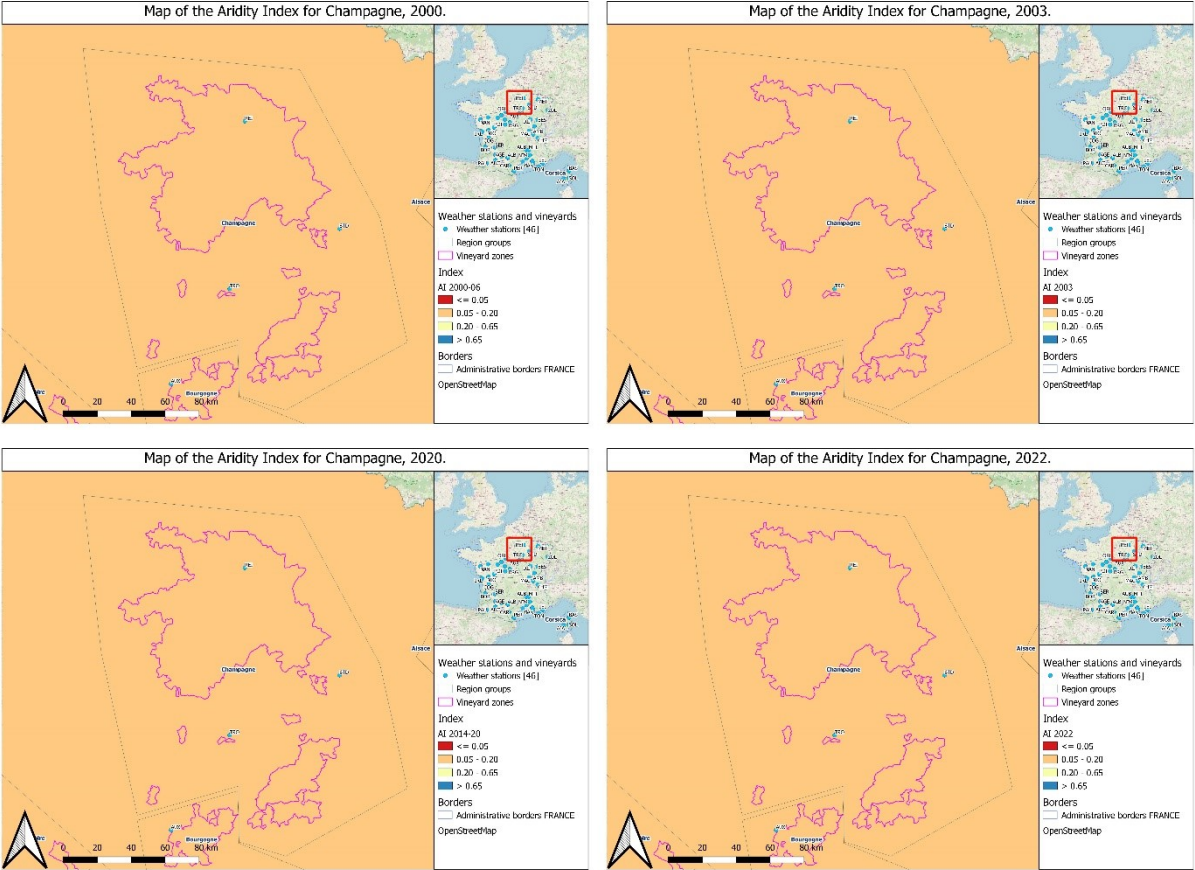


Figure 36 Champagne Aridity Index

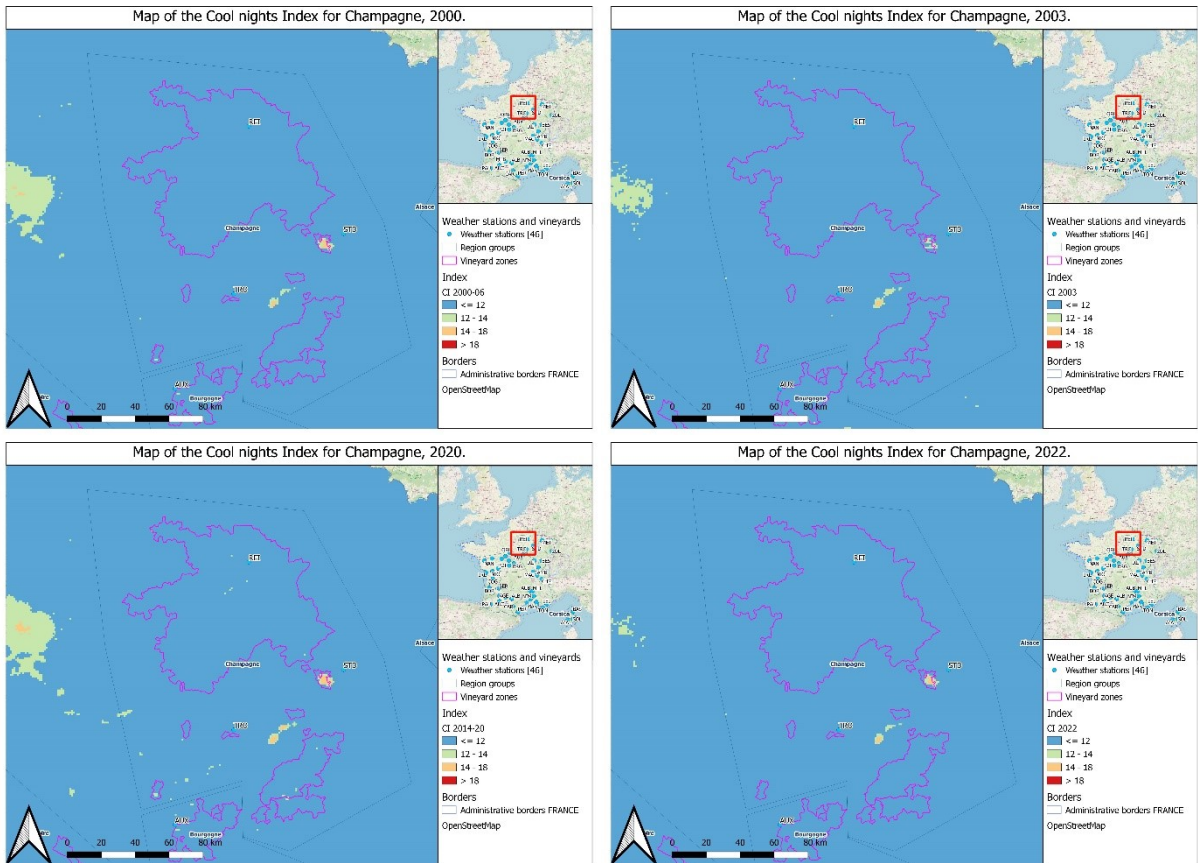


Figure 37 Champagne Cool Nights Index

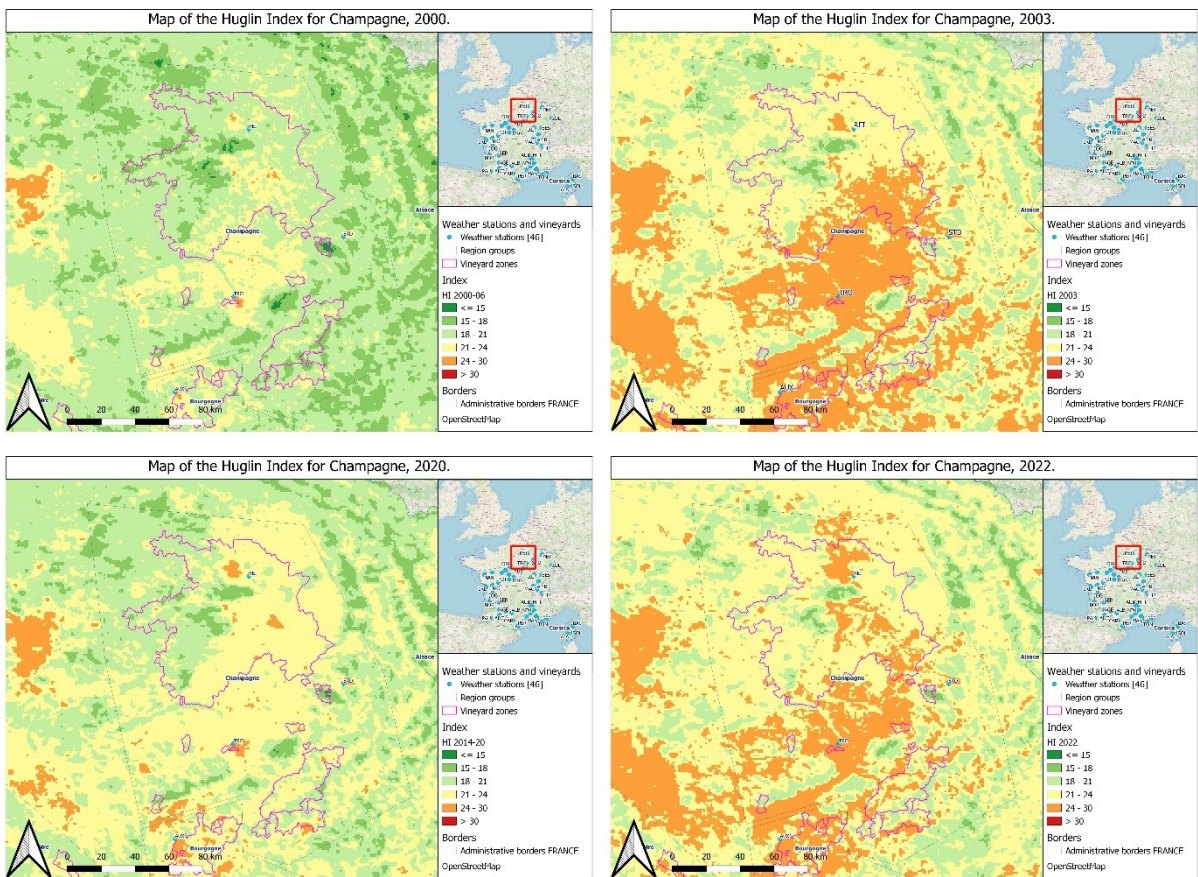


Figure 38 Champagne Hugin Index

3.2.6.3. Slopegraphs

We have 3 stations positioned in the Champagne region, two to the south near the towns of St-Dizier and Troyes (STD and TRO), and another in the city of Reims (REI). A dataset with only three spatial data points may not seem relevant enough, but knowing our aim is a national scale assessment and given the region's limited size, it aligns with our overall spatial resolution.

On our precipitation PT slopegraphs, we observe here that the values of each station start dissimilar one from another, but the trends seem to align more closely in the later years, and become more uniform, the pattern being more evident in July and September. The regression lines made by these values, however, are very similar in June and July, and diverge more for the months of April, May, August, and September. The regression coefficients of these lines, highlighted in blue in the table if significant, show that in April, the area around Reims has lost a significant amount of rainfall over the years, and that the same holds true for the entire region during the month of July. This latter pattern is part of a greater whole, as it also impacts the Loire region.

Examining our temperature slopegraphs TX reveals that the values share a very similar pattern, although a bit less close for Reims (REI) as it's situated much more to the north than the other stations. The regression lines are almost parallel to each other, going so far as to overlap in June for the stations of TRO and STD. Their overall trajectory also indicates a general rise in maximum temperature averages. The regression coefficient of Reims is also shown to be significant through the month of July, indicating an important rise in TX in the north of Champagne over the years.

All these information points out a general decrease in the region's precipitations as the same time as an increase in its maximum temperatures in the summer months. Though these changes don't seem to have affected the precipitation-evapotranspiration balance nor the night temperatures of the area, the increase in temperature extremes, fall in precipitations, coupled with the region's exposed terrain make the current situation faced by Champagne and its wine production a source of worry for the future of the iconic sparkling white wine.

Month	Stations	Regression Coeffs PT	p.value PT	Regression Coeffs TX	p.value TX
April	REI	-1.92	0.0416	0.137	0.0966
April	STD	-1.50	0.257	0.130	0.148
April	TRO	-1.47	0.185	0.128	0.124
May	REI	-0.468	0.711	0.0217	0.727
May	STD	-0.196	0.818	0.000390	0.995
May	TRO	1.06	0.351	0.00221	0.972
June	REI	1.29	0.154	0.0525	0.303
June	STD	1.22	0.213	0.0248	0.707

June	TRO	0.815	0.299	0.0274	0.653
July	REI	-2.87	0.0314	0.163	0.0324
July	STD	-3.83	0.0213	0.166	0.0754
July	TRO	-3.45	0.00960	0.158	0.0455
August	REI	-2.05	0.0984	0.113	0.130
August	STD	-1.98	0.231	0.112	0.221
August	TRO	-0.138	0.913	0.0983	0.254
September	REI	0.451	0.637	0.106	0.111
September	STD	-1.04	0.539	0.123	0.103
September	TRO	-0.0497	0.961	0.110	0.130

Table 12 Regression coefficients PT and TX with p-values for Champagne

Trends for Champagne

Precipitations and temperatures from April to June



Figure 39 Champagne Precipitation & Temperature Slopegraphs April to June

Trends for Champagne

Precipitations and temperatures from July to September



Figure 40 Champagne Precipitation & Temperature Slopegraphs July to September

3.2.7. Alsace

3.2.7.1. Geoclimatical Context

Located in the northeastern most part of France, the Alsace and Lorraine regions are often considered part of a same vineyard. They possess a unique landscape: the area is divided by the Vosges mountains, the western side in the Lorraine faces the Parisian basin while its eastern border in Alsace is shared with Germany. In the east, vineyards occupy the Alsacian Plain east of the Vosges along the Rhine River, and in the west, smaller vineyards on the other side of the mountains can be found along the Moselle River.

Because of this unique landscape, there is a separation of grape varieties across the Vosges mountains. The western side focuses at 95% on red wine production, the remaining 5% being white and yellow wines with grape varieties

- For reds: black pinot and gamay.
- For whites: only the auxerrois grape variety.

On the east side, 70% of the production goes towards white wines, the remaining 30% meant for rosés and red wines.

- For red wines: riesling, gewurztraminer, sylvaner, pinot gris, and muscat.
- For whites: pinot noir.

Both sides of the Vosges have a different climatic environment: the western side is exposed to the Parisian Basin and all its influences from the sea, while Alsace, on protected by the Vosges, has a more continental climate.

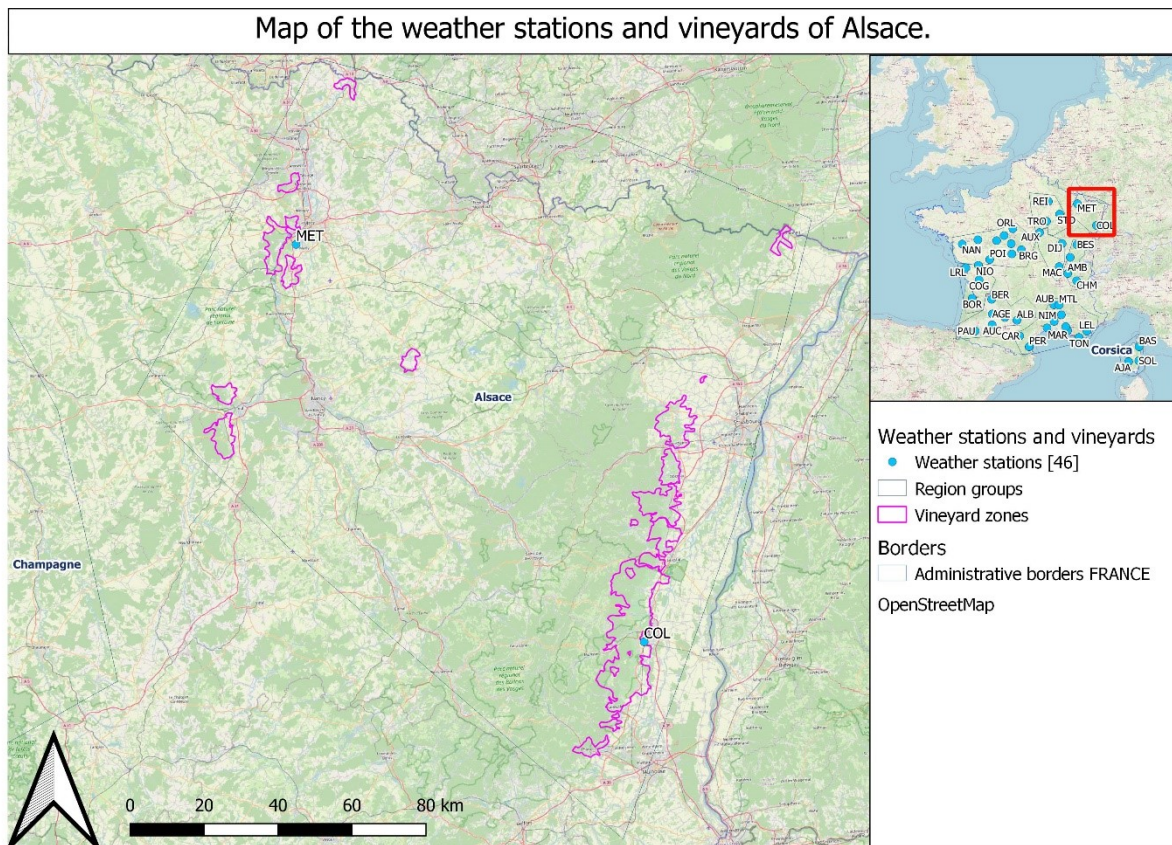


Figure 41 Alsace context

3.2.7.2. Index Shift Analysis

Study of the AI in this area reveals that in 2000, part of the Vosges close to the eastern vineyard area were in the semi-arid (+1) category. That zone has since disappeared, replaced by the arid (+2) category that already covered the rest of the region by 2020, and there were no significant changes to the region's AI since.

The HI shows us that in 2000, the region was predominantly in the temperate (-1) category, and vineyard sure ran the gamut between the warm-temperate (+1) and very cool (-3) categories in Alsace, while being shared between temperate (-1) and cool (-2) categories in Lorraine. By 2020, the plains had shifted in majority into the warm-temperate (+1) category, and the Alsace vineyards warmed enough to display spots of warm (+2) category temperatures along their length. The heatwaves of 2003 and 2022 had a similar but worse effect, worse in the case of 2003, as they made the warm (+2) temperatures become the majority in the plains of Lorraine as well as the Alsace Plain whereas the 2022 heatwaves mostly affected Alsace. In both instances, half the vineyard surface still shifted to the warm (+2) category, regardless of how the rest of the region was affected.

Analysing the CI, we discovered a shift in night temperatures between 2000 and 2020. In this warming trend, the Rhine valley's category started transitioning from the very cold (+2) that encompassed the whole region to the cold (+1) over these two decades, specifically over the vineyard area and at the edges of the Vosges du Nord National Park further north. In contrast, the heatwaves in 2003 and 2022 didn't affect the cold night conditions and instead, these years were firmly in the very cool (+2) category.

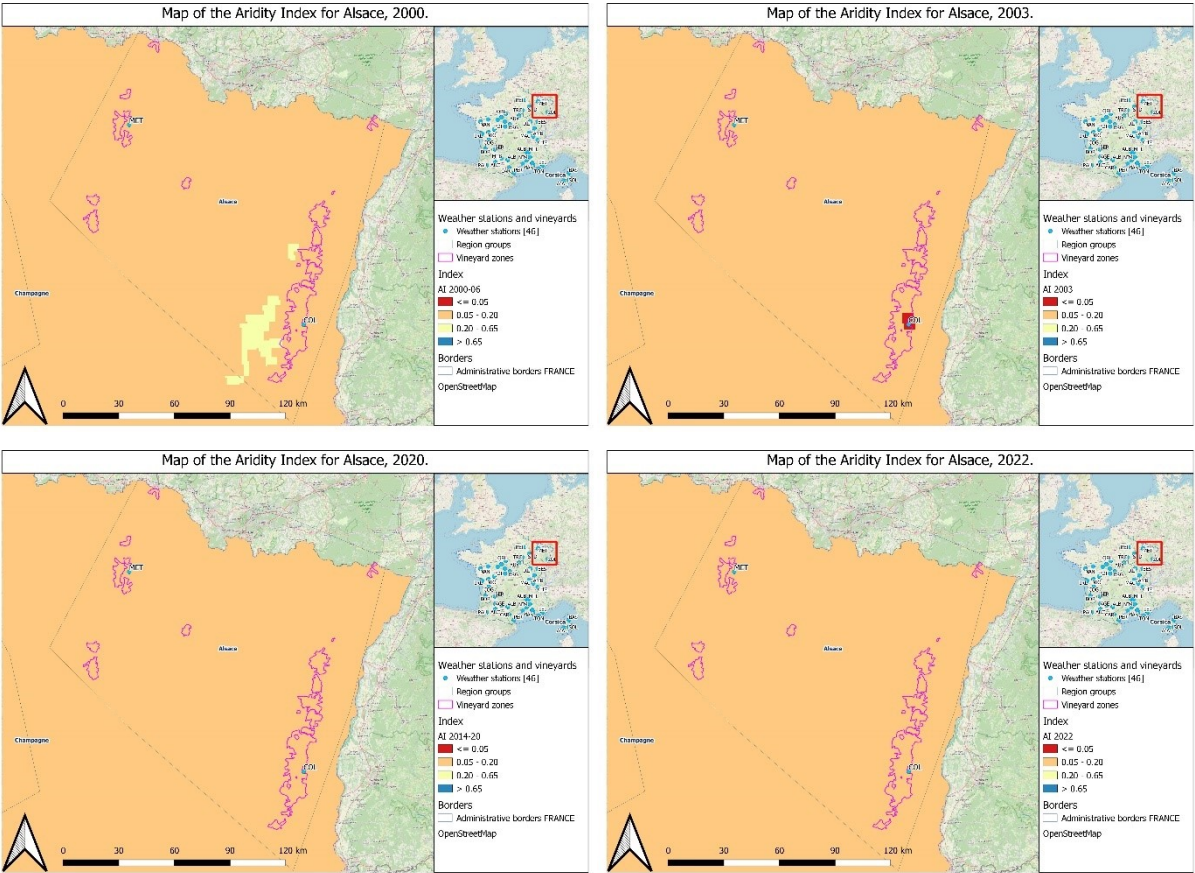


Figure 42 Alsace Aridity Index

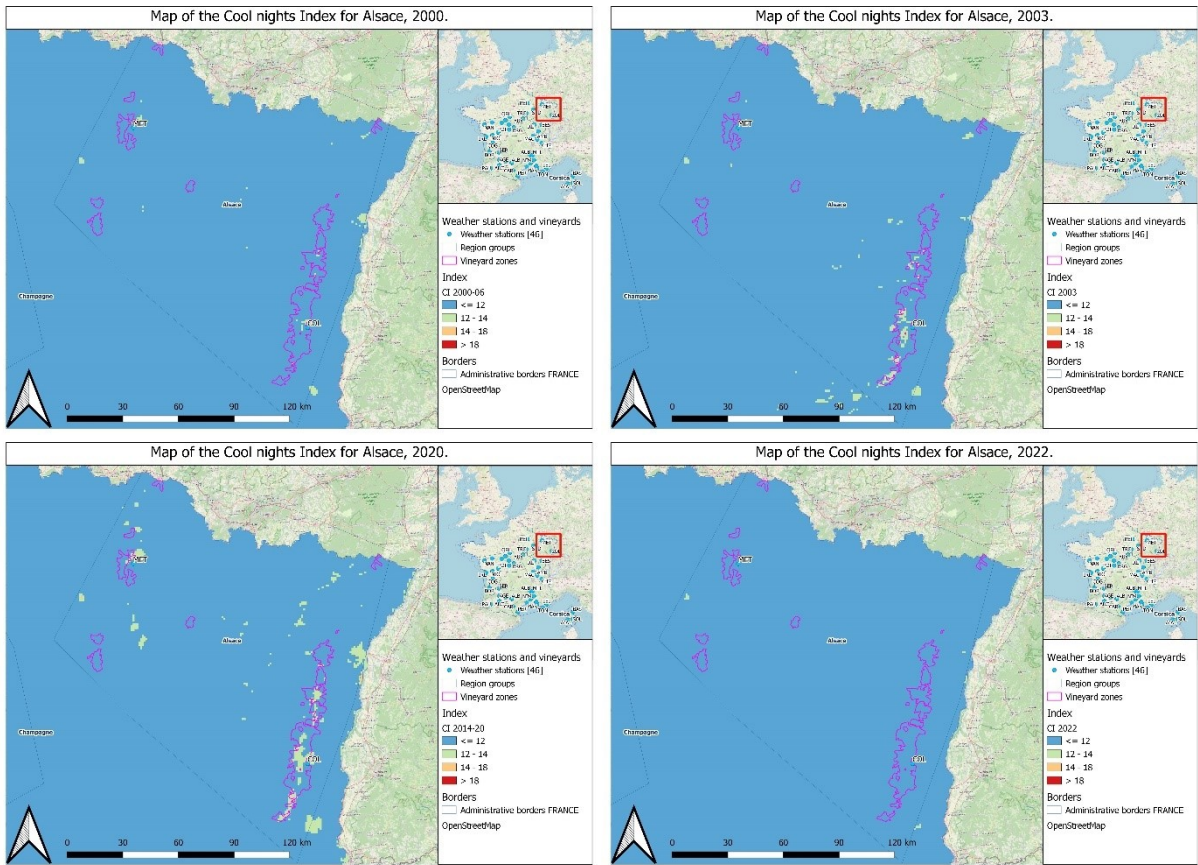


Figure 43 Alsace Cool Nights Index

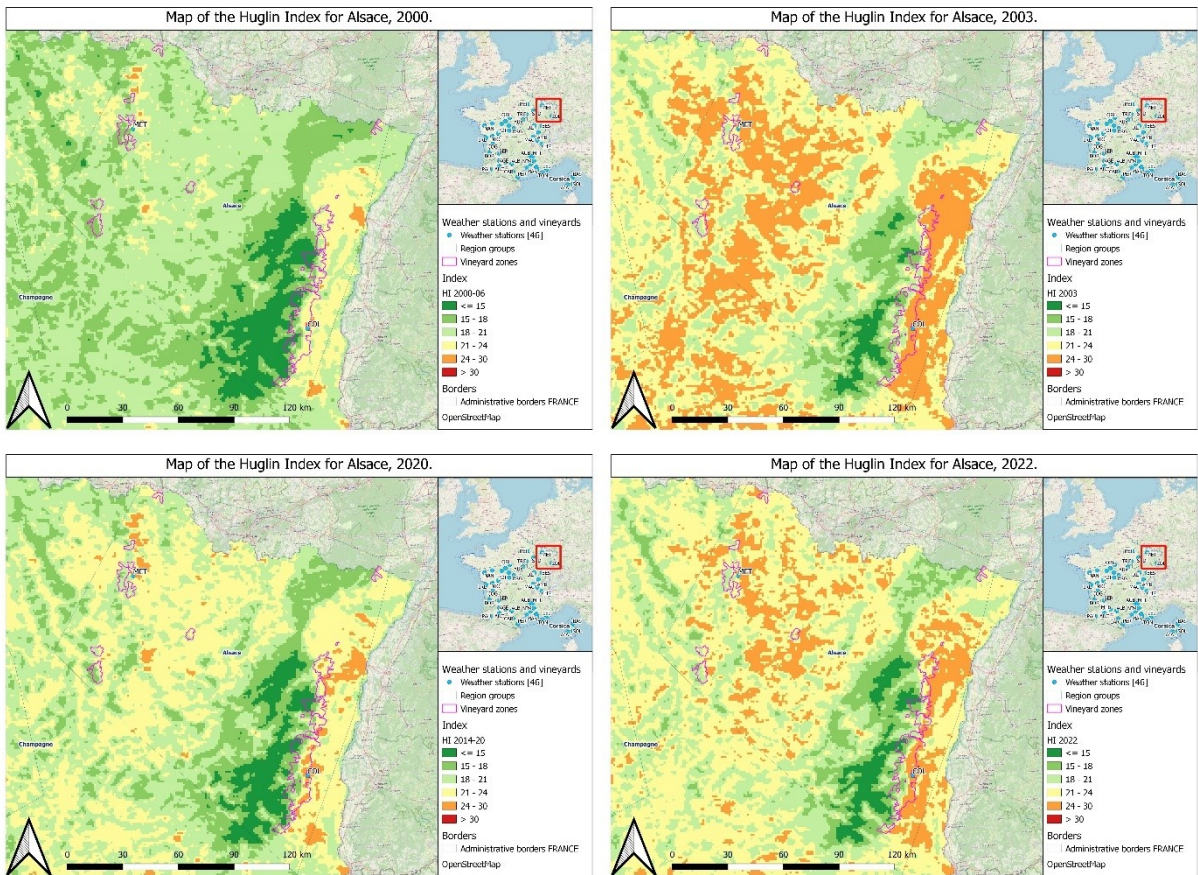


Figure 44 Alsace Huglin Index

3.2.7.3. Slopegraphs

In Alsace, data availability is limited since there are only two spatial data points, the city of Metz (MET) in Lorraine and Colmar (COL) in Alsace. Despite this small sample size, the placement of these points on opposing sides of the Vosges still serves to give them some significance, for with this arrangement we can effectively get readings from each side of the region.

Examining PT and TX slopegraphs, we see the values diverge noticeably from each other, rarely sharing the same pattern for PT, while they follow roughly the same pattern for TX. The readings from MET also seem lower than in COL. The regression lines computed through all these values don't show much in the first half of the study period months (from April to June), though in the later part (from July to September), the precipitation totals decrease over the years as the temperatures increase. For PT, the regression coefficient of MET in July especially, has a significant p-value, highlighted in blue in the table: the area is part of the larger phenomenon observed over the northern vineyards of a general decrease in precipitation over the years. For TX, the regression coefficient of COL is significant in July and September: the area is part of a larger warming phenomena present in several places over France over the years.

In conclusion, we can say that both regions of Alsace and Lorraine are different enough not to share much in terms of precipitation rates or temperature extremes.

Month	Stations	Regression Coeffs PT	p.value PT	Regression Coeffs TX	p.value TX
April	COL	-0.0814	0.936	0.130	0.149
April	MET	-0.670	0.527	0.104	0.248
May	COL	-0.975	0.389	-0.0290	0.689
May	MET	0.315	0.736	-0.00987	0.888
June	COL	0.578	0.584	0.0116	0.865
June	MET	1.75	0.0635	0.00870	0.884
July	COL	-1.58	0.219	0.176	0.0267
July	MET	-2.89	0.0426	0.135	0.108
August	COL	-1.33	0.250	0.104	0.253
August	MET	-2.20	0.123	0.0957	0.280
September	COL	-1.58	0.0890	0.146	0.0455
September	MET	-0.645	0.568	0.102	0.174

Table 13 Regression coefficients PT and TX with p-values for Alsace

Trends for Alsace

Precipitations and temperatures from April to June

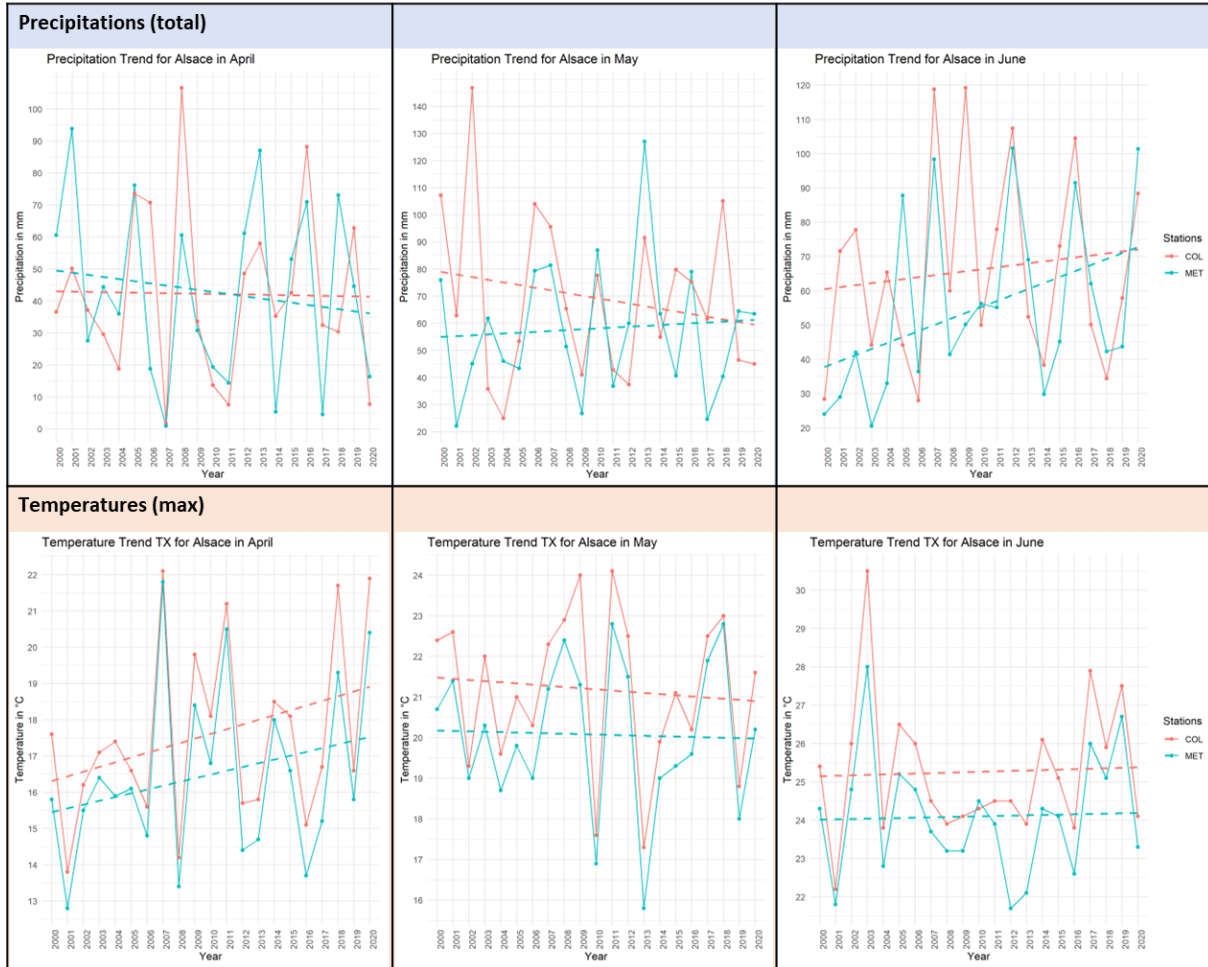


Figure 45 Alsace Precipitation & Temperature Slopegraphs April to June

Trends for Alsace

Precipitations and temperatures from July to September

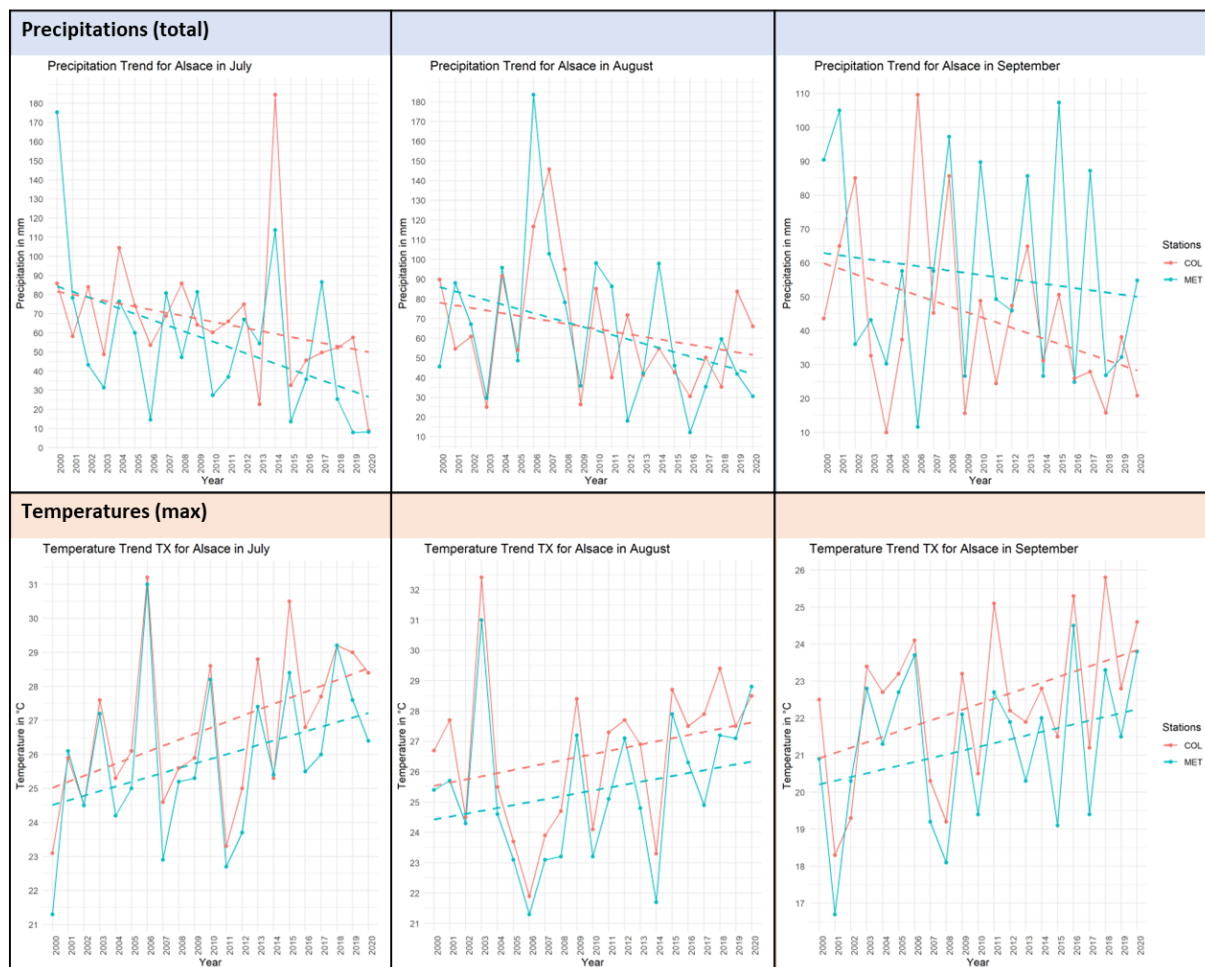


Figure 46 Alsace Precipitation & Temperature Slopegraphs July to September

3.2.8. Bourgogne

3.2.8.1. Geoclimatical Context

Positioned in the eastern part of France, just under the Champagne region, the Bourgogne vineyard occupies less than half of the region of the same name and spills south into the Rhône-Alpes region. It's located in the Saône valley between the Morvan mountains and the Jura and follows the course of the river south until reaching Lyon. The landscape alternates between plains and hills of varied slopes, and the climate is regulated by 3 great influences (continental through the east, oceanic through the northwest and Mediterranean through the south) that create a series of microclimates in the valley. The unique qualities of the area allow for the grape varieties grown there to reveal a new dimension to their character:

- For reds: black and grey Pinot and gamay
- For whites: Chardonnay, white Pinot and Aligoté

The wines of the region are historically known to be the best, rarest and thus the most expensive of France. Amongst them we count especially the Romanée-Conti, the Nuits-Saint-Georges, the Volnay, the Pouligny-Montrachet...

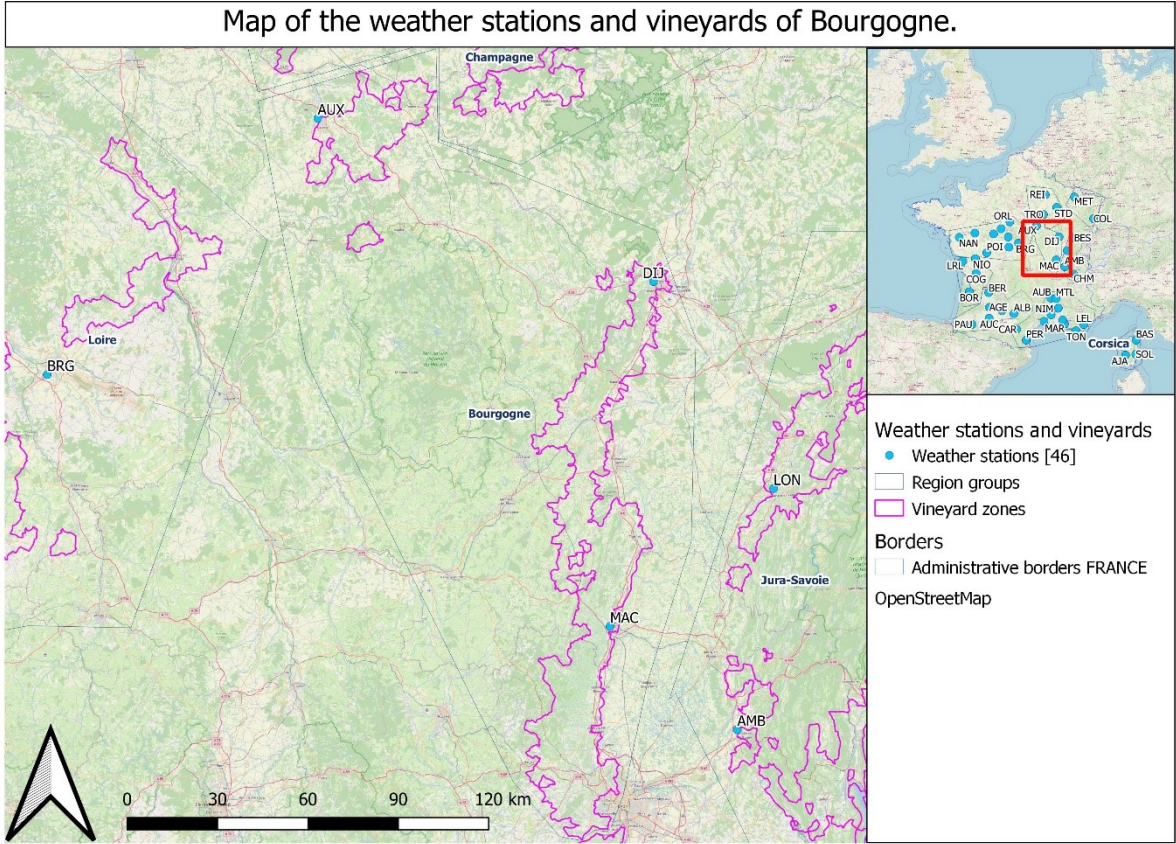


Figure 47 Bourgogne context

3.2.8.2. Index Shift Analysis

When assessing the AI for the region, we note that there hasn't been any change during the last 22 years, 2003 and 2022 included, as the area remains entirely in the arid (+1) category. This tells us that the precipitation-evapotranspiration balance of the region is stable.

The HI on the other hand gives us evidence of serious changes in the region's temperatures: what was in 2000 a region predominantly in the temperate (-1) and warm-temperate (+1) categories of the HI has since shifted. By 2020, a good part of the vineyard closest to the Saône River has gone in the warm (+2) category of the HI, especially near Dijon (DIJ) and south of Macon (MAC), from the warming influence of the Mediterranean. As for the year 2022, the heatwaves made the south of the area shift entirely into the orange warm (+2) category except for the Beaujolais mountains that remained cooler and stopped before reaching the Morvan mountains. The 2003 heatwave had an even worse effect: centered more on the middle of France

than its west like in 2022, they impacted the entire region and only stopped before the very top of the Morvan and Beaujolais mountains.

Analysis of the CI shows that the region, entirely in the very cool (+2) category in 2000, has very little changed since. The area closest to the Saône River has shifted categories into the cool (+1) from the rising influence of the Mediterranean through the valley. The 2003 and 2022 heatwaves had little effect on the CI, for the nights remained in the very cool category these two years.

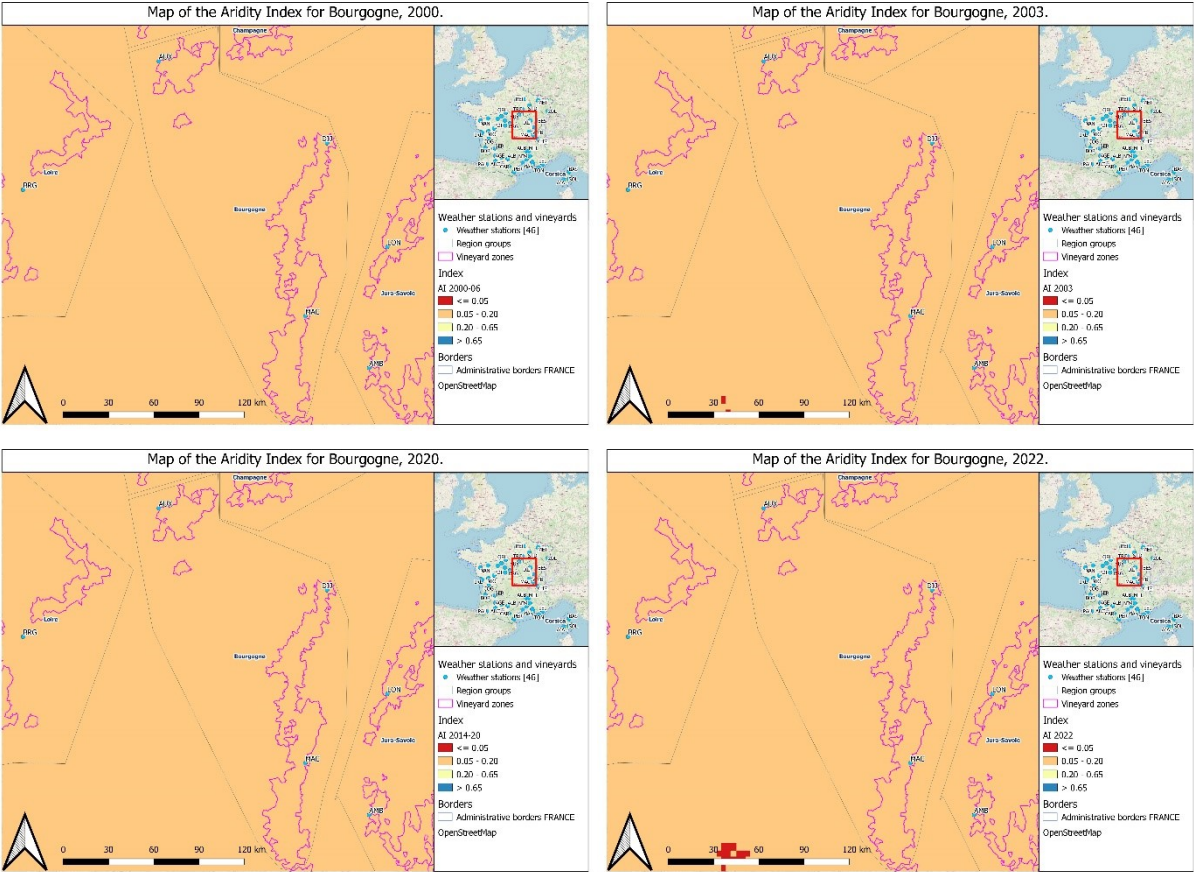


Figure 48 Bourgogne Aridity Index

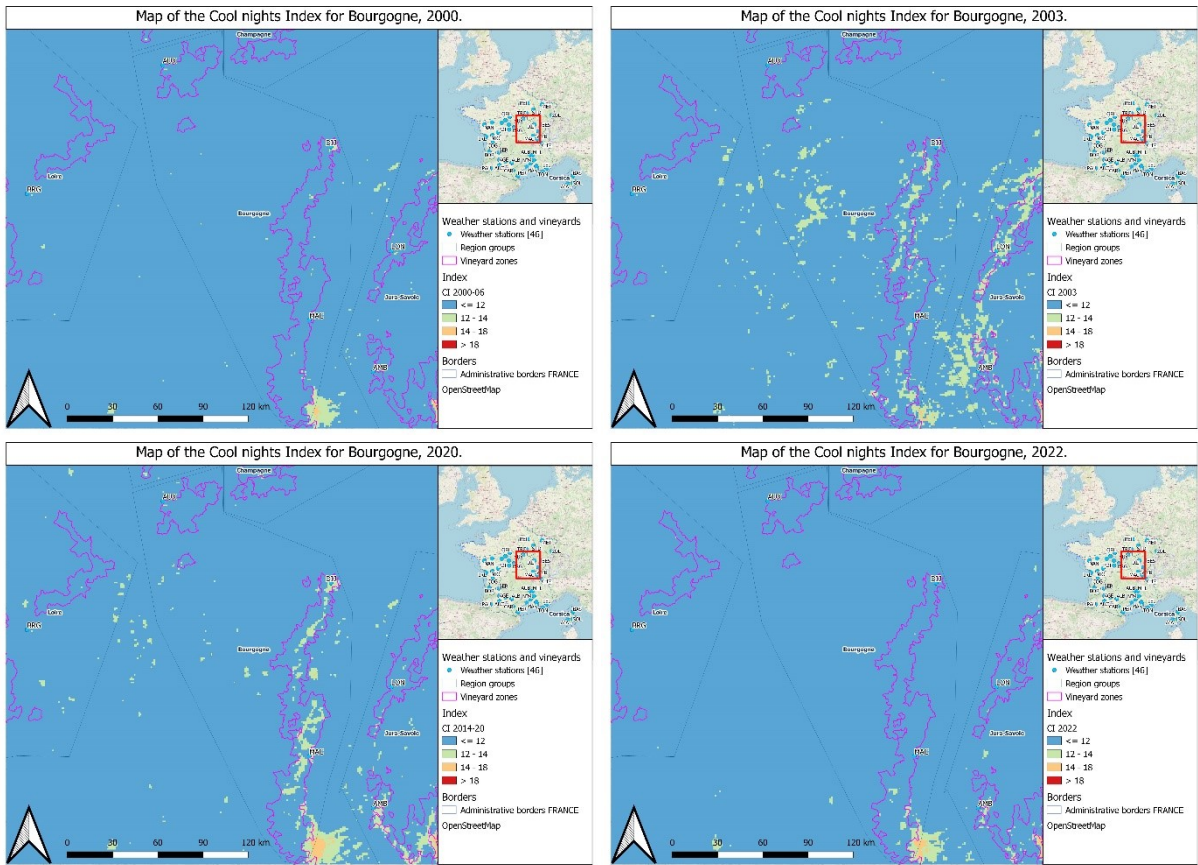


Figure 49 Bourgogne Cool Nights Index

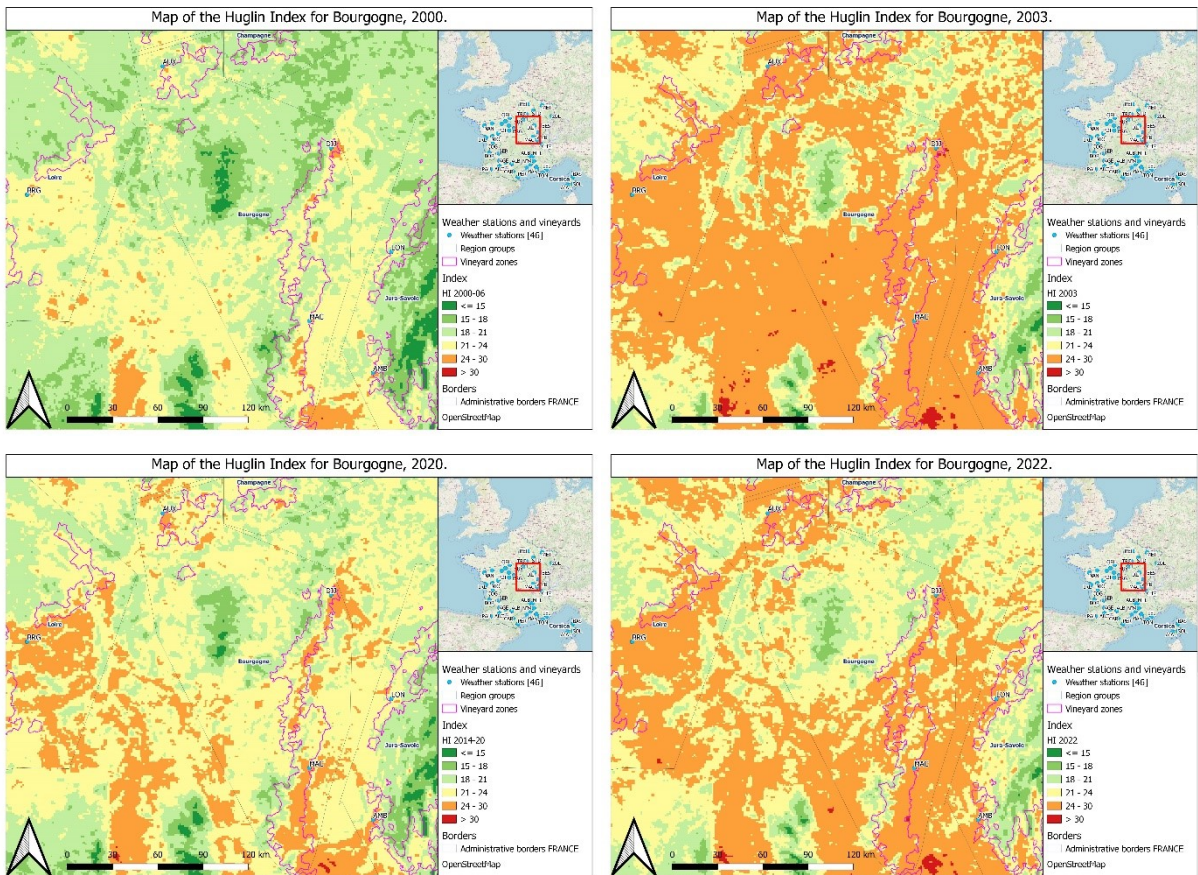


Figure 50 Bourgogne Hugin Index

3.2.8.3. Slopegraphs

The Bourgogne region only has 3 stations, but they are well-arranged in the north, south and middle of a very thin vineyard area and so remain relevant.

The PT values found on our slopegraphs are rather stable, as they rarely go over 120 mm per month, but the readings differ depending on the station. The regression lines however show a trend followed by the two stations in the south, Macon and Dijon (MAC and DIJ) that remains stable for most of the study period. However, the Auxerre station (AUX) more to the north sees a dramatic decrease of precipitations in July, that when calculating the p-values of the regression coefficients, proves to be significant.

Regarding the maximum temperature slopegraphs, we observe steep climbs and falls in temperature, very similar for all the stations, as well as the sharp peak up to 33°C in August 2003 caused by the heatwaves that hit the area that year. The regression lines of these values forms trends that tend to increase over the years, especially in July where, upon checking the p-values of the regression coefficients, we find the stations of Dijon and Macon (DIJ and MAC) recorded a significant increase in maximum temperatures of 2.5°C from 2000 to 2020.

These findings show that the Bourgogne Valley where most of the grape is cultivated is well-protected from droughts but less well from the rising temperatures caused by Climate Change, especially as they flow directly through the channel formed by the Rhône Valley from the Mediterranean.

Month	Stations	Regression Coeffs PT	p.value PT	Regression Coeffs TX	p.value TX
April	AUX	-1.43	0.274	0.116	0.200
April	DIJ	0.403	0.756	0.130	0.143
April	MAC	-0.621	0.710	0.135	0.0980
May	AUX	0.162	0.885	-0.0362	0.604
May	DIJ	0.379	0.772	-0.0204	0.763
May	MAC	-1.05	0.387	-0.0225	0.746
June	AUX	1.61	0.0699	-0.0443	0.516
June	DIJ	1.09	0.319	0.0114	0.876
June	MAC	1.24	0.320	-0.00455	0.949
July	AUX	-3.50	0.00325	0.149	0.0655
July	DIJ	-1.39	0.295	0.169	0.0422
July	MAC	-1.80	0.156	0.167	0.0448
August	AUX	-0.966	0.499	0.0875	0.352
August	DIJ	-0.572	0.617	0.102	0.242
August	MAC	-1.83	0.268	0.110	0.205
September	AUX	-0.677	0.388	0.116	0.111
September	DIJ	0.281	0.733	0.127	0.0983
September	MAC	0.294	0.775	0.144	0.0505

Table 14 Regression coefficients PT and TX with p-values for Bourgogne

Trends for Bourgogne

Precipitations and temperatures from April to June

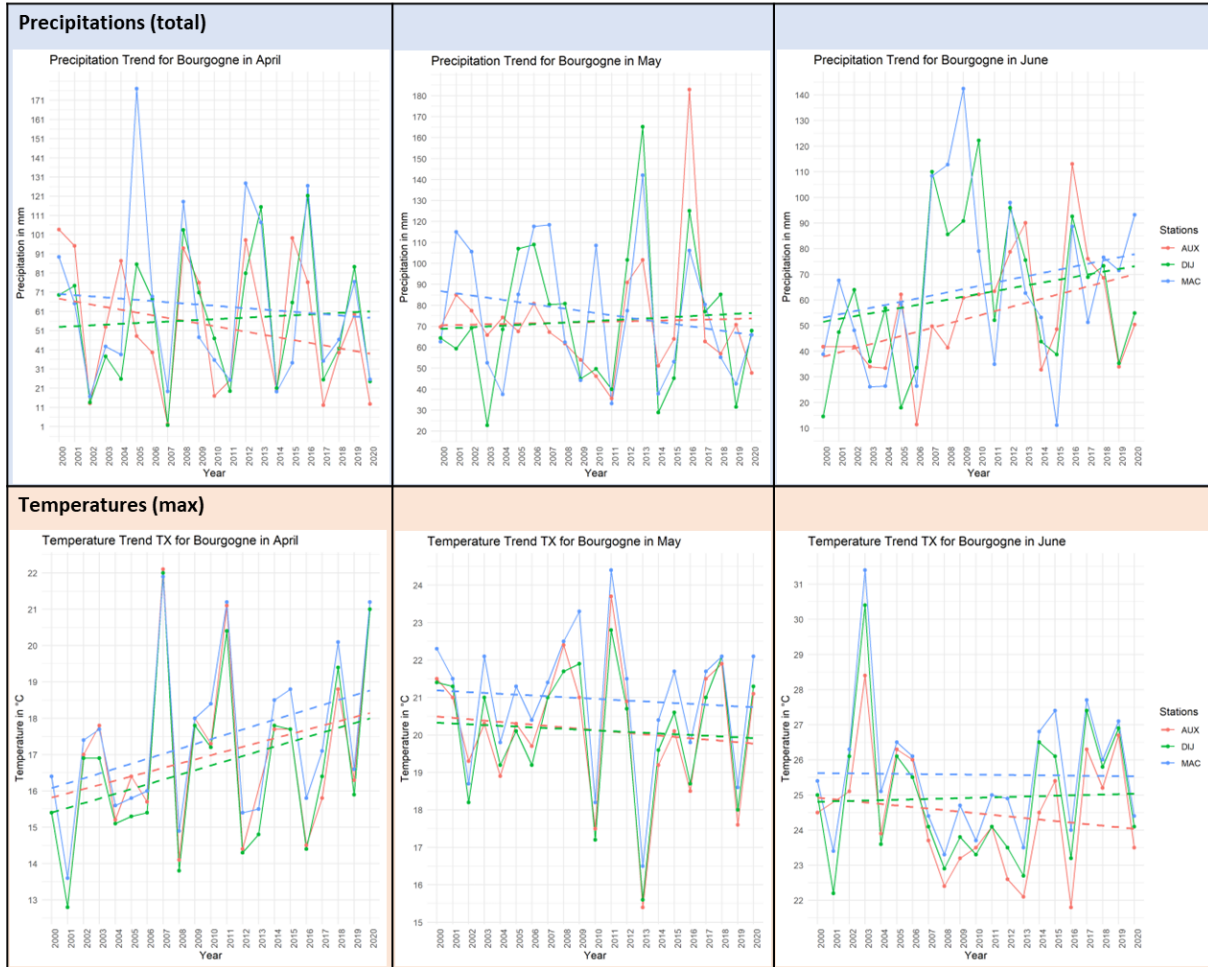


Figure 51 Bourgogne Precipitation & Temperature Slopegraphs April to June

Trends for Bourgogne

Precipitations and temperatures from July to September

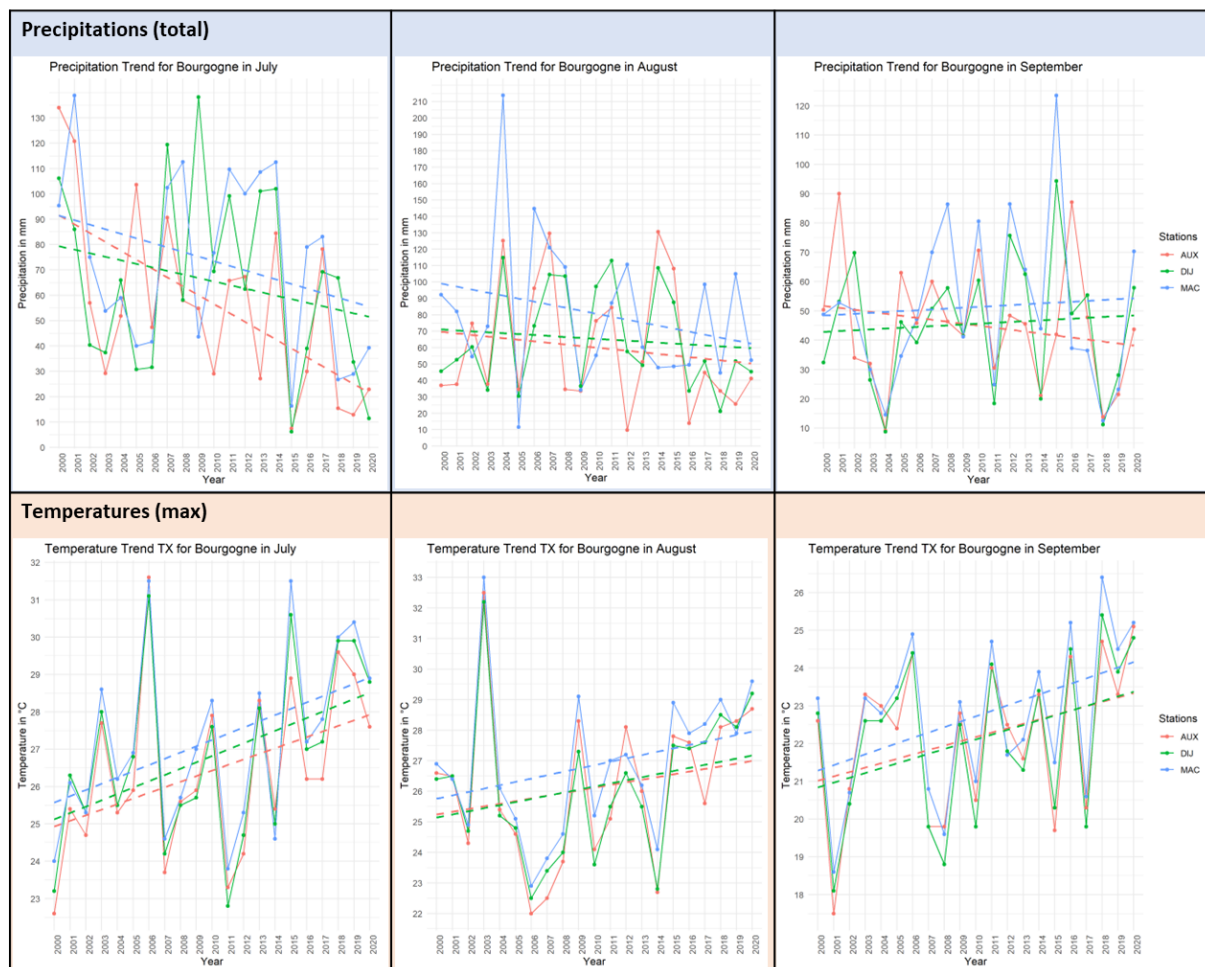


Figure 52 Bourgogne Precipitation & Temperature Slopegraphs July to September

3.2.9. Jura-Savoie

3.2.9.1. Geoclimatic Context

The region we call Jura-Savoie here is a vineyard area extending over both the Jura and Savoie regions. It's located to the east of the Bourgogne, against the Swiss border. The vineyards go around the Jura mountains on the west and south sides until they reach the Geneva Lake and the Swiss Alps, and south again along the Rhône River down to Chambéry (CHM). The varieties of grape grown in this mountainous region are:

- For red wines: the poulsard, the trousseau, black pinot, mondeuse and gamay.
- For whites: the savagnin, jacquère, roussanne, the altesse, chasselas, molette and chardonnay.

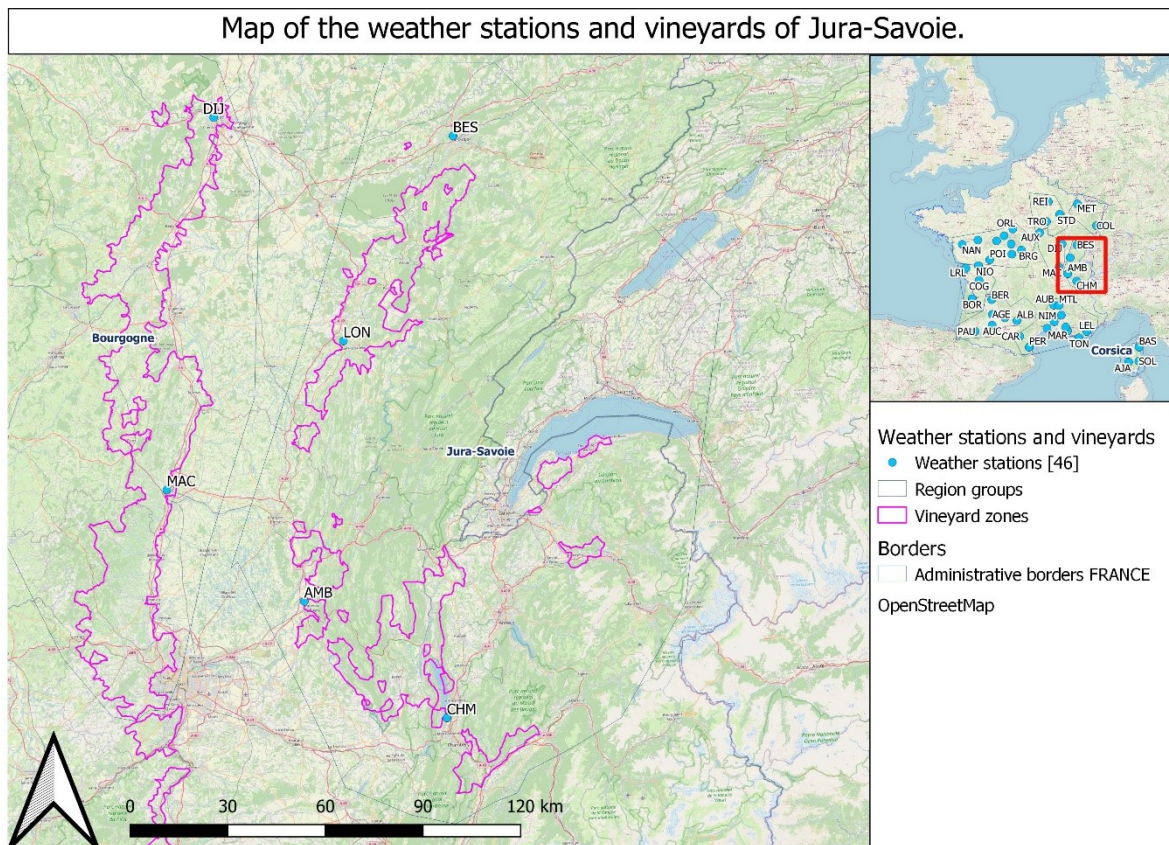


Figure 53 Jura-Savoie context

3.2.9.2. Index Shift Analysis

The region's closeness to the Swiss Alps and great Swiss lakes had lent the area around the border a semi-arid (-1) climate that we could observe in 2000, though the rest of the region was, as the majority of France, in the arid (+1) category. By 2020, the occurrence had regressed some from the region and though still apparent near the border, it was nowhere near the vineyard surface areas. We also saw in 2003 and 2022, the heatwaves caused the semi-arid (-1) area to regress even further, which is worrying: the area being used to a semi-arid climate, the rising aridity caused by climate change is sure to have a greater effect here than on other areas already used to more arid conditions.

Regarding the evolution of the HI, the proximity to the Jura mountains had given the region cool temperatures putting most of the region into the cool (-2) category and the entire vineyard surface in the temperate (-1) category, hinting at a warm-temperate (+1) category in the west from the valleys. By 2020, the vineyard surface had gone into the warm-temperate (+1) category, with even some warm (+2) category seen in its western parts spreading from the vicinity of Lyon and the Bourgogne region. The 2003 and 2022 heatwaves an acceleration of this trend, as most of the vineyard surface turned to the warm (+2) category and the rest fully into the warm-temperate (+1) for these two years. The effect on the region was similar for both years, though slightly worse in 2003, where the warm (+2) spread a bit further.

About our analysis of the CI, we first must note that although the region is fully into the very cool (+2) category, some warm (+1) spots are present: these are lakes and the city of Chambéry (CHM). In the 22 following years, the night temperatures didn't warm enough to change categories, except on the edges of the Rhône River, where they shifted to cool (+1). They also weren't much affected by the heatwaves of 2022, though the one from 2003 caused a smattering of cool (+1) zones to appear along the western edge of the Jura mountains where the northern vineyards of the region are settled.

This analysis shows that the Jura-Savoie region, although small and mountainous, has been affected by climate change through the advance of a warm and dry influence from the west, coming from the Mediterranean through the Bourgogne.

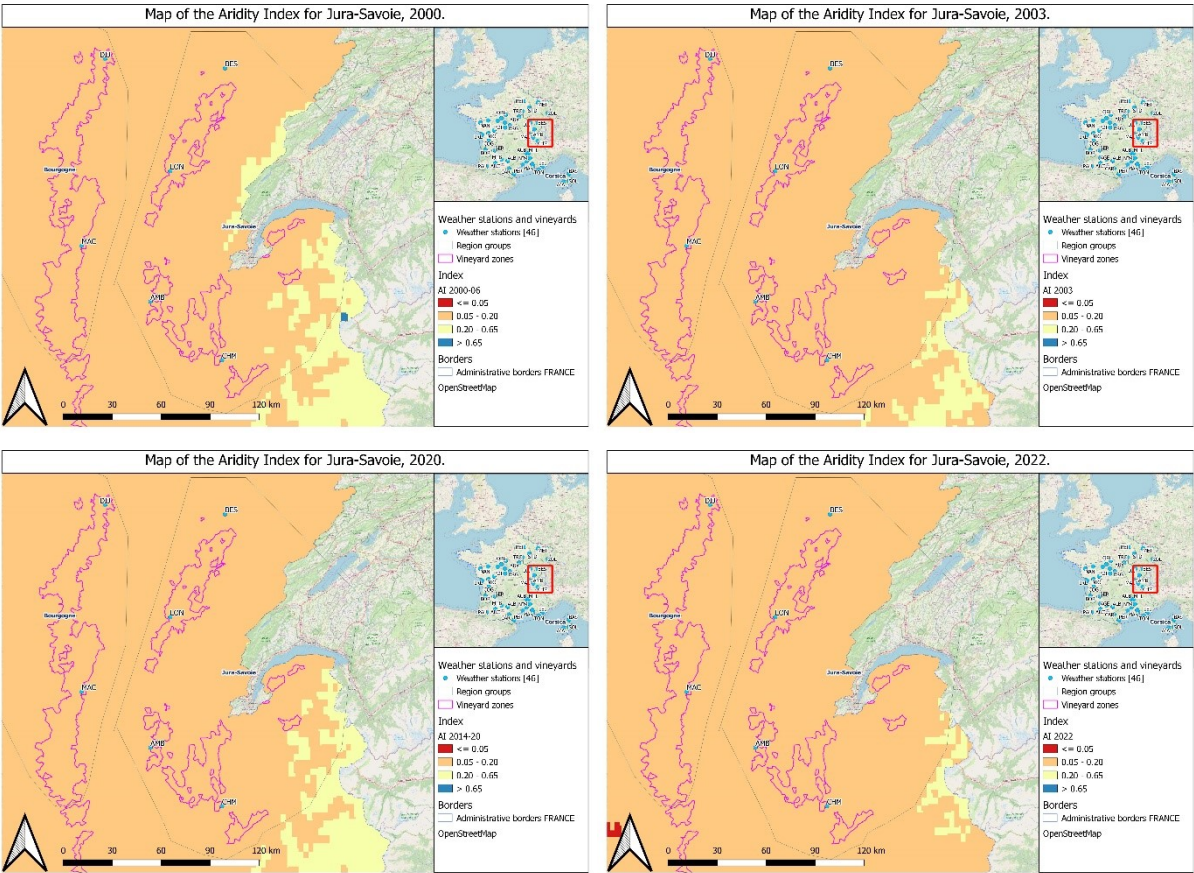


Figure 54 Jura-Savoie Aridity Index

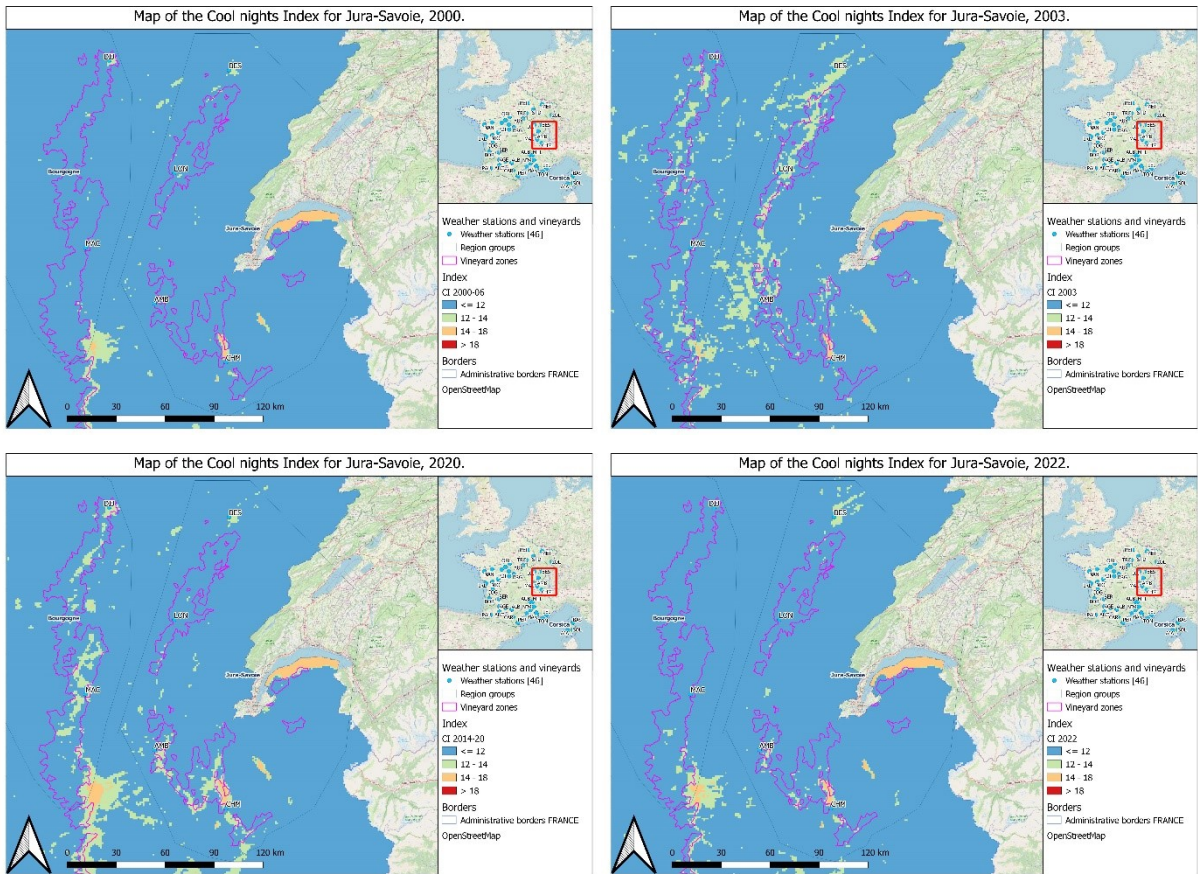


Figure 55 Jura-Savoie Cool Nights Index

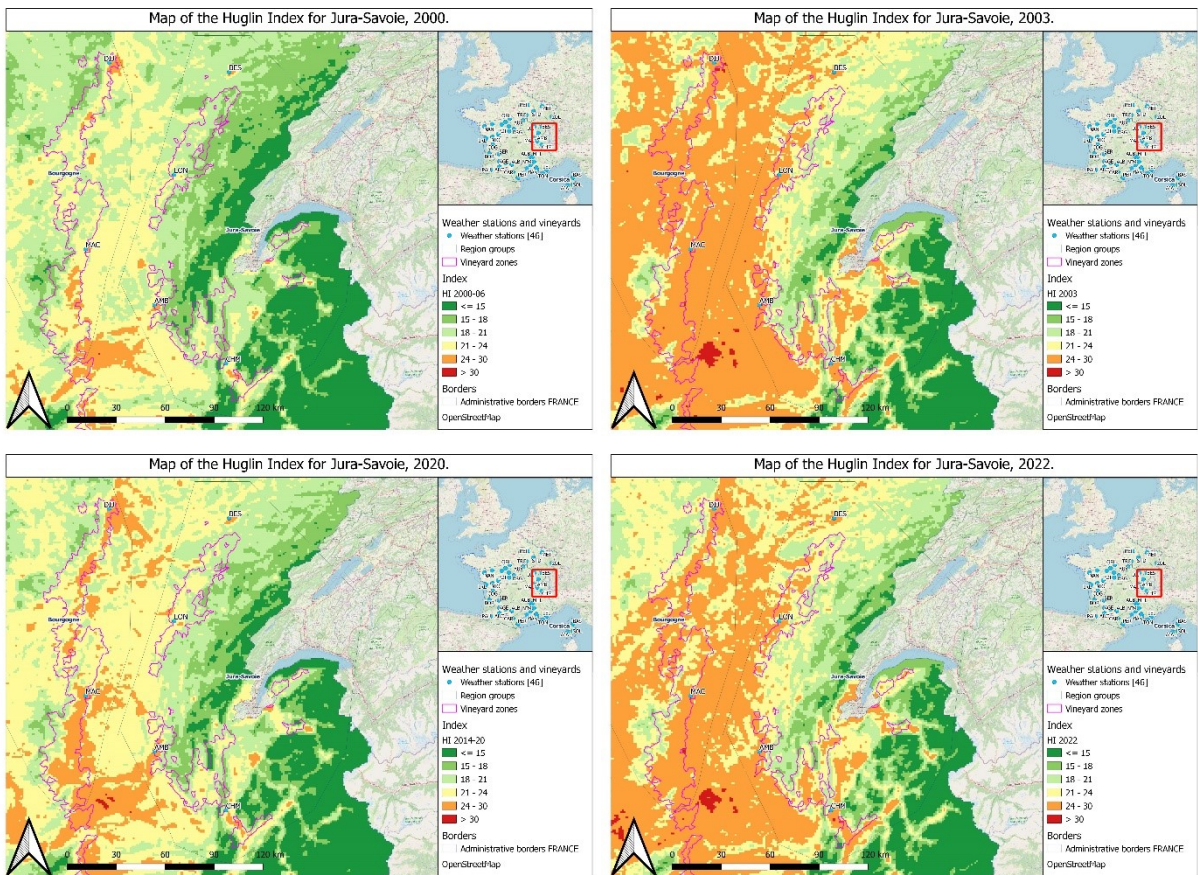


Figure 56 Jura-Savoie Huglin Index

3.2.9.3. Slopegraphs

We have 4 weather stations along the Jura-Savoie region, three of them, Besançon, Lons-sur-Saunier and Ambérieu (BES, LON and AMB) are along the western edge of the Jura, and the fourth, Chambéry (CHM) is next to the Rhône River. This configuration allows us to get a thorough view of the entire vineyard surface.

Regarding our precipitation slopegraphs: the values are a bit spread apart, and reach extremes to 20 to 150 mm every month depending on the year. However, their regression lines form trends clustered together very closely, with a stable trend, give or take 30 mm depending on the month. The only outlier to this tendency being Chambéry (CHM) in June: during that month, the station has recorded rising precipitation rates that we noticed through the regression coefficient p-values. For this city and its surroundings in June, the regression line has seen a rise of 70 mm in 21 years.

Concerning the temperature slopegraphs, we find the values are clustered in two parts: one for the northern stations of Besançon and Lons (BES and LON), and another for the southern ones of Ambrieu and Chambéry (AMB and CHM), with the northern stations noticeably colder than the others. We also find the spike in temperatures in August 2003 corresponding to that year's heatwaves. The regression lines formed by these values form 2 trends over the months, one following both Ambrieu and Chambéry (AMB and CHM) and the other, a bit colder but with the same direction, for Besançon and Lons (BES and LON).

The p-values calculated from these regression coefficients show two cities underwent a significant increase in TX over the years in July, as well as 3 for September. In July, the stations of Ambérieu and Besançon (AMB and BES) saw an increase of 3.5°C for their regression lines, and in September, AMB, BES and CHM saw an increase of 3°C for AMB, against 2.5°C for CHM and BES.

These findings tell us that in the region, precipitations have tended to fall over the years while temperatures increased, which is a worrying course of events for the region's climate.

Month	Stations	Regression Coeffs PT	p.value PT	Regression Coeffs TX	p.value TX
April	AMB	-1.37	0.536	0.139	0.0819
April	BES	-0.544	0.802	0.122	0.158
April	CHM	-1.33	0.469	0.132	0.0848
April	LON	-0.990	0.650	0.124	0.142
May	AMB	-0.0197	0.993	-0.0218	0.768
May	BES	1.73	0.272	-0.0334	0.646
May	CHM	2.63	0.0550	-0.0403	0.573
May	LON	0.593	0.717	-0.0294	0.682
June	AMB	1.96	0.129	-0.0186	0.808
June	BES	2.20	0.216	0.00234	0.973
June	CHM	3.38	0.0173	-0.0390	0.582

June	LON	1.15	0.479	-0.00104	0.989
July	AMB	-1.76	0.378	0.175	0.0363
July	BES	-3.32	0.106	0.172	0.0443
July	CHM	-1.00	0.632	0.158	0.0538
July	LON	-3.43	0.0915	0.154	0.0681
August	AMB	-2.99	0.0841	0.114	0.213
August	BES	-1.60	0.413	0.105	0.261
August	CHM	-1.32	0.401	0.102	0.214
August	LON	-2.94	0.106	0.0917	0.326
September	AMB	-0.785	0.653	0.163	0.0193
September	BES	-0.522	0.698	0.146	0.0469
September	CHM	-0.934	0.604	0.138	0.0350
September	LON	0.215	0.888	0.134	0.0634

Table 15 Regression coefficients PT and TX with p-values for Jura-Savoie

Trends for Jura-Savoie

Precipitations and temperatures from April to June

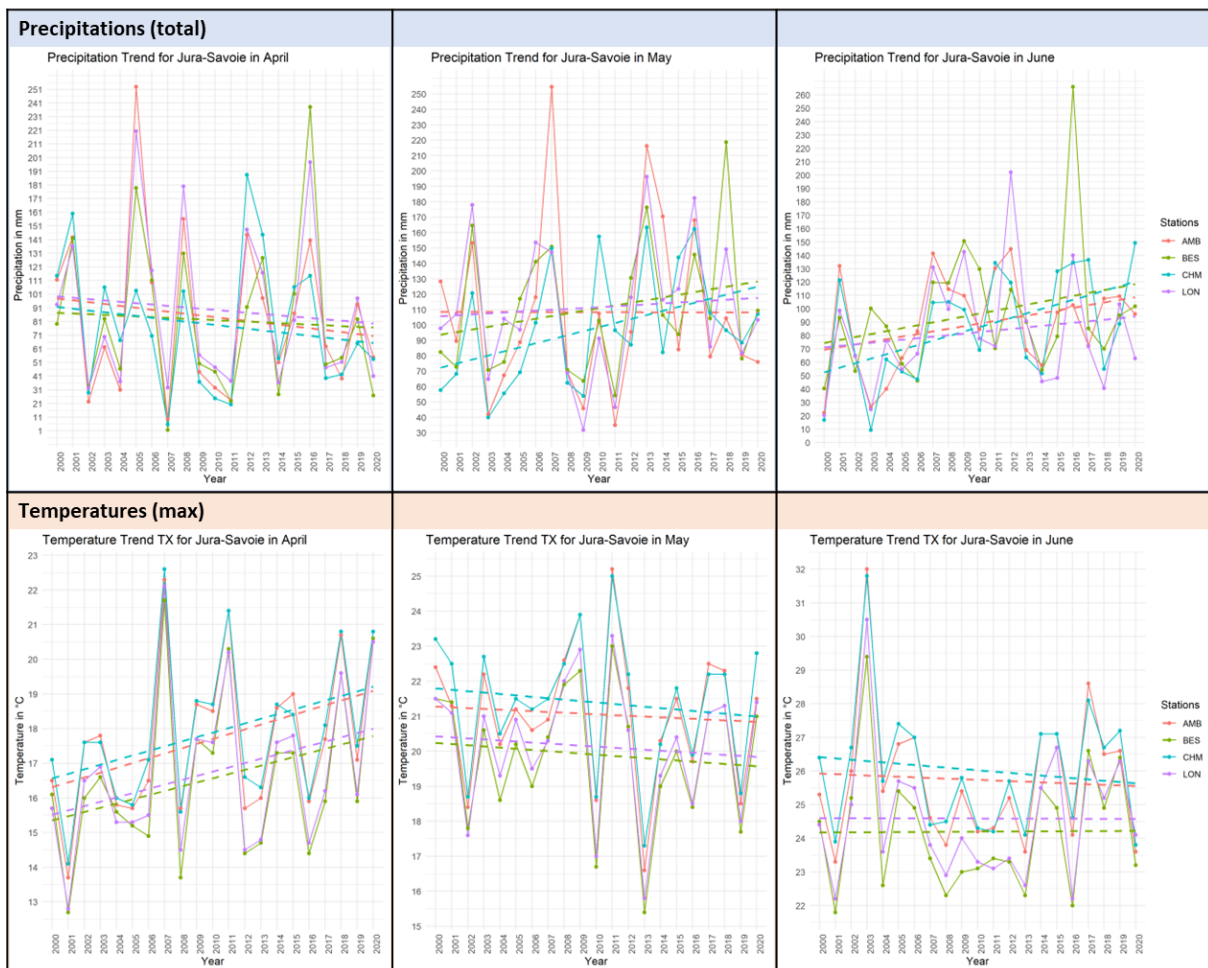


Figure 57 Jura-Savoie Precipitation & Temperature Slopegraphs April to June

Trends for Jura-Savoie

Precipitations and temperatures from July to September

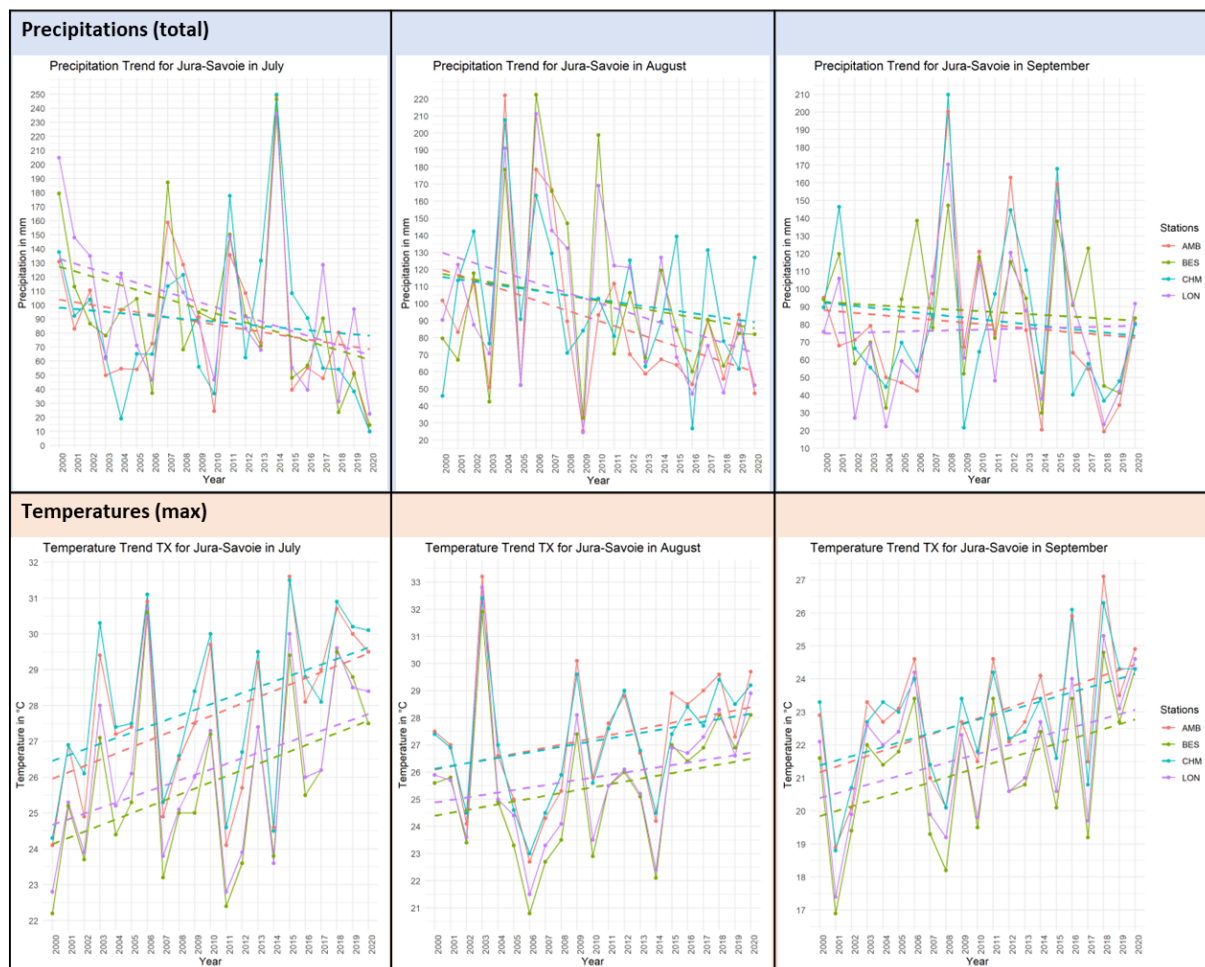


Figure 58 Jura-Savoie Precipitation & Temperature Slopegraphs July to September

3.3. Regression coefficients graphic representation

Through our analysis of the regression coefficients of the slopegraphs in each city for each month of the study, we created maps with the slope of the coefficients spatially represented as a points vector layer onto our QGIS project. We repeated this process for each of the 6 months of our study and for the PT and TX values, for a total of 12 maps. At the same time, we know that several of these values denoted a significant increase or decrease of PT or TX over the years in certain areas. To better visualize their spatial distribution and any possible trends, we manually input the concerned stations onto a polygon vector layer on the maps of the corresponding regression coefficients.

3.3.1. Precipitations PT

The patterns taken by PT regression coefficient values indicate a significant decrease of precipitation from 2000 to 2020 in April, in the vicinity of Reims (REI). The month of June sees a significant increase in precipitations over these years, on the Atlantic front and covering

parts of the Loire, Bordeaux-Charentes and Midi regions, as well as the city of Chambéry (CHM) in the Jura-Savoie, which has probably seen an increase in Mediterranean episodes. We observe in July a significant decrease in precipitations affecting the entire north side of France, and impacting the Loire, Champagne, and parts of the Bordeaux-Charentes, Bourgogne and Alsace regions. September only sees a significant decrease in precipitation in Orange (ORA), which is probably an outlier.

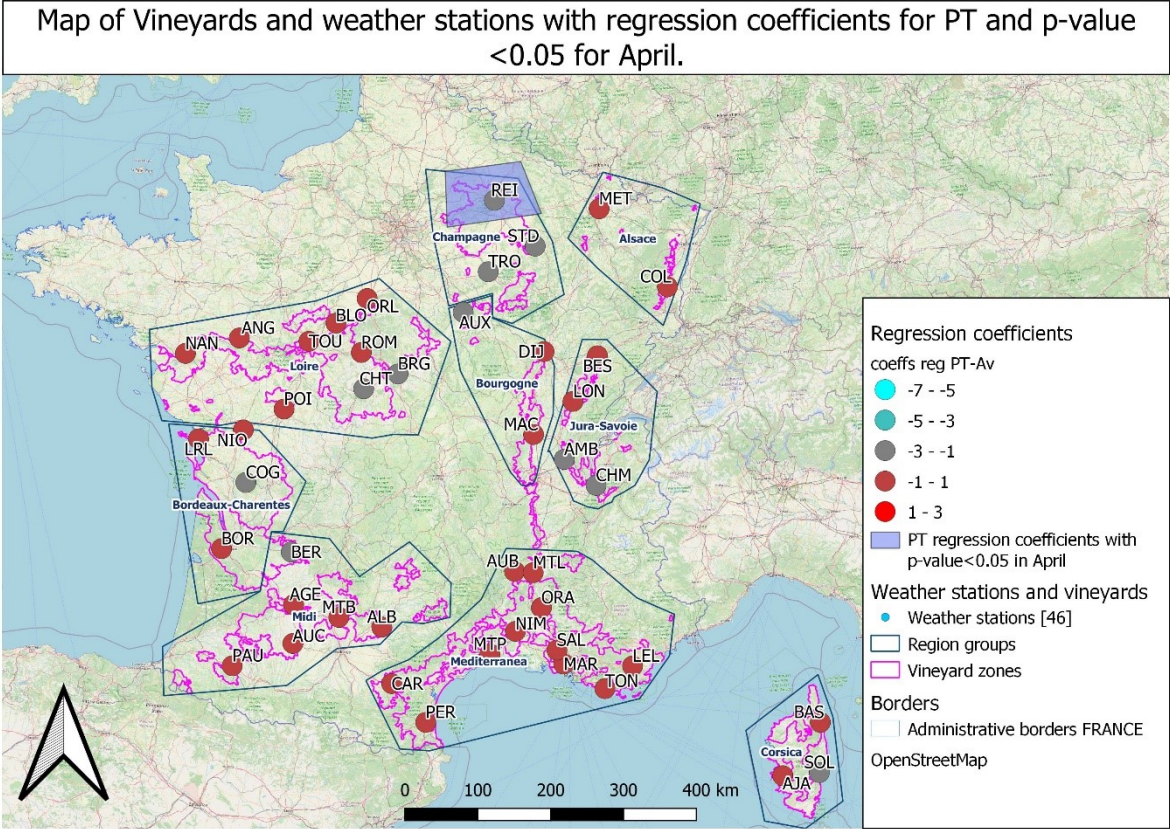


Figure 59 Regression coefficients for Precipitation in April

Map of Vineyards and weather stations with regression coefficients for PT for May.

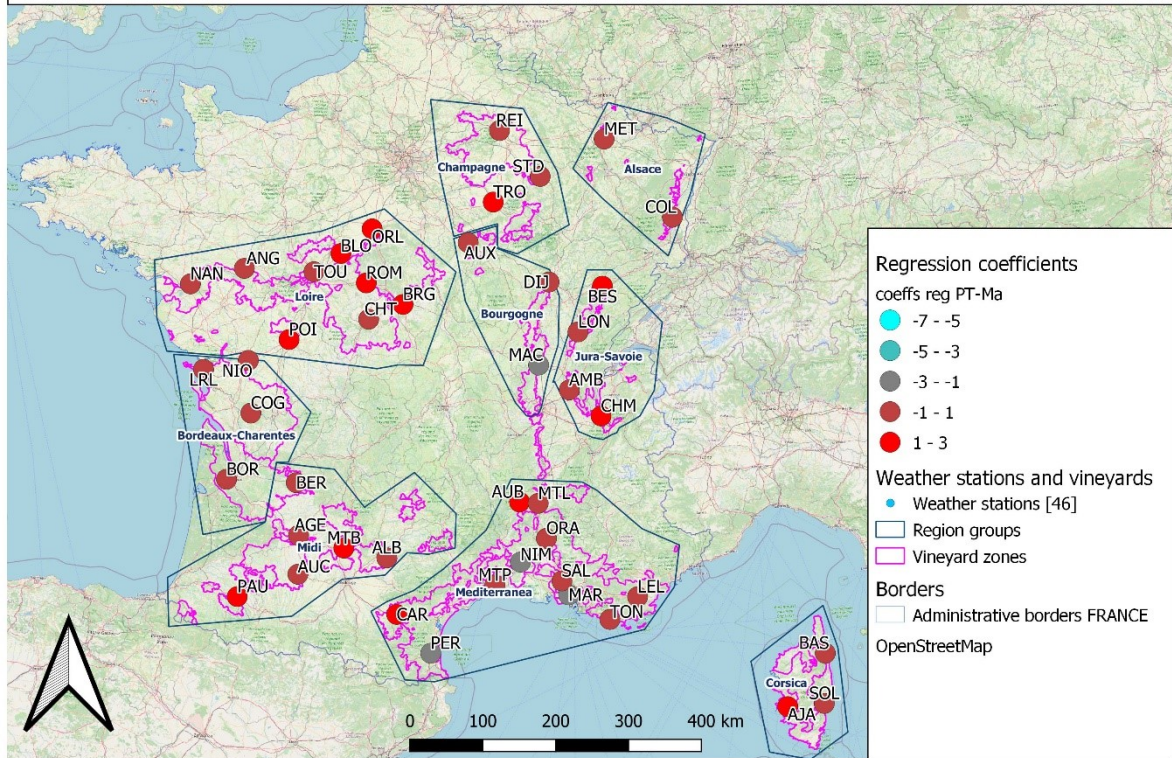


Figure 60 Regression coefficients for Precipitation in May

Map of Vineyards and weather stations with regression coefficients for PT and p-value <0.05 in June.

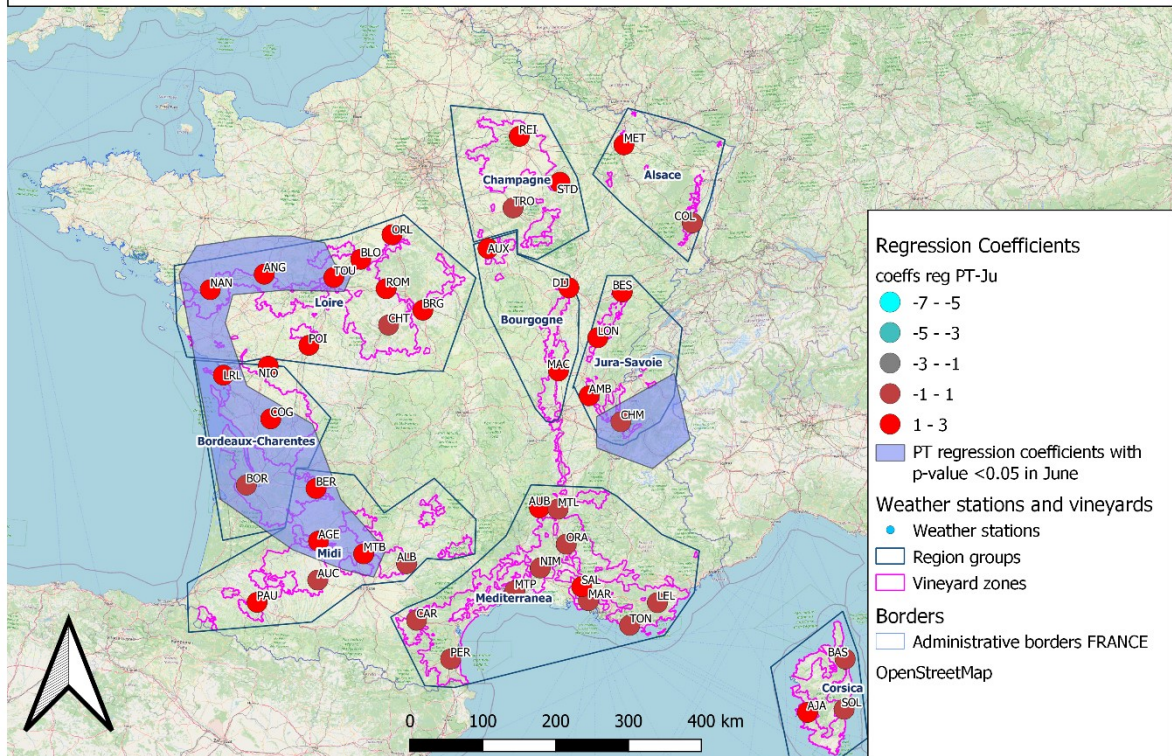


Figure 61 Regression coefficients for Precipitation in June

Map of Vineyards and weather stations with regression coefficients for PT and p-value <0.05 for July.

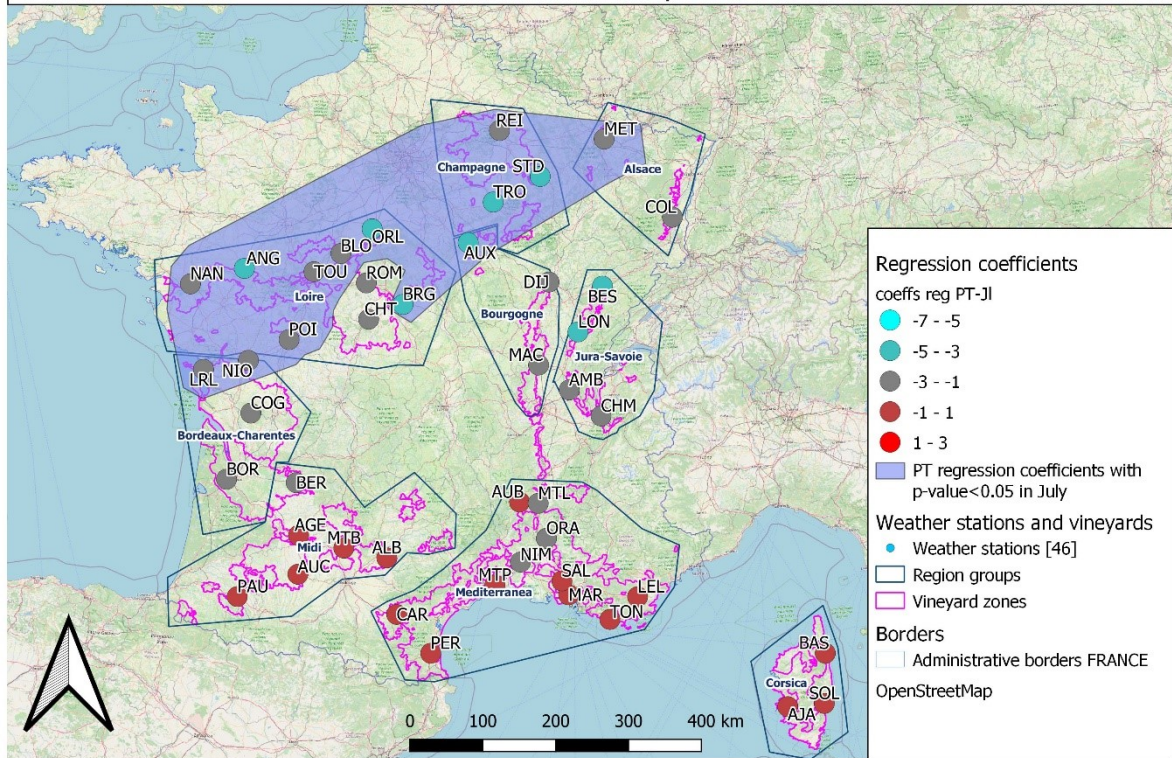


Figure 62 Regression coefficients for Precipitation in July

Map of Vineyards and weather stations with regression coefficients for PT for August.

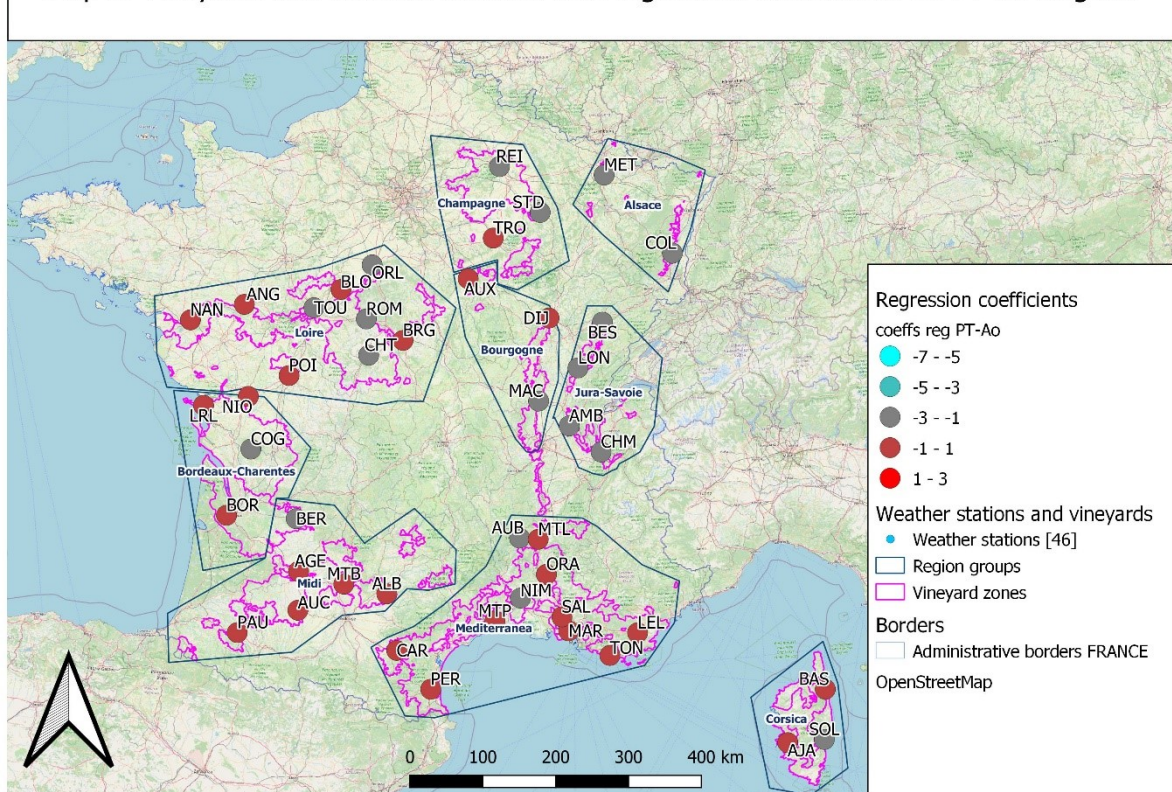


Figure 63 Regression coefficients for Precipitation in August

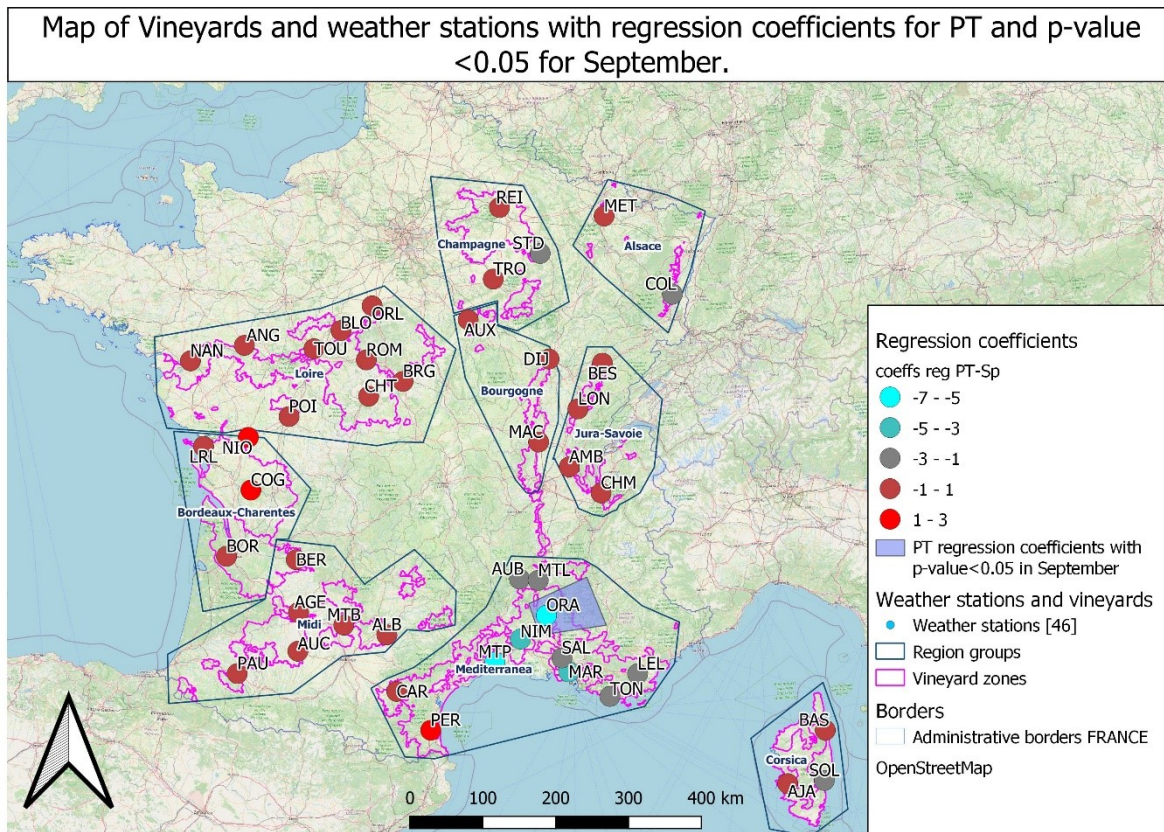


Figure 64 Regression coefficients for Precipitation in September

3.3.2. Maximum Temperatures TX

The patterns taken by TX regression coefficient values indicate a significant increase of maximum temperatures, only present in Corsica for April, and going inland through the Mediterranean and the Atlantic in July while impacting parts or the entirety of almost all the regions. Another significant increase of temperature is present in September through the Mediterranean Sea and covering Corsica, Mediterranean, and going north through the Jura-Savoie to reach Alsace.

Map of Vineyards and weather stations with regression coefficients for TX and p-value <0.05 for April

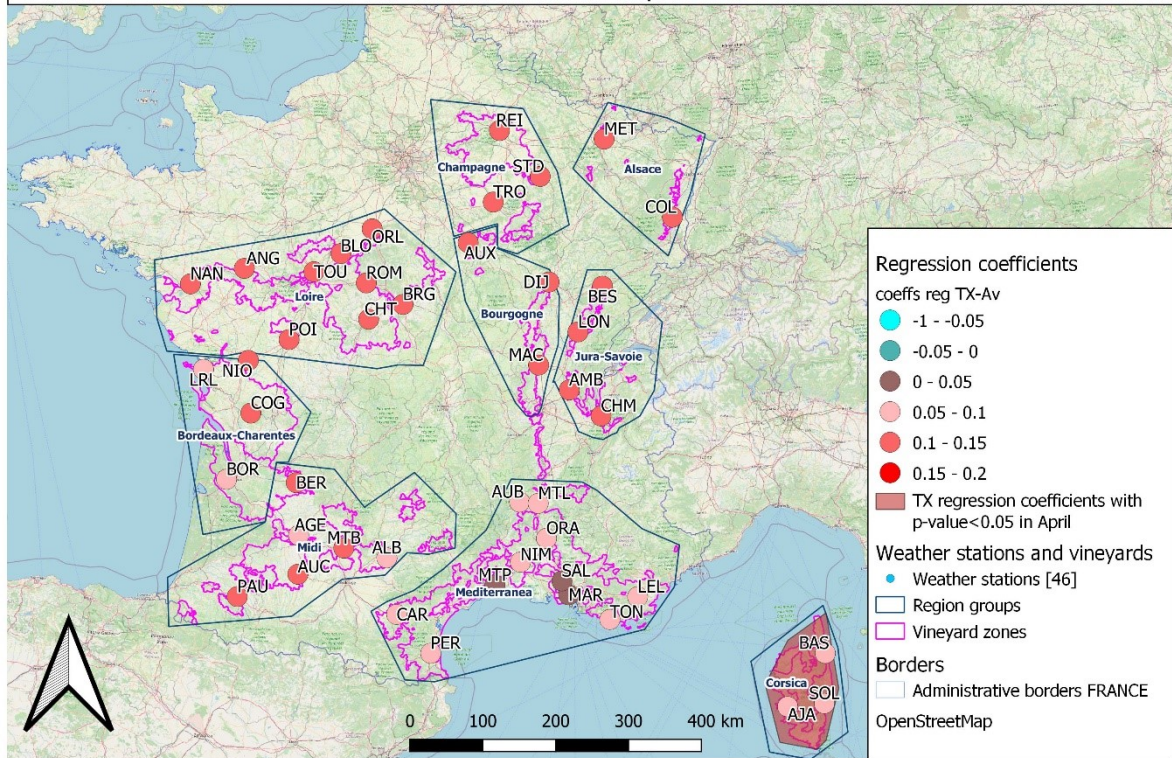


Figure 65 Regression coefficients for Maximum Temperatures in April

Map of Vineyards and weather stations with regression coefficients for TX for May.

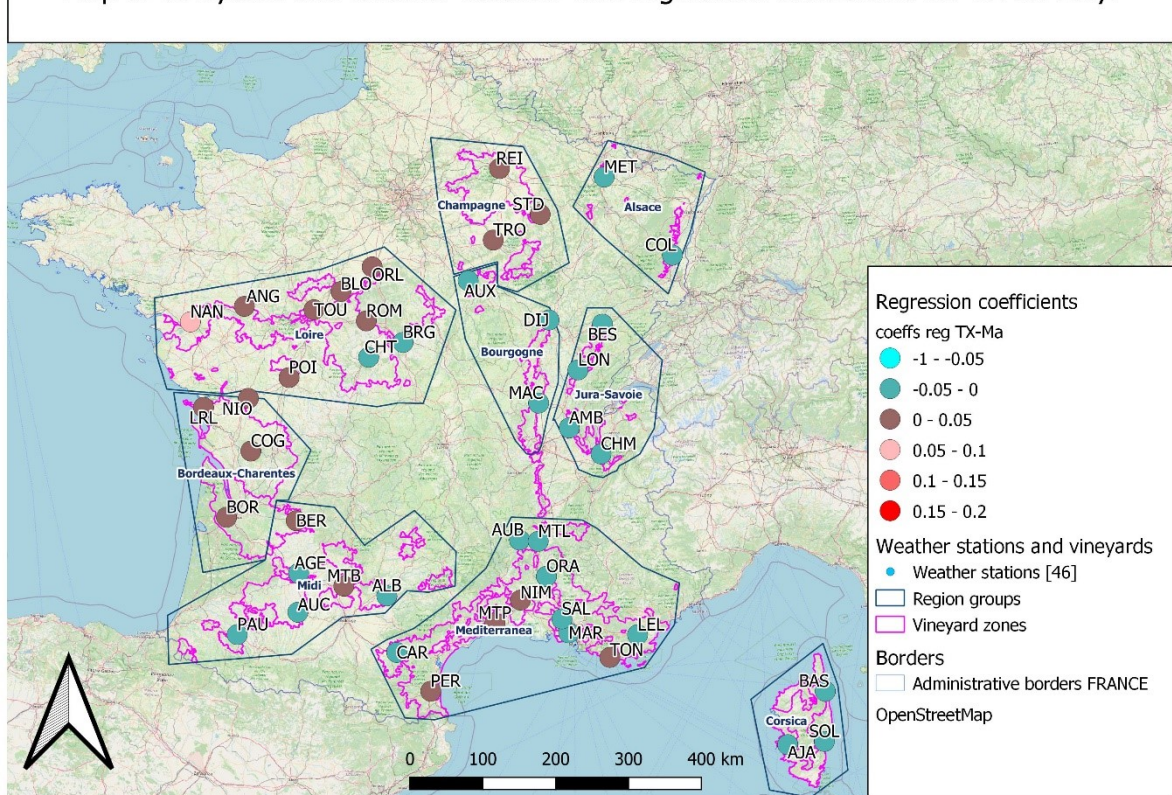


Figure 66 Regression coefficients for Maximum Temperatures in May

Map of Vineyards and weather stations with regression coefficients for TX for June.

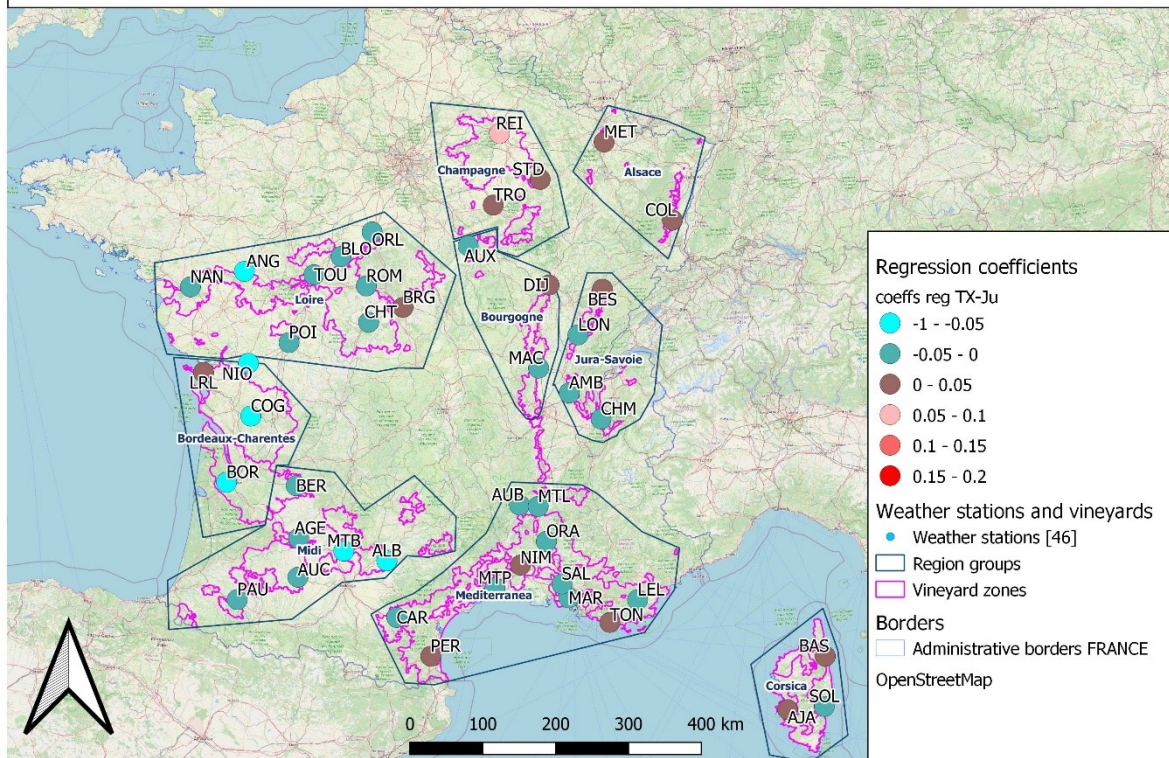


Figure 67 Regression coefficients for Maximum Temperatures in June

Map of Vineyards and weather stations with regression coefficients for TX and p-value <0.05 for July.

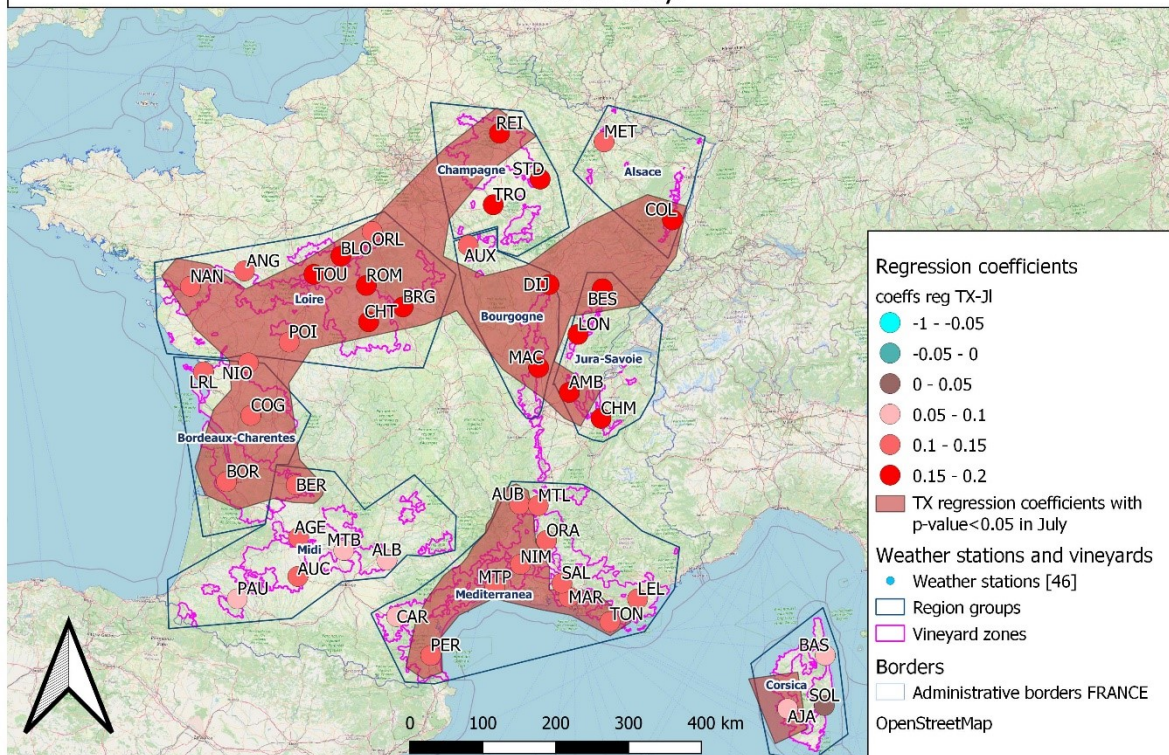


Figure 68 Regression coefficients for Maximum Temperatures in July

Map of Vineyards and weather stations with regression coefficients for TX for August.

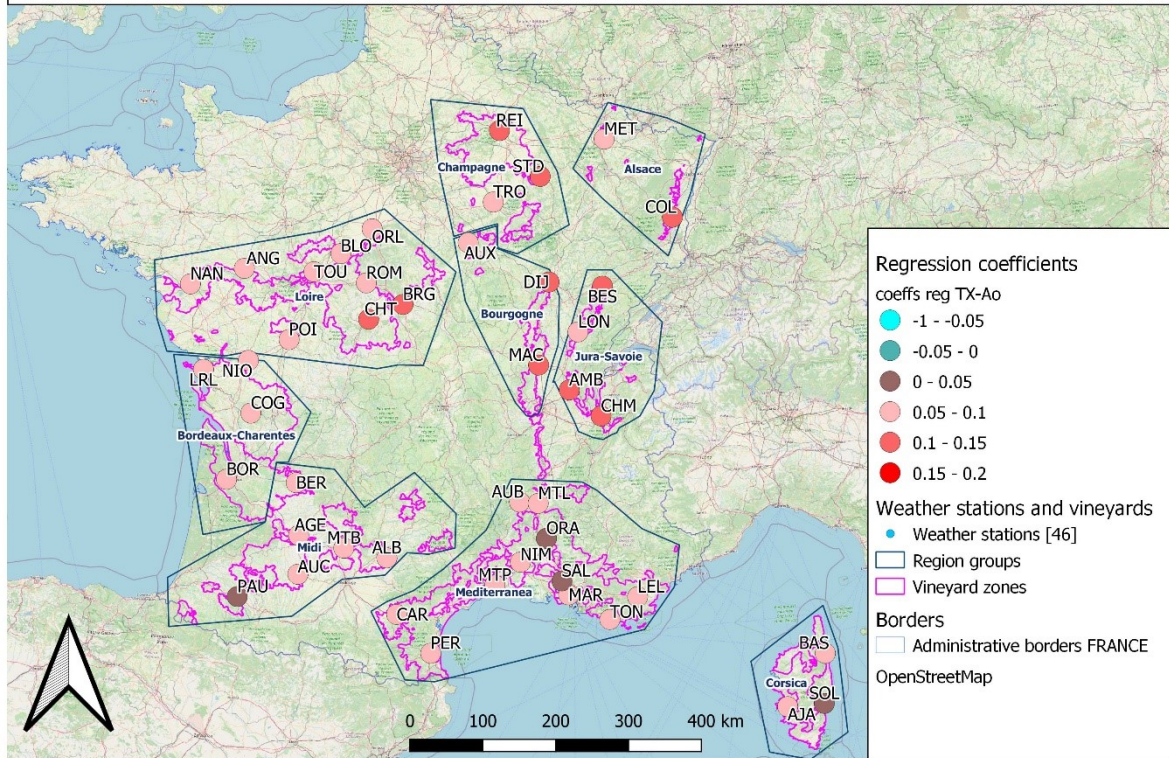


Figure 69 Regression coefficients for Maximum Temperatures in August

Map of Vineyards and weather stations with regression coefficients for TX and p-value <0.05 in September.

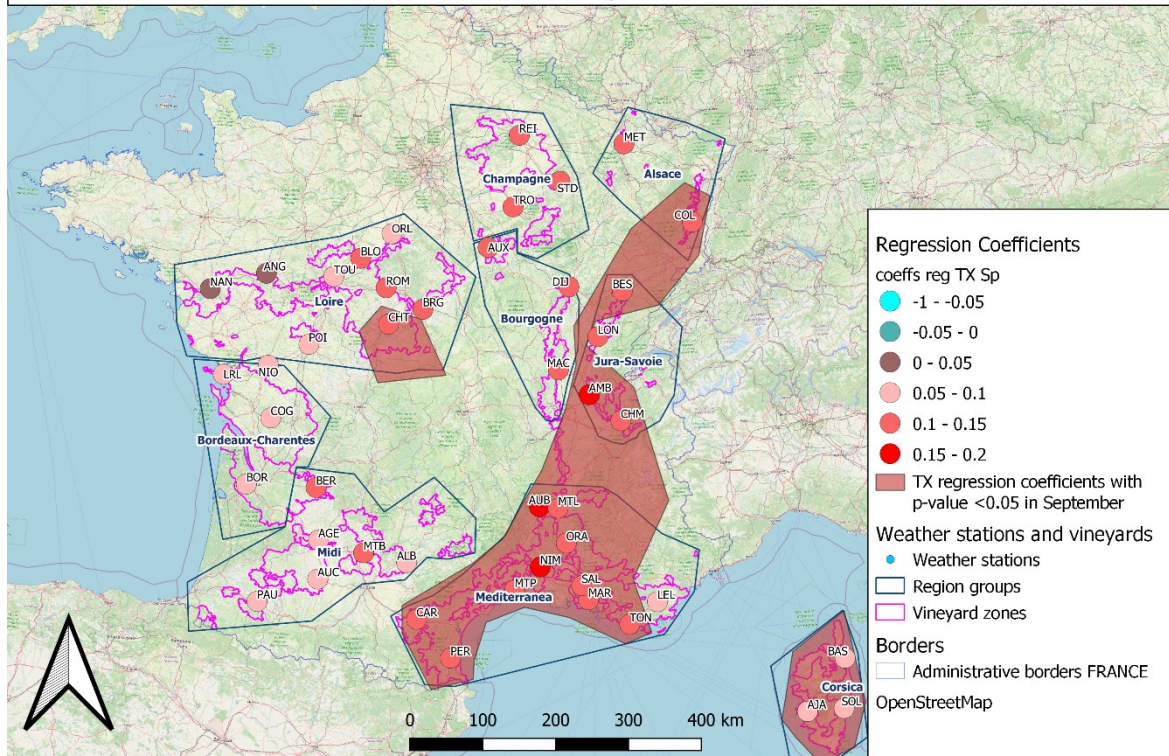


Figure 70 Regression coefficients for Maximum Temperatures in September

4. Discussion

4.1. Key Findings and their Implications

In this section, we will discuss the key findings of our study according to our research objectives, list the consequences the observed climatic shifts we observed have on the winemaking regions of France, future opportunities, ongoing research on these topics, and limits of the analysis.

First, we wish to discuss the temperature and precipitation trends and the consequences of their influence on the grape producing regions. We will cover their origin, spatial impacts, impact on the night temperatures and aridity index. Then, we'll look at potential impact on separate regions.

4.1.1. High Temperature Origins and Dynamics

In July, warm winds coming from Spain transport heat North through the Atlantic currents and around the Pyrénées mountains to hit the west of France on the Aquitaine Basin. The same way in July and September, the Mediterranean region's significant increase in maximum temperatures most likely originates from North Africa and are carried to France through the Mediterranean Sea. These two increasing warming trends travel respectively up the Loire Valley and through the Rhone Valley after impacting the coasts. The country's geography explains why the spread of these high temperature trends reaches far inland.

The severe heatwaves that occurred in France in both 2003 and 2022 both hit equally hard even being 20 years apart, but had distinctly different impacts, both in affected areas and propagation patterns. Moreover, though climate change has a visible effect on September night temperatures, it seems to be reduced in the years of heatwave occurrence. This anomaly might be a result of the increased evaporation during heatwaves leading to sudden precipitations and a general cooling of the air.

4.1.2. Region-Specific Trends, Risks, and Opportunities brought on by Climate Change:

In the northern regions of France, a significant loss in precipitation during July over the years 2000 to 2020 has been increasing the hydric stress of the plants during the summer months without compensatory rainfall in June or in the later months, which is more likely to happen in coastal areas. In the case of Reims in the heart of the Champagne grape production area, we face heightened drought risks, with notable precipitation decreases in April and July coupled

with a significant increase in temperatures, also during July. Because of this, the Champagne region encounters risks regarding wine production volumes and winemaking processes.

The observed warming trend in the Loire region can be attributed in part to the influx of warmth originating from Spain via the Atlantic. This warming primarily affects the area south of the Loire River and extends far inland. Additionally, July witnesses a noteworthy decrease in PT across most of the region, effectively prolonging the dry period ahead of the summer months.

The Alsace region is experiencing differing trends: while the vineyards in the Lorraine plains have been impacted by a significant loss of PT in July as part of the same phenomenon as the rest of the northern regions, the eastern territories in the Vosges are seeing a significant increase in temperatures for July and September. Furthermore, as the Lorraine plain is exposed to winds from the west, it's also very vulnerable to the heatwaves and the vineyards there might become at risk of flash droughts during the summer months in the future years. The Alsace vineyard on the side of the Vosges however, being both protected by the mountains and its closeness to the Rhine River, might not suffer as much from the shift in temperatures.

June sees a significant uptick in precipitation on the Atlantic front, along with an equally significant decrease in July for the north of France. While this results in an unchanged total PPT for the shared area between the two phenomena, it extends their period of hydric stress starting earlier in the summer. Indeed, significant increase in maximum temperatures in July and CI category changes are now permanent. Though the Bordeaux-Charentes region remains relatively spared from the drying influences which spread further to the north, the rise in precipitation in June might also create better conditions for mildew and other cryptogamous species to thrive in. As such, the region might become more vulnerable to changes beyond the immediate effects of climate change.

Shielded from warm Spanish influences by the Pyrénées, the Midi region remains quite exposed to Atlantic precipitation. While it has experienced a significant PT increase in June, it notably stands as the only French region not affected by the rising TX trends in July. However, it remains vulnerable to heatwaves, given its location in the heart of the Aquitaine Basin.

Corsica's climate, already warm for grape cultivation as shown by the high categories in its AI, HI, and CI, now experiences significant warming, starting earlier in April and extending into September. This prolonged warmth has obvious implications for Corsica's viticulture.

Mediterranea faces rising temperatures induced by warm African influences, impacting both coastal and inland areas, especially in July and September. Additionally, the region's night temperatures are influenced by persistent warmth, exacerbating overall warming trends.

Mediterranea faces worsening conditions, punctuated by exceptional events such as significant September precipitations near Orange, attributed to Mediterranean episodes.

Bourgogne experiences significant climate change effects, particularly in July, marked by rising temperatures and declining PT. This region, pivotal for French winemaking, faces potential risks due to its proximity to swiftly changing neighboring areas.

The Jura region stands as a unique example in France, finding some benefits in the consequences of climate change. Traditionally situated on the lower climatic range of suitable grapevine growth conditions, it is now approaching more optimal conditions for viticulture. An article found on the IFV (Lempereur et al., 2016) says the same of the Beaujolais, on the other side of the Rhone valley from the Jura-Savoie region.

4.2. Future research developments:

The Institut Français de la Vigne et du Vin (French Institute for Grapevine and Wine) or IFV is the main research organization for viticultural activities, and it is there we have found most innovation projects concerning viticulture methods in the face of Climate Change. In view of their investigations and our findings, we would also like to propose some avenues of research.

- The LACCAVE project, begun in 2012, coordinates efforts from the INRAE, CNRS and several French Universities to study the impacts of climate change on the country's wine industry and develop adaptation strategies (Touzard & Ollat, 2014). The consequences of the rising temperatures and lowered precipitation are already being felt: limited production, berry ripening difficulties or with a growing time lag, affected health of the plants, scalding or flash drying from lack of rainfall coupled with high winds... 7 areas of focus have been defined:
 - Information gathering, climate simulations, elaboration of literature reviews focusing on plant health, evaluating the wine industry actors' perceptions of CC...
 - Determining grapevine responses to the changing climatic parameters and the mechanisms involved. Model methodologies for vine performance simulations.
 - Developing techniques and practices to adapt the vines to the changing conditions. Analysis of viticulture practices, design of ideotypes for varieties and cultures based on their requirements, potential yield, and qualities.

- Evaluating CC impacts on the local scale, comparing traditional and new viticultural practices to measure the impact on the long-term of their implementation. Considers the local resources as well.
 - Analysis of the economic context and strategies to be made regarding the new types of wine. Consumer willingness to pay, new marketing strategies, placement of France in the international wine industry, etc.
 - Data management support, building and securing databases, methodologies for analysis and integration of complex viticulture data for the participants.
 - Strategies on the possible scenarios for 2050. 4 strategies: a conservative one with minimal changes, an innovative one with implementation of new techniques, a migration one where the vineyards would have to be moved, and a control. Of course, it's very likely that a single strategy will not suffice, and it will be necessary to implement a mix of different strategies in each territory to be efficient.
- We observed that, at least in the Languedoc-Roussillon area, as harvest time started in the middle of a heatwave in 2023, the workers operated during the night.
 - Shading the grapevines is an experimental way to protect them from rising temperatures. A series of experiments over the years (Pallotti et al., 2023) have shown that the application of a 50% shading mesh halfway across the vine plant to put the grapes in the shade has had an impact on grape phenology: studies have stated that a microclimate formed at the level of the grapes and reduced the daily maximum temperature of 1 to 2°C, causing a delay of one week in maturity compared to the control stands, though this delay isn't impacted by the installation date of the mesh. This shift is strengthened by the increase in shading intensity, but the shading seems to have no effect on hydric stress. The comparison of the oenological parameters revealed a tendency towards a slight decrease in total acidity but the impact on colour and organoleptic parameters of the resulting wine seem to vary depending on the environment. More studies are currently ongoing to study the long-term effects of this method by IFV though it might be a response to the problem of the rising maximum temperatures trend in most of France's vineyards.
 - Another method considered by the IFV is to artificially lower the alcohol levels in the wine through dealcoholisation (Davaux & Cottureau, 2023). 3 methods have been considered to do so:

- First, by stripping 30% of the leaves from the apex of the vines, the photosynthesis is then reduced, and the glucose/fructose content of the grapes lessen. Experiments in Languedoc-Roussillon were made, starting in 2016. They efficiently contribute to lower the alcohol degree by 0.1° to 0.8°.
- Second, by selecting different maturities of the grape when harvesting. In 2019, an experiment made on Merlot patches from the PDO Gaillac saw the harvest of an early maturity of the grapes at 11% potential alcohol and another maturity at 14%. The assembly plan developed that same year resulted in an alcoholic degree gradient of 11.8% vol. to 13.7% vol. The wines also presented a modified acid balance. More studies are conducted on the impact of the method on the quality of tannins. The long-term consequences of these practices on the vine's health and the sustainability of the method remains to be evaluated.
- A third option is to ventilate the grape must during the fermentation process. 8 hours of ventilation in a room with 80% humidity causes the evaporation of 2% of the alcohol content. But it can also cause contamination of the must by acetic bacteria and *Brettanomyces*, which hasn't been considered in this study.
- The CEP (Champs Électriques Pulsés) or electromagnetic field technique is used on the experimental level to better extract polyphenols from the grape skin and seeds before fermentation of red wines. It uses electrical pulses to burst the cell walls of the grapes and release the contained anthocyanins and tannins. It enhances the colour, aromatic components, and organoleptic properties of the resulting wine. This technique may also be used to sterilize the must. It has been proven efficient and eventually accepted by the International Organisation of Vine and Wine (OIV) after presentation of the works from the IFV (Davaux et al., 2018).
- Clonal selection is a practice that was officially approved in France by the viticulture branch of the Permanent Technical Committee for Selection (CTPS) of the Variety and Seed Study and Control Group ("Inscription des variétés de vigne au Catalogue - GEVES," n.d.) in 2018, for over 40 clone strains (*Catalogue Officiel Des Variétés de Vigne | FranceAgriMer - Établissement National Des Produits de l'agriculture et de La Mer*, n.d.) that were selected mainly for their resistance to viruses, fungi, and bacteria, as well as for their gustative qualities and production rates. For the most part they weren't selected with climatic resistance in mind.

- The use of rootstocks is also an interesting option, in which the stem of the desired variety would be grafted onto the root system of a foreign grape variety, better adapted to high temperatures and/or drought conditions. Experiments are still underway by the Institute of Grapevine and Wine Sciences (ISVV) and INRAE in Bordeaux (Audeguin et al., 2015).

Migrating vineyards north to escape the impacts of climate change has been considered before but might only be a valid option up to a certain point. Indeed, a study made in Belgium (Doutreloup et al., 2022) indicates the cultivation of grapevines beyond 50° latitude is not recommended, as day length is too short, and late frosts are too prevalent in the budding season of the grapevine. However, the vine plant itself is very resistant to cold temperatures, as demonstrated by the presence of vineyards in Quebec and Canada. Taking the example of the Jura-Savoie region whose conditions are becoming more optimal to grape cultivation and observing the movement of the hot temperatures through the years of our study, our results suggest it might be an option in the future to move the vineyards up the slopes of mountain ranges as the heat tends to accumulate in valleys and are less impacted by heatwave events. This method would in theory allow the plants to escape the rising temperature trends while remaining in their assigned area and thus retaining their PDOs. Furthermore, as climate change progresses, the risk of late frost events killing the buds would lessen even in those relatively higher altitudes. As most vineyards of France are situated near mountain ranges, this option is interesting enough to be worth considering further research on.

4.3. Limitations:

After filtering the data points of our original dataset on MeteoFrance for relevance, only 46 weather stations were considered, which lessened the precision of our analysis in some regions with few stations like Alsace, Champagne, and Bourgogne. However, the weather stations' official and complete readings are not freely available in France yet and obtaining them would have required more time and budget. As there weren't any stations in proximity of the Beaujolais vineyards, it was instead integrated to the Bourgogne region, to which it was geographically closest.

To limit interannual variation while making indexes, the means of the data over 7 years were calculated and used in the raster maps. However, this caused the loss of the intra-variability factor.

Grape production data was not available in this study for they were either not complete enough for the it's needs (years 2000 to 2020 uninterrupted) and/or are considered an industrial secret or the private intellectual property of the domain.

The methodology laid out by the MCCS for assessing climate suitability for grapevine cultivation required use of the Dryness Index (Tonietto & Carbonneau, 2004). This option was discarded due to a lack of data. The Aridity Index from the World Atlas of Desertification was used instead but seemed ill-suited to the scale of our study. Slopegraphs were used to mitigate this problem with a linear regression model. For a 20 years-long study period, such a model seems to suffice, however for a longer time period, the use of a polynomial regression model would need to be considered.

5. Conclusion

Climate change is a reality which we must adapt to, for it is already too late to delay or reverse its effects. In this study, we demonstrated that they impact the whole French metropolis in different ways. The results we obtained show a significant decrease in total precipitation early in the summer in the northern territories, along with a significant increase in temperature, mostly in July and September, which advances the onset of the dry season by a month and prolongs the summer, impacting the grape volume production.

The southern part of France mostly suffers from a significant increase in temperatures brought on by dominant warm winds from Spain in the West and North Africa in the South. Most likely driven by warm winds, the Cool Nights Index has upgraded by at least on level since 2000, which disturbs harvest times and challenges wine quality. Through the Huglin Index and the data gathered from the heatwaves in 2003 and 2022, we determined that the heat has spread deep in mountain ranges through the bottom of the valleys, and low-elevation areas all over the French territory are at a much higher risk of permanent warming than mid-elevation sectors. These conditions cause economic and social changes, as PDO are linked to specific geographical areas, working conditions have worsened and innovations in current practices are required.

The wine industry's stakeholders are aware of the challenges these issues represent for their livelihood and the future of French wines notoriety, and research has been made specifically to devise solutions and techniques to help grape production adapt to the current and future conditions. However, most solutions designed are still at the experimental or pilot local implementation stage, upon which we count short-term solutions (shading vines, night harvests, artificially altering the alcohol or phenol contents of the must) and long-term ones (rootstocks of more drought-resistant varieties, genetic selection, migration of the vineyards). Hindering

the implementation of these innovations is the weight of tradition in French viticulture. The competitive advantage until now conferred to the geographical locations of the vineyards by PDOs is now being lost as these locations become unsustainable for growing grapes with the qualities required for winemaking, and any changes made to the famous vintages might influence their standing in the global marketplace. Therefore, it will be necessary to take all these concerns into account when implementing management strategies so that they are appropriate for every region's specific viticultural needs.

6. Bibliography

abacchus, pascal. (2021, August 7). Les cépages français par région: La carte qui résume tout ! - 50 Cépages. *Blog Vin Abacchus*. <https://shop.abacchus.fr/blog-vin/cepages-francais-par-region-la-carte/>

Agenis-Nevers, M. (2006). *Impacts du changement climatique sur les activités Viti-vinicoles*. <https://doi.org/10.13140/RG.2.1.4045.4163>

Audeguin, L., Sereno, C., & Olivier, Y. (2015). *Variétés de vigne de demain: Évolutions attendues, attentes professionnelles et sociétales, challenges*. 05002. <https://doi.org/10.1051/oivconf/20150505002>

Briche, É., Quenol, H., & Beltrando, G. (2011). Changement climatique dans le vignoble champenois. L'année 2003, préfigure-t-elle les prévisions des modèles numériques pour le xxie siècle ? *L'Espace géographique*, 40(2), 164–175. <https://doi.org/10.3917/eg.402.0164>

broom package—RDocumentation. (n.d.). Retrieved September 9, 2023, from <https://www.rdocumentation.org/packages/broom/versions/1.0.4>

Buesa, I., Yeves, A., Guerra, D., Sanz, F., Chirivella, C., & Intrigliolo, D. S. (2023). Testing field adaptation strategies for delaying grape ripening and improving wine composition in a cv. Macabeo Mediterranean vineyard. *Frontiers in Plant Science*, 14. Scopus. <https://doi.org/10.3389/fpls.2023.1155888>

Carte du relief français. (n.d.). Retrieved September 9, 2023, from <https://www.cartesfrance.fr/geographie/cartes-relief/carte-relief-francais.html>

Cartes des grandes régions productrices de vins AOP en France—Data.gouv.fr. (n.d.).

Retrieved September 8, 2023, from <https://www.data.gouv.fr/fr/datasets/cartes-des-grandes-regions-productrices-de-vins-aop-en-france/>

Catalogue officiel des variétés de vigne | FranceAgriMer—Établissement national des produits de l'agriculture et de la mer. (n.d.). Retrieved September 7, 2023, from <https://www.franceagrimer.fr/filieres-Vin-et-cidre/Vin/Accompagner/Dispositifs-par-filiere/Normalisation-Qualite/Bois-et-plants-de-vigne/Catalogue-officiel-des-varietes-de-vigne>

Davaux, F., & Cottereau, P. (2023). Comparaison de pratiques d'acidification en vinification en rouge: Impacts sur l'acidité, les caractéristiques chromatiques et organoleptiques des vins. *BIO Web of Conferences*, 56, 02014. <https://doi.org/10.1051/bioconf/20235602014>

Davaux, F., Royant, L., & Leroy, J.-B. (2018, January 11). *Quelles applications concrètes pour les champs électriques pulsés en Œnologie ?*

Données Publiques de Météo-France—Bulletins climatiques de France métropolitaine et outre-mer. (n.d.). Retrieved September 8, 2023, from https://donneespubliques.meteofrance.fr/?fond=produit&id_produit=129&id_rubrique=52

Doutreloup, S., Bois, B., Pohl, B., Zito, S., & Richard, Y. (2022). Climatic comparison between Belgium, Champagne, Alsace, Jura and Bourgogne for wine production using the regional model MAR. *OENO One*, 56(3), Article 3. <https://doi.org/10.20870/oeno-one.2022.56.3.5356>

dplyr package—RDocumentation. (n.d.). Retrieved September 9, 2023, from <https://www.rdocumentation.org/packages/dplyr/versions/1.0.10>

Fraga, H., García de Cortázar Aauri, I., Malheiro, A. C., & Santos, J. A. (2016). Modelling climate change impacts on viticultural yield, phenology and stress conditions in

- Europe. *Global Change Biology*, 22(11), 3774–3788.
<https://doi.org/10.1111/gcb.13382>
- GADM. (n.d.). Retrieved September 8, 2023, from
https://www.gadm.org/download_country.html
- ggplot2 package—RDocumentation. (n.d.). Retrieved September 8, 2023, from
<https://www.rdocumentation.org/packages/ggplot2/versions/3.4.3>
- Gutiérrez-Gamboa, G., Zheng, W., & Martínez de Toda, F. (2021). Current viticultural techniques to mitigate the effects of global warming on grape and wine quality: A comprehensive review. *Food Research International*, 139, 109946.
<https://doi.org/10.1016/j.foodres.2020.109946>
- Infographie—La viticulture française. (n.d.). Ministère de l’Agriculture et de la Souveraineté alimentaire. Retrieved September 8, 2023, from
<https://agriculture.gouv.fr/infographie-la-viticulture-francaise>
- Inscription des variétés de vigne au Catalogue—GEVES. (n.d.). <https://www.geves.fr/>. Retrieved September 7, 2023, from <https://www.geves.fr/expertises-varietes-semences/vignes/inscription-des-varietes/>
- Knauss, Z. A. (n.d.). *Mapping the Impacts of Climate Change on Mediterranean Viticulture*.
- Lempereur, V., Chatelet, B., Cahurel, J.-Y., & Honoré-Chedozeau, C. (2016, July 10). *Représentation holistique d’une dynamique pluridisciplinaire suite à la cartographie des sols en Beaujolais*.
- Liu, P.-H., Vrigneau, C., Salmon, T., Hoang, D. A., Boulet, J.-C., Jégou, S., & Marchal, R. (2018). Influence of Grape Berry Maturity on Juice and Base Wine Composition and Foaming Properties of Sparkling Wines from the Champagne Region. *Molecules*, 23(6), Article 6. <https://doi.org/10.3390/molecules23061372>
- Madelin, M., Bois, B., & Chabin, J.-P. (2010). Modification des conditions de maturation du raisin en Bourgogne viticole liée au réchauffement climatique. *EchoGéo*, 14, Article 14. <https://doi.org/10.4000/echogeo.12176>

- Müller, M. D. (2011). Effects of Model Resolution and Statistical Postprocessing on Shelter Temperature and Wind Forecasts. *Journal of Applied Meteorology and Climatology*, 50(8), 1627–1636. <https://doi.org/10.1175/2011JAMC2615.1>
- Ollat, N., Zito, S., Richard, Y., Aigrain, P., Brugière, F., Duchêne, E., Cortazar-Atauri, I. G. D., Gautier, J., Giraud-Héraud, E., Hannin, H., Touzard, J.-M., & Bois, B. (2021). La diversité des vignobles français face au changement climatique: Simulations climatiques et prospective participative. *Climatologie*, 18, 3. <https://doi.org/10.1051/climat/202118003>
- Pallotti, L., Silvestroni, O., Dottori, E., Lattanzi, T., & Lanari, V. (2023). Effects of shading nets as a form of adaptation to climate change on grapes production: A review. *OENO One*, 57(2), Article 2. <https://doi.org/10.20870/oenone.2023.57.2.7414>
- Pluies diluviennes sur le Languedoc et la Corse—Pluies extrêmes en France métropolitaine.* (n.d.). Retrieved September 9, 2023, from <http://pluiesextremes.meteo.fr/france-metropole/Pluies-diluviennes-sur-le-Languedoc-et-la-Corse.html>
- raster package—RDocumentation.* (n.d.). Retrieved September 8, 2023, from <https://www.rdocumentation.org/packages/raster/versions/3.6-23>
- readxl package—RDocumentation.* (n.d.). Retrieved September 8, 2023, from <https://www.rdocumentation.org/packages/readxl/versions/1.4.3>
- Roucher, A., Aristodemou, L., & Tietze, F. (2022). Predicting wine prices based on the weather: Bordeaux vineyards in a changing climate. *Frontiers in Environmental Science*, 10. Scopus. <https://doi.org/10.3389/fenvs.2022.1020867>
- Salazar-Parra, C., Aranjuelo, I., Pascual, I., Aguirreolea, J., Sánchez-Díaz, M., Irigoyen, J. J., Araus, J. L., & Morales, F. (2018). Is vegetative area, photosynthesis, or grape C uploading involved in the climate change-related grape sugar/anthocyanin decoupling in Tempranillo? *Photosynthesis Research*, 138(1), 115–128. <https://doi.org/10.1007/s11120-018-0552-6>

- sp package—RDocumentation*. (n.d.). Retrieved September 8, 2023, from <https://www.rdocumentation.org/packages/sp/versions/2.0-0>
- Toda, F. M. de, & Balda, P. (2015). Quantifying the effect of temperature on decoupling anthocyanins and sugars of the grape (*Vitis vinifera* L. 'Maturana Tinta de Navarrete'). *VITIS - Journal of Grapevine Research*, 54(3), Article 3. <https://doi.org/10.5073/vitis.2015.54.117-120>
- Tonietto, J., & Carbonneau, A. (2004). A multicriteria climatic classification system for grape-growing regions worldwide. *Agricultural and Forest Meteorology*, 124(1), 81–97. <https://doi.org/10.1016/j.agrformet.2003.06.001>
- Touzard, J.-M., & Ollat, N. (2014). Long-term adaptation to climate change in viticulture and enology: The Laccave project. *Journal International Des Sciences de La Vigne et Du Vin*, 1–7.
- van Leeuwen, C., Darriet, P., Pons, A., & Dubernet, M. (2016). *Effet du changement climatique sur le comportement de la vigne et la qualité du vin*.
- Verdugo-Vásquez, N., Orrego, R., Gutiérrez-Gamboa, G., Reyes, M., Silva, A. Z., Balbontín, C., Gaete, N., & Salazar-Parra, C. (2023). Trends and climatic variability in the Chilean viticultural production zones: Three decades of climatic data (1985-2015). *OENO One*, 57(1), Article 1. <https://doi.org/10.20870/oenone.2023.57.1.7151>
- Vin-Vigne: Le guide des vins et des vignes de France*. (n.d.). Retrieved September 9, 2023, from <http://www.vin-vigne.com/>
- WAD | World Atlas of Desertification*. (n.d.). Retrieved September 8, 2023, from <https://wad.jrc.ec.europa.eu/patternsaridity>
- Zomer, R. J., Xu, J., & Trabucco, A. (2022). Version 3 of the Global Aridity Index and Potential Evapotranspiration Database. *Scientific Data*, 9(1), Article 1. <https://doi.org/10.1038/s41597-022-01493-1>

7. Annexes

7.1. Annex 1 : Weather station names and 3-letter codes

City names	3-letter code
Agen-La Garenne	AGE
Ajaccio	AJA
Albi	ALB
Ambérieu	AMB
Angers	ANG
Aubenas	AUB
Auch	AUC
Auxerre	AUX
Bastia	BAS
Bergerac	BER
Besançon	BES
Blois	BLO
Bordeaux-Mérignac	BOR
Bourges	BRG
Carcassonne	CAR
Chambéry-Aix	CHM
Châteauroux-Déols	CHT
Cognac	COG
Colmar-Inra	COL
Dijon	DIJ
Le Luc	LEL
Lons Le Saunier	LON
La Rochelle-Ile de Ré	LRL
Macon	MAC
Marignane	MAR
Metz-Frescaty	MET
Montauban	MTB
Montélimar	MTL
Montpellier	MTP
Nantes	NAN
Nîmes-Courbessac	NIM
Niort	NIO
Orange	ORA
Orléans	ORL
Pau-Uzein	PAU
Perpignan	PER
Poitiers-Biard	POI
Reims	REI
Romorantin	ROM
Salon de Provence	SAL
Solenzara	SOL
St Dizier	STD
Toulon	TON
Tours	TOU
Troyes-Barberey	TRO

Table 16 City names and codes

PRINCIPAUX VIGNOBLES ET CEPAGES DE FRANCE

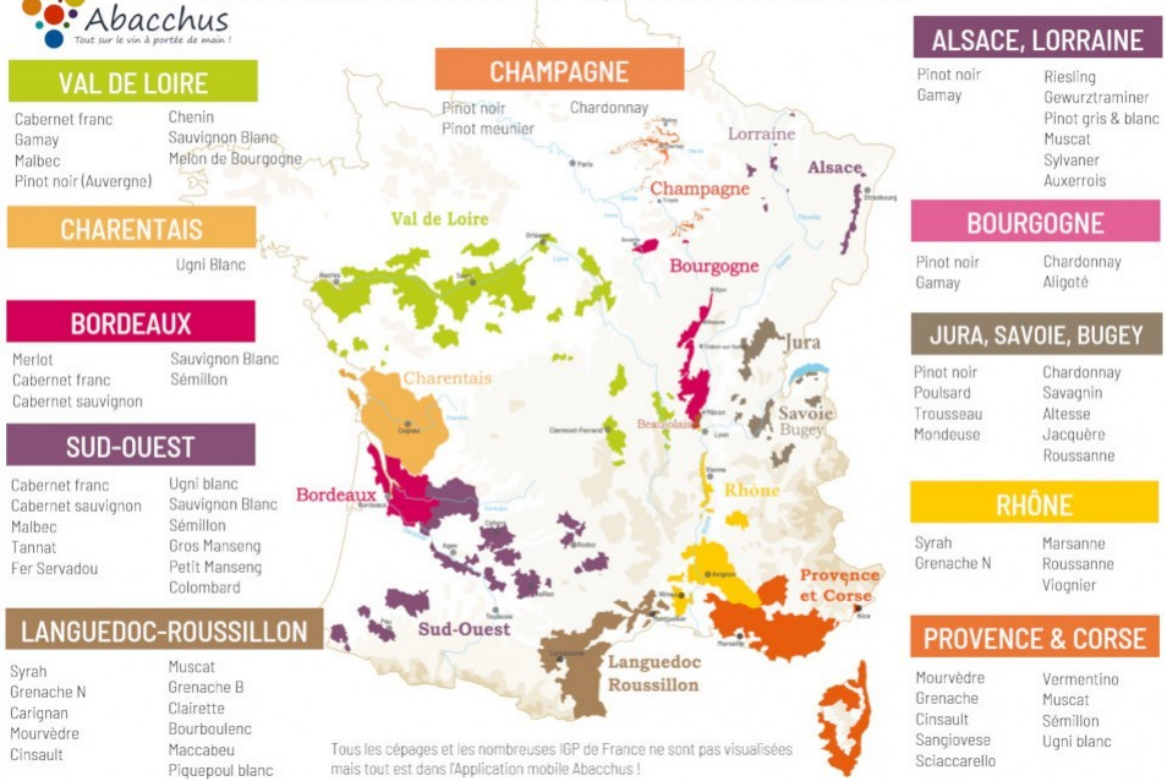


Figure 72 Map of grapevine varieties by regions of France, source: (abacchus, 2021)